Eur. Phys. J. C (2024) 84:338
https://doi.org/10.1140/epjc/s10052-024-12692-y

THE EUROPEAN PHYSICAL JOURNAL C

Check for updates

Regular Article - Theoretical Physics

$(g-2)_{e,\mu}$ anomalies and decays $h \to e_a e_b$, $Z \to e_a e_b$, and $e_b \to e_a \gamma$ in a two Higgs doublet model with inverse seesaw neutrinos

T. T. Hong[1,2,a], **Q. Duyet Tran**[1,2,b], **T. Phong Nguyen**[3,c], **L. T. Hue**[4,d], **N. H. T. Nha**[4,5,e]

[1] An Giang University, Long Xuyen 880000, Vietnam
[2] Vietnam National University, Ho Chi Minh City 700000, Vietnam
[3] Department of Physics, Can Tho University, 3/2 Street, Can Tho, Vietnam
[4] Subatomic Physics Research Group, Science and Technology Advanced Institute, Van Lang University, Ho Chi Minh City, Vietnam
[5] Faculty of Applied Technology, School of Technology, Van Lang University, Ho Chi Minh City, Vietnam

Received: 21 December 2023 / Accepted: 20 March 2024
© The Author(s) 2024, corrected publication 2024

Abstract The lepton flavor violating decays $h \to e_b^{\pm} e_a^{\mp}$, $Z \to e_b^{\pm} e_a^{\mp}$, and $e_b \to e_a \gamma$ will be discussed in the framework of the Two Higgs doublet model with presence of new inverse seesaw neutrinos and a singly charged Higgs boson that accommodate both 1σ experimental data of $(g-2)$ anomalies of the muon and electron. Numerical results indicate that there exist regions of the parameter space supporting all experimental data of $(g-2)_{e,\mu}$ as well as the promising LFV signals corresponding to the future experimental sensitivities.

1 Introduction

In the two Higgs doublet model (2HDM) framework with presence of new seesaw neutrinos, a recent study on lepton flavor violating (LFV) decays of charged leptons $e_b \to e_a \gamma$, (Standard Model-like) SM-like Higgs and neutral gauge bosons $Z, h \to e_b^{\pm} e_a^{\mp}$, showed that the $Z \to e_b^{\pm} e_a^{\mp}$ decays are suppressed even with the future experimental searches, in contrast with the promoting signal of the remaining LFV decays [1]. On the other hand, the experimental data of charged lepton anomalies $(g-2)_{e,\mu}$ [2–4] can be accommodated in the 2HDM adding a singly charged Higgs bosons and new heavy leptons [5,6] such as neutrinos used to explain the neutrino oscillation data through the inverse seesaw (ISS) mechanism. The new ISS heavy neutrinos give large one-loop contributions, named as "chirally-enhanced" ones, to both $(g-2)_{e,\mu}$ and LFV decays of charged leptons (cLFV) [7]. The same contributions also predict large LFV decays of the SM-like Higgs boson (LFVh) in the 3-3-1 model [8]. In contrast, the LFV decay rates were predicted to be suppressed in many beyond the SM, including the 3-3-1 models [9]. Therefore, we expect that there may appear promising signals of LFV decays of the gauge boson Z (LFVZ) in the allowed regions accommodating the $(g-2)_{e,\mu}$ data the mentioned models with ISS neutrinos. This is our main aim in this work.

Moreover, our work here will be useful for further investigation another class of the beyond the SM (BSM) consisting of both singly charged Higgs bosons and singly charged vector-like (VL) leptons, which also give "chirally-enhanced" contributions to accommodate the $(g-2)_{\mu}$ data [7,10–16]. Namely, when the future $(g-2)_e$ data is confirmed experimentally, the couplings of these VL particles to both muon and electron can result in interesting consequences on LFV decay rates which should be explored more precisely elsewhere.

For the 2HDM adding a singly charged Higgs boson χ and six ISS neutrinos (2HDM$N_{L,R}$) we choose to study LFV decays in this work, although the one-loop contributions from the $W^{\pm}$ in the loop do not affect the new deviations of $(g-2)_{e,\mu}$ from the SM predictions, they affect strongly the cLFV decay rates Br$(e_b \to e_a \gamma)$ which are now constrained strictly by experiments. Consequently, the LFVh decay rates are also constrained more strict than the experimental sensitivities, especially in the ISS extension of the SM without new Higgs bosons [17–19]. The same conclusions for the LFVZ

[a] e-mail: tthong@agu.edu.vn
[b] e-mail: tqduyet@agu.edu.vn
[c] e-mail: thanhphong@ctu.edu.vn
[d] e-mail: lethohue@vlu.edu.vn
[e] e-mail: nguyenhuathanhnha@vlu.edu.vn (corresponding author)

Published online: 30 March 2024

decays, where maximal decay rates are orders of $\mathcal{O}(10^{-7})$ for $Z \to \tau^{\pm}e^{\mp}, \tau^{\pm}\mu^{\mp}$ [20–23], even for the 2HDM with standard seesaw neutrinos [1]. Therefore, new contributions from new singly charged Higgs bosons may give opposite signs to relax the maximal values of these decays rates.

One-loop contributions from diagrams with virtual $W^{\pm}$ used in this work will be computed in both unitary and 't Hooft–Feynman gauges, using the same notations introduced in Ref. [1]. These formulas can be transformed into the forms given in Ref. [23] used to discussed in a simple ISS extension of the SM. Formulas calculated in the unitary without any need of information of Goldstone boson couplings will be a great advantage applicable for calculating one-loop contributions of new charged gauge boson to the LFVZ decay amplitudes or new heavy neutral gauge bosons appearing in BSM being searched for at LHC [24].

Experimental data for $(g-2)_{e,\mu}$ anomalies have been updated recently. In this work we will discuss on the parameter spaces of a 2HDM satisfying the following experimental data:

- $a_\mu \equiv (g-2)_\mu/2$ data has been updated from Ref. [4] showing a deviation from the SM prediction of $a_\mu^{\rm SM} = 116591810(43)\times 10^{-11}$ [25] combined from various different contributions based on the dispersion approach [26–52]. In this work we will use the following deviation [53]

$$\Delta a_\mu^{\rm NP} \equiv a_\mu^{\rm exp} - a_\mu^{\rm SM} = (2.49 \pm 0.48)\times 10^{-9}(5.1\sigma). \tag{1}$$

- The recent experimental a_e data was reported from different groups [2,3,54,55], leading to the two inconsistent deviations between experiments and the SM prediction [56–61]. In this work, we accept the following value:

$$\Delta a_e^{\rm NP} \equiv a_e^{\rm exp} - a_e^{\rm SM} = (3.4 \pm 1.6)\times 10^{-13}, \tag{2}$$

  where the latest experimental data for $a_e^{\rm exp}$ was given in Ref. [3]. There is another $a_e^{\rm SM}$ value derived from the measurement of the fine-structure constant of Cs-133 atoms [2], leading to $\Delta a_e^{\rm NP} = (-10.2 \pm 2.6)\times 10^{-13}$, implying the 3.9σ deviation from the earlier. Although our numerical investigation will use only the 1σ range given in Eq. (2), the two $(g-2)_e$ data have the same order of magnitudes, therefore the two qualitative results will be the same.
- The cLFV rates are constrained experimentally as follows [62–64]:

$$\begin{aligned} &{\rm Br}(\tau \to \mu\gamma) < 4.4\times 10^{-8},\\ &{\rm Br}(\tau \to e\gamma) < 3.3\times 10^{-8},\\ &{\rm Br}(\mu \to e\gamma) < 4.2\times 10^{-13}. \end{aligned} \tag{3}$$

  Future sensitivities for these decay will be ${\rm Br}(\mu \to e\gamma) < 6\times 10^{-14}$, ${\rm Br}(\tau \to e\gamma) < 9.0\times 10^{-9}$, ${\rm Br}(\tau \to \mu\gamma) < 6.9\times 10^{-9}$ [65,66].
- The latest experimental constraints for LFVh decay rates are

$$\begin{aligned} &{\rm Br}(h \to \tau\mu) < 1.5\times 10^{-3}\ [67],\\ &{\rm Br}(h \to \tau e) < 2.2\times 10^{-3}\ [67],\\ &{\rm Br}(h \to \mu e) < 6.1\times 10^{-5}\ [68]. \end{aligned} \tag{4}$$

  The future sensitivities at the HL-LHC and e^+e^- colliders may be orders of $\mathcal{O}(10^{-4})$ [69–71], $\mathcal{O}(10^{-4})$, and $\mathcal{O}(10^{-5})$ [69] for the three above LFVh decays, respectively .
- The latest experimental constraints for LFVZ decay rates are

$$\begin{aligned} &{\rm Br}(Z \to \tau^{\pm}\mu^{\mp}) < 6.5\times 10^{-6}\ [72],\\ &{\rm Br}(Z \to \tau^{\pm}e^{\mp}) < 5.0\times 10^{-6}\ [72],\\ &{\rm Br}(Z \to \mu^{\pm}e^{\mp}) < 2.62\times 10^{-7}\ [73], \end{aligned} \tag{5}$$

  The future sensitivities will be 10^{-6}, 10^{-6}, and 7×10^{-8} at HL-LHC [74]; and 10^{-9}, 10^{-9}, and 10^{-10} at FCC-ee [74,75], respectively.

Our work is arranged as follows. In Sect. 2, we discuss on the one-loop contributions of the W mediation to the decay amplitudes $Z \to e_b^{\pm}e_a^{\mp}$, using the notations introduced in Ref. [1]. In Sect. 3, we will investigate the three LFV decay classes, namely $e_b \to e_a\gamma$, $Z \to e_b^{\pm}e_a^{\mp}$, and $h \to e_b^{\pm}e_a^{\mp}$ in the 2HDM$N_{L,R}$ framework, concentrating on the regions of the parameter space accommodating the 1σ range of the $(g-2)_{e,\mu}$ experimental data.

2 One-loop contributions of W mediation to the decay amplitude $Z \to e_b^+e_a^-$

In this section we will determine analytic formulas of all diagrams relevant to one-loop contributions of the gauge boson $W^{\pm}$ to the decay amplitude $Z \to e_b^+e_a^-$ in the unitary gauge, using the notations introduced in Ref. [1]. Although the calculation is limited in the two Higgs doublet models, in which the results in the 't Hooft–Feynman gauge were introduced [1], the calculations in the unitary gauge can be generalized for many BSM predicting new neutral and charged gauge bosons. This is very convenient because the relevant couplings of new goldstone bosons can be ignored.

In the 2HDM framework, the one-loop contributions of the $W^{\pm}$ to the decay amplitude $Z \to e_a^+e_b^-$ will be calculated

in the unitary gauge, based on the well-known Lagrangian parts constructed previously [1,76]. We summarize here the necessary ingredients.

- We consider the 2HDM model consists of K exotic right-handed neutrinos N_{IR} $(I = 1, 2, \ldots, K)$ as $SU(2)_L$ singlets, in stead of 3 discussed in Ref. [1]. Because all exotic N_R are $SU(2)_L$ singlets, they do not couple to gauge bosons Z and $W^{\pm}$. Lagrangian for the charged current is the same form given in Ref. [1], namely

$$\mathcal{L}_{cc} = \frac{e}{\sqrt{2}s_W}\sum_{a=1}^{3}\sum_{i=1}^{K+3}\left(U_{ai}\overline{e_a}\gamma^{\mu}P_L n_i W_{\mu}^{-} + U_{ai}^{*}\bar{n}_i\gamma^{\mu}P_L e_a W_{\mu}^{+}\right), \tag{6}$$

where U_{ai} is the $3 \times (K+3)$ mixing matrix of three active neutrinos and new heavy ones, $UU^{\dagger} = I$, which is defined as a submatrix of the following total $(K+3) \times (K+3)$ neutrino mixing matrix:

$$U^{\nu} := \begin{pmatrix} U \\ X^{*} \end{pmatrix}. \tag{7}$$

Here we used the general from of neutrino mixing matrix introduced in Ref. [1], in which the total neutrino mass matrix is a $(K+3) \times (K+3)$ symmetric one denoted as $\mathcal{M}^{\nu}$. The original basis is $\nu_L' := (\nu_L, (N_R)^c)^T$ and $\nu_R' := (\nu_L)^c = ((\nu_L)^c, N_R)^T$. The respective physical basis of neutrinos is $n_{L,R} := (n_{1L,R}, n_{2L,R}, \ldots, n_{(K+3)L,R})^T$, which consist of left and right components of the physical Majorana states $n_i = n_i^c \equiv (n_{iL}, n_{iR})^T$ with $n_{iR} = (n_{iL})^c$. Useful relations are:

$$\begin{aligned} \mathcal{L}_{\text{mass}}^{\nu} &= -\frac{1}{2}\overline{\nu_R'}\mathcal{M}^{\nu}\nu_L + \text{H.c.}, \\ U^{\nu T}\mathcal{M}^{\nu}U^{\nu} &= \hat{\mathcal{M}}^{\nu} = \text{diag}\left(\hat{m}_{\nu}, \hat{M}_N\right), \\ \nu_L' &= U^{\nu}n_L, \ \ \nu_R' = U^{\nu *}n_R. \end{aligned} \tag{8}$$

We note here that $\mathcal{M}^{\nu}$ considered here is more general than the standard seesaw (ss) form. Three physical active neutrinos have masses being included in the matrix $\hat{m}_{\nu} = \text{diag}(m_{n_1}, m_{n_2}, m_{n_3})$, which must guarantee the neutrino oscillation data. As the charged lepton states are assumed to be physical from the beginning, $\equiv U_{ab}$ $\forall a, b = 1, 2, 3$ can be derived in terms of the experimental parameters relating to the neutrino oscillation data. The sub-matrices have the following properties.

$$\begin{aligned} \left(UU^{\dagger}\right)_{ab} &= \left(U^{\nu}U^{\nu}\right)_{ab} = \delta_{ab} \quad \forall a, b = 1, 2, 3; \\ \left(X^{*}X^{T}\right)_{IJ} &= \left(U^{\nu}U^{\nu}\right)_{(I+a)(J+b)} \\ &= \delta_{(I+a)(J+b)} \quad \forall a, b = 1, 2, 3; \ I, \\ & J = 1, 2, \ldots, K. \end{aligned} \tag{9}$$

They are originated from the unitary property and dependent to the particular form of $\mathcal{M}^{\nu}$.

- Lagrangian for the neutral current in this model is:

$$\mathcal{L}_{nc} = eZ_{\mu}\sum_{a=1}^{3}\bar{e}_a\gamma^{\mu}\left[t_L P_L + t_R P_R\right]e_a + \frac{eZ_{\mu}}{4s_W c_W}\sum_{i,j=1}^{K+3}\bar{n}_i\gamma^{\mu}\left[q_{ij}P_L - q_{ji}P_R\right]n_j, \tag{10}$$

where

$$t_R = \frac{s_W}{c_W}, \ t_L = \frac{s_W^2 - c_W^2}{2s_W c_W}, \ q_{ij} = \left(U^{\dagger}U\right)_{ij}, \ -\frac{1}{t_R} = 2t_L - t_R. \tag{11}$$

- The triple-gauge-boson couplings ZWW, which is changed into the momentum notations, is written as follows:

$$\begin{aligned} \mathcal{L}_{ZWW} &= -\frac{e}{t_r}Z_{\mu}W_{\nu}^{+}W_{\alpha}^{-}\Gamma^{\mu\nu\alpha}(p_0, p_+, p_-), \\ \Gamma^{\mu\nu\alpha}(p_0, p_+, p_-) &\equiv g^{\nu\alpha}(p_+ - p_-)^{\mu} + g^{\alpha\mu} \\ &\times (p_- - p_0)^{\nu} + g^{\mu\nu}(p_0 - p_+)^{\alpha}. \end{aligned} \tag{12}$$

To calculate in the 't Hooft–Feynman gauge, one needs more particular information of the goldstone boson couplings. Namely, Lagrangian for couplings of the goldstone boson $G_W^{\pm}$ corresponding to $W^{\pm}$ is

$$\begin{aligned} \mathcal{L}^{G} = \sum_{a=1}^{3}\sum_{i=1}^{6}\frac{g}{\sqrt{2}m_W}\Big[&G_W^{-}\bar{e}_a U_{ai}^{\nu}\left(m_i P_R - m_{e_a}P_L\right)n_i \\ &+G_W^{+}\bar{n}_i U_{ai}^{\nu *}\left(m_i P_L - m_{e_a}P_R\right)e_a\Big] \\ &-et_R m_W Z_{\mu}\left(W^{+\mu}G_W^{-} + \text{h.c.}\right) - iet_L Z_{\mu}\Big[\left(\partial^{\mu}G_W^{+}\right)G_W^{-} \\ &-G_W^{+}\partial^{\mu}G_W^{-}\Big]. \end{aligned} \tag{13}$$

The Feynman rules for $Z\overline{e_a}e_a$ and $Z\overline{n_i}n_j$ couplings are shown in Table 1.

It is emphasized that the factor for $Z\overline{n_i}n_j$ vertex for two Majorana neutrinos in Table 1 is different from that appears

Table 1 Feynman rules for one-loop contributions to $Z \to e_b^{+}e_a$

Vertex	Factor	Vertex	Factor
$Z_{\mu}\overline{e_a}e_a$	$i\gamma^{\mu}\left(t_L P_L + t_R P_R\right)$	$Z\overline{n_i}n_j$	$\frac{ie}{2s_W c_W}\gamma^{\mu}\left[q_{ij}P_L - q_{ji}P_R\right]$

in Lagrangian (10) by a factor two, which consistent with Refs. [1,77].[1]

In the unitary gauge, the propagator of Goldstone boson $\Delta^{(u)}_{G_W} = 0$, therefore all contributions from diagrams consisting of goldstone propagators vanish. In this work, we will give all relevant one-loop contributions in the unitary gauge, then we compare them with the previous results calculated in the 't Hoof–Feynman gauge.

2.1 Decays $Z \to e_b^+ e_a^-$

The effective amplitude for the decays $Z \to e_b^{\pm}(p_2) e_a^{\mp}(p_1)$ is written following the notations introduced in Refs. [1,21], namely:

$$i\mathcal{M}(Z \to e_b^+ e_a^-) = \frac{ie}{16\pi^2}\overline{u}_a \left[\not{\varepsilon}\left(\bar{a}_l P_L + \bar{a}_r P_R\right) + (p_1.\varepsilon)\left(\bar{b}_l P_L + \bar{b}_r P_R\right)\right] v_b, \tag{14}$$

where $\varepsilon_\alpha(q)$ is the polarization of Z and $u_a(p_1)$, and $v_b(p_2)$ Dirac spinors of e_a^- and e_b^+. We also used the relation $q.\varepsilon = 0$ to derive that $p_2.\varepsilon = -p_1.\varepsilon$, hence simplify the relevant expression introduced in Ref. [1]. In this work, the form factors $\bar{a}_{l,r}$ and $\bar{b}_{l,r}$ get contributions from one-loop corrections. The on-shell conditions of the final leptons and Z are $p_1^2 = m_1^2 = m_a^2$, $p_2^2 = m_2^2 = m_b^2$, and $q^2 = m_Z^2$. The respective partial decay width is

$$\Gamma(Z \to e_b^+ e_a^-) = \frac{\sqrt{\lambda}}{16\pi m_Z^3} \times \left(\frac{e}{16\pi^2}\right)^2 \left(\frac{\lambda M_0}{12 m_Z^2} + M_1 + \frac{M_2}{3m_Z^2}\right), \tag{15}$$

where $\lambda = m_Z^4 + m_b^4 + m_a^4 - 2(m_Z^2 m_a^2 + m_Z^2 m_b^2 + m_a^2 m_b^2)$, and

$$\begin{aligned} M_0 &= (m_Z^2 - m_a^2 - m_b^2)\left(|\bar{b}_l|^2 + |\bar{b}_r|^2\right) - 4m_a m_b \mathrm{Re}\left[\bar{b}_l \bar{b}_r^*\right] \\ &\quad - 4m_b \mathrm{Re}\left[\bar{a}_r^* \bar{b}_l + \bar{a}_l^* \bar{b}_r\right] - 4m_a \mathrm{Re}\left[\bar{a}_l^* \bar{b}_l + \bar{a}_r^* \bar{b}_r\right], \\ M_1 &= 4m_a m_b \mathrm{Re}\left[\bar{a}_l \bar{a}_r^*\right], \\ M_2 &= \left[2m_Z^4 - m_Z^2\left(m_a^2 + m_b^2\right) - \left(m_a^2 - m_b^2\right)^2\right]\left(|\bar{a}_l|^2 + |\bar{a}_r|^2\right). \end{aligned} \tag{16}$$

In the unitary gauge, the relevant 4 one-loop diagrams relating to the $W^{\pm}$ mediation are shown in Fig. 1.

Detailed steps to derive the form factors by hand are given in Appendix B. Consequently, the one-loop contributions to the form factors $\bar{a}_{l,r}^{nWW}$ and $\bar{b}_{l,r}^{nWW}$ corresponding to the diagram (1) in Fig. 1 are written in terms of the Passarino–Veltman (PV) functions [78] defined in appendix A, namely:

$$\begin{aligned} \bar{a}_l^{nWW} &= \frac{e^2}{2s_W^2 t_R}\sum_{i=1}^{K+3} U_{ai}^{\nu} U_{bi}^{\nu *}\left\{\left[-4 + \frac{(m_Z^2 - 2m_W^2)m_{n_i}^2}{m_W^4}\right] C_{00} \right. \\ &\quad + 2\left(m_Z^2 - m_a^2 - m_b^2\right) X_3 \\ &\quad - \frac{1}{m_W^2}\left[m_Z^2\left(2m_{n_i}^2 C_0 + m_a^2 C_1 + m_b^2 C_2\right)\right. \\ &\quad \left.\left. - m_{n_i}^2\left(B_0^{(1)} + B_0^{(2)}\right) - m_a^2 B_1^{(1)} - m_b^2 B_1^{(2)}\right]\right\}, \end{aligned} \tag{17}$$

$$\begin{aligned} \bar{a}_r^{nWW} &= \frac{e^2 m_a m_b}{2s_W^2 t_R}\sum_{i=1}^{K+3} U_{ai}^{\nu} U_{bi}^{\nu *}\left[\left(-4 + \frac{m_Z^2}{m_W^2}\right) X_3 \right. \\ &\quad \left. + \frac{m_Z^2 - 2m_W^2}{m_W^4} C_{00}\right], \end{aligned} \tag{18}$$

$$\begin{aligned} \bar{b}_l^{nWW} &= \frac{e^2 m_a}{2s_W^2 t_R}\sum_{i=1}^{K+3} U_{ai}^{\nu} U_{bi}^{\nu *}\left[4\left(X_3 - X_1\right)\right. \\ &\quad \left. + \frac{m_Z^2 - 2m_W^2}{m_W^4}\left(m_{n_i}^2 X_{01} + m_b^2 X_2\right) - \frac{2m_Z^2}{m_W^2} C_2\right], \end{aligned} \tag{19}$$

$$\begin{aligned} \bar{b}_r^{nWW} &= \frac{e^2 m_b}{2s_W^2 t_R}\sum_{i=1}^{K+3} U_{ai}^{\nu} U_{bi}^{\nu *}\left[4\left(X_3 - X_2\right)\right. \\ &\quad \left. + \frac{m_Z^2 - 2m_W^2}{m_W^4}\left(m_{n_i}^2 X_{02} + m_a^2 X_1\right) - \frac{2m_Z^2}{m_W^2} C_1\right], \end{aligned} \tag{20}$$

where $B_{0,1}^{(k)} = B_{0,1}^{(k)}(p_k^2; m_{n_i}^2, m_W^2)$, $C_{00,0,k,kl} = C_{00,0,k,kl}(m_a^2, m_Z^2, m_b^2; m_{n_i}^2, m_W^2, m_W^2)$, and $X_{0,k,kl}$ are defined in terms of the PV-functions in Eq. (A4) for all $k, l = 1, 2$.

Similarly, the one-loop contributions from diagram (2) in Fig. 1 are:

$$\begin{aligned} \bar{a}_l^{Wnn} &= \frac{e^2}{4m_W^2 s_W^3 c_W} \\ &\quad \times \sum_{i,j=1}^{K+3} U_{ai}^{\nu} U_{bj}^{\nu *}\left\{q_{ij}\left[m_W^2\left(4C_{00} + 2m_a^2 X_{01}\right.\right.\right. \\ &\quad + 2m_b^2 X_{02} - 2m_Z^2\left(C_{12} + X_0\right)\Big) \\ &\quad - \left(m_{n_i}^2 - m_a^2\right) B_0^{(1)} - \left(m_{n_j}^2 - m_b^2\right) B_0^{(2)} + m_a^2 B_1^{(1)} \\ &\quad + m_b^2 B_1^{(2)} \\ &\quad + \left(m_{n_j}^2 m_a^2 + m_{n_i}^2 m_b^2 - m_a^2 m_b^2\right) X_0 - m_{n_i}^2 m_{n_j}^2 C_0 \\ &\quad - m_{n_i}^2 m_b^2 C_1 - m_{n_j}^2 m_a^2 C_2\Big] \\ &\quad + q_{ji} m_{n_i} m_{n_j}\left[2m_W^2 C_0 - 2C_{00} - m_a^2 C_{11} - m_b^2 C_{22}\right. \\ &\quad \left.\left.\left. + \left(m_Z^2 - m_a^2 - m_b^2\right) C_{12}\right]\right\}, \end{aligned} \tag{21}$$

[1] This factor does not appear for the Feynman rule in Ref. [23].

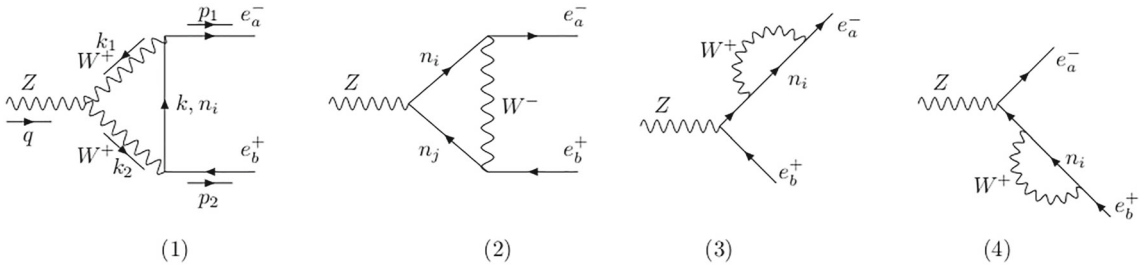

Fig. 1 One-loop Feynman diagrams in the unitary gauge

$$\bar{a}_r^{Wnn} = \frac{e^2 m_a m_b}{4m_W^2 s_W^3 c_W} \sum_{i,j=1}^{K+3} U_{ai}^{\nu} U_{bj}^{\nu *} q_{ij} \times \Big[2C_{00} + 2m_W^2 X_0 + m_a^2 X_1 + m_b^2 X_2 - m_Z^2 C_{12} - m_{n_i}^2 C_1 - m_{n_j}^2 C_2 \Big], \tag{22}$$

$$\bar{b}_l^{Wnn} = \frac{2e^2 m_a}{4m_W^2 s_W^3 c_W} \sum_{i,j=1}^{K+3} U_{ai}^{\nu} U_{bj}^{\nu *} \times \Big[q_{ij} \left(-2m_W^2 X_{01} - m_b^2 X_2 + m_{n_j}^2 C_2 \right) + q_{ji} m_{n_i} m_{n_j} (X_1 - C_1) \Big], \tag{23}$$

$$\bar{b}_r^{Wnn} = \frac{2e^2 m_b}{4m_W^2 s_W^3 c_W} \sum_{i,j=1}^{K+3} U_{ai}^{\nu} U_{bj}^{\nu *} \times \Big[q_{ij} \left(-2m_W^2 X_{02} - m_a^2 X_1 + m_{n_i}^2 C_1 \right) + q_{ji} m_{n_i} m_{n_j} (X_2 - C_2) \Big], \tag{24}$$

where $B_{0,1}^{(1)} = B_{0,1}^{(1)}(p_1^2; m_W^2, m_{n_i}^2)$, $B_{0,1}^{(2)} = B_{0,1}^{(2)}(p_2^2; m_W^2, m_{n_j}^2)$, and $C_{00,0,k,kl} = C_{00,0,k,kl}(m_a^2, m_Z^2, m_b^2; m_W^2, m_{n_i}^2, m_{n_j}^2)$ for all $k, l = 1, 2$.

The form factors for sum contributions from two diagrams (3) and (4) in Fig. 1 are

$$\bar{a}_l^{nW} = \frac{e^2 t_L}{2m_W^2 s_W^2 (m_a^2 - m_b^2)} \sum_{i=1}^{K+3} U_{ai}^{\nu} U_{bi}^{\nu *} \times \Big\{ 2m_{n_i}^2 (m_a^2 B_0^{(1)} - m_b^2 B_0^{(2)}) + m_a^4 B_1^{(1)} - m_b^4 B_1^{(2)} + \Big[2m_W^2 + m_{n_i}^2 \Big] \left(m_a^2 B_1^{(1)} - m_b^2 B_1^{(2)} \right) \Big\}. \tag{25}$$

$$\bar{a}_r^{nW} = \frac{e^2 m_a m_b t_R}{2m_W^2 s_W^2 (m_a^2 - m_b^2)} \sum_{i=1}^{K+3} U_{ai}^{\nu} U_{bi}^{\nu *} \times \Big\{ 2m_{n_i}^2 (B_0^{(1)} - B_0^{(2)}) + m_a^2 B_1^{(1)} - m_b^2 B_1^{(2)} + \left(2m_W^2 + m_{n_i}^2 \right) \left(B_1^{(1)} - B_1^{(2)} \right) \Big\}, \tag{26}$$

$$\bar{b}_l^{nW} = \bar{b}_r^{nW} = 0, \tag{27}$$

where $B_{0,1}^{(k)} = B_{0,1}^{(1)}(p_k^2; m_{n_i}^2, m_W^2)$ with $k = 1, 2$.

We have used $d = 4$ for all finite parts, and the unitary property of U^{ν}: $\sum_{i=1}^{K+3} U_{ai}^{\nu} U_{bi}^{\nu *} = \delta_{ab}$, and $\sum_{i,j=1}^{K+3} U_{ai}^{\nu} U_{bi}^{\nu *} q_{ij} = \delta_{ab}$, based on brief explanations given in Appendix B. The results of all form factors listed above were also crosschecked using FORM package [79,80]. They are also consistent with those introduced in Ref. [6] for decay amplitude $e_b \to e_a \gamma$ in the limit $t_R = t_L = 1$ and $g^R = 0$. For completeness, we list in Appendix B the one-loop contributions from singly charged Higgs bosons to the LFVZ amplitude, which is totally consistent with previous results [1]. We note that the results calculated in the unitary gauge presented in our work and Ref. [23] are consistent in general, except two parts expressed more detailed in Appendix B.3.

In the 't Hooft–Feynman gauge, apart from 4 diagrams listed in Fig. 1, the relevant diagrams consisting the goldstone boson exchanges are shown in Fig. 2.

The one-loop form factors are contributions from 10 diagrams discussed in Ref. [1], which were checked carefully by us to confirm the complete consistency with the results derived from our calculation, see the detailed discussion in Appendix B. We also show that the two results calculated in both unitary and 't Hooft–Feynman gauges are the same. The proof is summarized as follows. The first diagram in Fig. 1 relates to the class of four relevant diagrams in the 't Hooft Feynman gauge, in which the W propagators may be replaced with those of the respective Goldstone boson $G_W^{\pm}$. Consequently, we denote the following deviations between the two gauges:

$$\begin{aligned} \delta\bar{a}_l^{nWW} &\equiv \bar{a}_l^{nWW} - \bar{a}'_{nWW,l} - \bar{a}'_{nGW,l} - \bar{a}'_{nWG,l} - \bar{a}'_{nGG,l} \\ &= \frac{e^2}{2m_W^2 s_W^2 t_R} \sum_{i=1}^{K+3} U_{ai}^{\nu} U_{bi}^{\nu *} \Big\{ m_{n_i}^2 \left(B_0^{(1)} + B_0^{(2)} \right) + m_a^2 B_1^{(1)} + m_b^2 B_1^{(2)} \Big\} \\ &= \frac{e^2}{4m_W^2 s_W^2 t_R} \times \sum_{i=1}^{K+3} U_{ai}^{\nu} U_{bi}^{\nu *} \Big\{ 2A_0(m_{n_i}^2) - \left(m_a^2 B_0^{(1)} + m_b^2 B_0^{(2)} \right) + \left(3m_{n_i}^2 - m_W^2 \right) \left(B_0^{(1)} + B_0^{(2)} \right) \Big\}, \end{aligned}$$

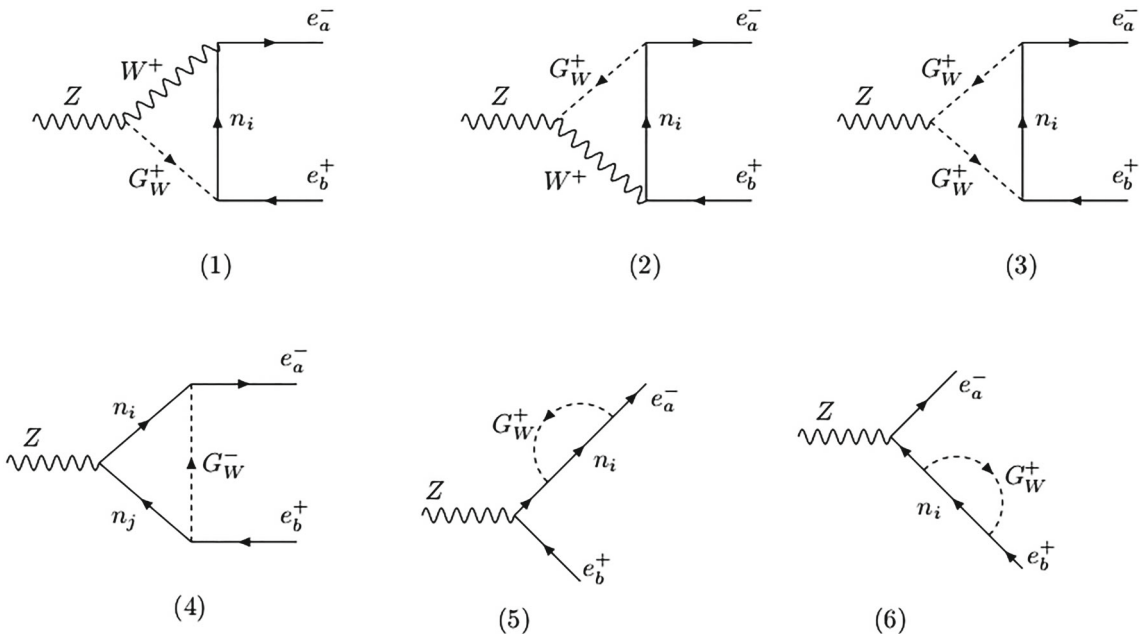

Fig. 2 One-loop Feynman diagrams consisting of goldstone boson exchanges

$$\begin{aligned}
\delta\bar{a}_r^{nWW} &= \bar{a}_r^{nWW} - \bar{a}'_{nWW,r} - \bar{a}'_{nGW,r} - \bar{a}'_{nWG,r} - \bar{a}'_{nGG,r} \\
&= 0, \\
\delta\bar{b}_l^{nWW} &= \bar{b}_l^{nWW} - \bar{b}'_{nWW,l} - \bar{b}'_{nGW,l} - \bar{b}'_{nWG,l} - \bar{b}'_{nGG,l} \\
&= 0, \\
\delta\bar{b}_r^{nWW} &= \bar{b}_r^{nWW} - \bar{b}'_{nWW,r} - \bar{b}'_{nGW,r} - \bar{b}'_{nWG,r} - \bar{b}'_{nGG,r} \\
&= 0,
\end{aligned} \tag{28}$$

where $B_0^{(k)} = B_0^{(k)}\left(p_k^2; m_{n_i}^2, m_W^2\right)$ with $k = 1, 2$; $t_{L,R}$ given in Eq. (11), and $m_Z = m_W/c_W$ were used to derive the zero values of $\delta\bar{b}_{nWW,l}$ and $\delta\bar{b}_{nWW,r}$. The functions $B_1^{(k)}$ is replaced with Eq. (A3) to obtain the final results of $\delta\bar{a}_{nWW,l}$.

Similarly, we consider the second class of the diagrams containing two neutrino propagators as follows:

$$\begin{aligned}
\delta\bar{a}_l^{Wnn} &= \bar{a}_l^{Wnn} - \bar{a}'_{Wnn,l} - \bar{a}'_{Gnn,l} \\
&= \frac{e^2}{4m_W^2 s_W^3 c_W} \sum_{i,j=1}^{K+3} q_{ij} \left[-m_{n_i}^2 B_0^{(1)} - m_{n_j}^2 B_0^{(2)} \right. \\
&\quad \left. + m_a^2 B_1^{(1)} + m_b^2 B_1^{(2)} + m_a^2 B_0^{(1)} + m_b^2 B_0^{(2)} \right], \\
&= \frac{e^2}{4m_W^2 s_W^3 c_W} \sum_{i=1}^{K+3} \left[-m_{n_i}^2 \left(B_0^{(1)} + B_0^{(2)} \right) + m_a^2 B_1^{(1)} \right. \\
&\quad \left. + m_b^2 B_1^{(2)} + m_a^2 B_0^{(1)} + m_b^2 B_0^{(2)} \right] \\
&= -\frac{e^2}{8m_W^2 s_W^3 c_W} \sum_{i=1}^{K+3} \left\{ 2A_0(m_{n_i}^2) \right. \\
&\quad - \left(m_a^2 B_0^{(1)} + m_b^2 B_0^{(2)} \right) \\
&\quad \left. + \left(3m_{n_i}^2 - m_W^2 \right) \left(B_0^{(1)} + B_0^{(2)} \right) \right\}, \\
\delta\bar{a}_r^{Wnn} &= \delta\bar{b}_l^{Wnn} = \delta\bar{b}_r^{Wnn} = 0,
\end{aligned} \tag{29}$$

where

$$B_0^{(k)} = B_0^{(k)}\left(p_k^2; m_W^2, m_{n_i}^2\right) = B_0^{(k)}\left(p_k^2; m_{n_i}^2, m_W^2\right),$$

and $k = 1, 2$. We note that the relation (A5) relating to C_{00} results in $\delta\bar{a}_{nWW,r} = 0$.

Finally, the class of the two-point diagrams give the following deviations:

$$\begin{aligned}
\delta\bar{a}_l^{nW} &= \bar{a}_l^{nW} - \bar{a}'_{nW,l} - \bar{a}'_{nG,l} \\
&= \frac{e^2 t_L}{2m_W^2 s_W^2} \sum_{i=1}^{K+3} U_{ai}^{\nu} U_{bi}^{\nu *} \left[m_{n_i}^2 \left(B_0^{(1)} + B_0^{(2)} \right) \right. \\
&\quad \left. + m_a^2 B_1^{(1)} + m_b^2 B_1^{(2)} \right] \\
&= \frac{e^2 t_L}{4m_W^2 s_W^2} \\
&\quad \times \sum_{i=1}^{K+3} U_{ai}^{\nu} U_{bi}^{\nu *} \left\{ 2A_0(m_{n_i}^2) - \left(m_a^2 B_0^{(1)} + m_b^2 B_0^{(2)} \right) \right. \\
&\quad \left. + \left(3m_{n_i}^2 - m_W^2 \right) \left(B_0^{(1)} + B_0^{(2)} \right) \right\}, \\
\delta\bar{a}_r^{nW} &= \bar{a}_r^{nW} - \bar{a}'_{nW,r} - \bar{a}'_{nG,r} = 0,
\end{aligned} \tag{30}$$

Table 2 Particle content of the 2HDM$N_{L,R}$

Symmetry	L_L	e_R	N_L	N_R	H_1	H_2	φ	χ^-
$SU(3)_C$	**1**	**1**	**1**	**1**	**1**	**1**	**1**	**1**
$SU(2)_L$	**2**	**1**	**1**	**1**	**2**	**2**	**1**	**1**
$U(1)_Y$	$-\frac{1}{2}$	-1	0	0	$\frac{1}{2}$	$\frac{1}{2}$	0	-1
$\mathbb{Z}_2$	$-$	$-$	$+$	$+$	$-$	$+$	$+$	$-$

where $B_0^{(k)} = B_0^{(k)}\left(p_k^2; m_{n_i}^2, m_W^2\right)$ with $k = 1, 2$. As a result, it is easy to derive that

$$\delta\bar{a}_l^{nWW} + \delta\bar{a}_l^{Wnn} + \delta\bar{a}_l^{nW} \propto \frac{e^2}{4m_W^2 s_W^2} \times \left(\frac{1}{t_R} - \frac{1}{2s_W c_W} + t_L\right) = 0, \tag{31}$$

i.e., the two results calculated in the two unitary and 't Hooft–Feynman gauges coincide with each other.

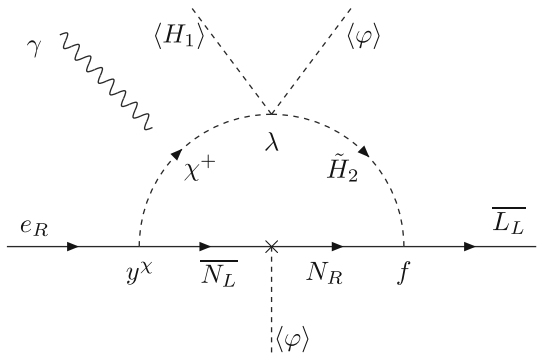

Fig. 3 One-loop Feynman diagram for chirally-enhanced contribution for $(g-2)_{e_a}$ and cLFV decays $e_b \to e_a\gamma$

3 The 2HDM with inverse seesaw neutrinos

3.1 Particle content and couplings

In this work, we will study a model discussed recently to explain experimental data of $(g-2)_{e,\mu}$ anomalies, where all LFV processes mentioned above will be discussed, namely the particle content is of the leptons and Higgs sector is listed in Table 2, which is a particular model (2HDM$N_{L,R}$) mentioned in Ref. [6].

This model is also a simple version without the gauge symmetry $U(1)_{B-L}$ mentioned in Ref. [5]. We do not mention the quark sector because it is irrelevant with our discussions and can be found in many well-known works, see reviews in Refs. [5,81].

Accordingly, the electric charge operator and covariant derivative corresponding to the electroweak gauge group $SU(2)_L \times U(1)_Y$ are:

$$Q = T^3 + Y, \tag{32}$$

$$D_\mu = \partial_\mu - ig_2 T^a W_\mu^a - g_1 Y B_\mu, \tag{33}$$

where $a = \overline{1,3}$, g_2, and g_1 are respectively the gauge couplings of the gauge fields G_μ^a, W_μ^a, B_μ, and B'_μ. The Higgs doublets are expanded as follows:

$$H_i = \begin{pmatrix} H_i^+ \\ H_i^0 \end{pmatrix},$$

$$H_i^0 = \frac{v_i + r_i + iz_i}{\sqrt{2}}, \quad \varphi = \frac{v_\varphi + r' + iz'}{\sqrt{2}}; i = 1, 2. \tag{34}$$

The Yukawa Lagrangian of leptons is [5]

$$-\mathcal{L}_Y^\ell = \overline{L_L} y_\ell H_1 e_R + \overline{L_L} f \tilde{H}_2 N_R + \overline{N_L} y^\chi e_R \chi^+ + \overline{N_L} y_N N_R \varphi + \overline{(N_L)^C} \frac{\lambda_L}{\Lambda} N_L \varphi^2 + \text{h.c.}, \tag{35}$$

where $\tilde{H}_2 = i\sigma_2 H_2^*$, y_ℓ, f, Y_N, y^χ, and λ_L are 3×3 matrices, with respective entries $y_{\ell,ab}$, f_{ab}, g_{ab}, and $\lambda_{L,ab}$ with $a, b = 1, 2, 3$. The five-dimension effective matrix μ_L generates small Majorana values consistent with the ISS form. We note that to forbid unnecessary Yukawa couplings appearing in Eq. (35), a gauge symmetry $U(1)_{B-L}$ or a discrete symmetry like Z_3 introduced respectively in Ref. [5] or [6] must be imposed. These new symmetries will not affect our results in the limit of large v_φ hence we will not discuss details here.[2]

As we will show details below, the Yukawa part in Eq. (35) generates one-loop contributions containing chirally-enhancement corresponding to the Feynman diagram shown in Fig. 3, see a similar diagram discussed in Ref. [82]. The quartic Higgs-self coupling λ comes from the Higgs potential listed in Appendix D.

The mass of leptons are derived from Eq. (35), keeping the VEV terms as follows

$$-\mathcal{L}_{\ell,\text{mass}}^Y = m_{e_a}\bar{e}_a e_a + \left[\frac{1}{2}\left(\overline{(\nu_L)^C},\ \overline{N_R},\ \overline{(N_L)^C}\right)\right.$$

[2] We thank the referee for pointing out this point.

$$\times \mathcal{M}^{\nu}\left(\nu_L,\ (N_R)^C,\ N_L\right)^T + \text{H.c.}\Big], \tag{36}$$

where

$$\mathcal{M}^{\nu} = \begin{pmatrix} \mathcal{O}_{3\times 3} & M_D^T \\ M_D & M_N \end{pmatrix},\ M_D = \begin{pmatrix} m_D \\ \mathcal{O}_{3\times 3} \end{pmatrix},$$
$$M_N = \begin{pmatrix} \mathcal{O}_{3\times 3} & M_R \\ M_R^T & \mu_L \end{pmatrix},$$
$$m_D \equiv \frac{f^{\dagger} v_2}{\sqrt{2}},\ M_R \equiv y_N^{\dagger}\frac{v_{\varphi}}{\sqrt{2}},\ \mu_L \equiv \lambda_L v_{\varphi}^2/\Lambda, \tag{37}$$

and $\mathcal{O}_{3\times 3}$ is a zero matrix. The total mass matrix $\mathcal{M}^{\nu}$ will be identified with that given in Eq. (8), where $K = 6$. The analytic form of the Dirac mass matrix m_D was chosen generally following Ref. [83].

The first term in Eq. (35) generate charged lepton masses, i.e., Eq. (36), where we choose the diagonal form to avoid tree level cLFV decay:

$$m_{e_a} = \frac{(y_{\ell})_{aa}\, v_1}{\sqrt{2}} \to (y_{\ell})_{aa} = \frac{g m_a}{\sqrt{2} m_W c_{\beta}}, \tag{38}$$

where

$$t_{\beta} \equiv \tan\beta = v_2/v_1,\ s_{\beta} = \sin\beta,\ c_{\beta} = \cos\beta. \tag{39}$$

The neutrino mass matrix is diagonalized through the following mixing matrix [84]:

$$U^{\nu T}\mathcal{M}^{\nu}U^{\nu} = \widehat{\mathcal{M}}^{\nu} = \text{diag}(m_{n_1}, m_{n_2}, \ldots, m_{n_9})$$
$$= \text{diag}(\widehat{m}_{\nu}, \widehat{M}_N), \tag{40}$$

where $\widehat{m}_{\nu} = \text{diag}(m_{n_1}, m_{n_2}, m_{n_3})$ and $\widehat{M}_N$ consist of active and new heavy neutrinos, respectively. The relations between the flavor and mass base are

$$\nu_L' = U^{\nu} n_L,\ \text{and}\ (\nu_L')^c = U^{\nu *}(n_L)^c = U^{\nu *} n_R, \tag{41}$$

where four-component spinor for Majorana neutrinos $n_i = (n_{iL}, n_{iR})^T$, and

$$\nu_L' \equiv \left(\nu_L,\ (N_R)^C,\ N_L\right)^T \leftrightarrow (\nu_L')^C$$
$$\equiv \left((\nu_L)^C,\ N_R,\ (N_L)^C\right)^T,$$
$$n_L \equiv (n_{1L},\ n_{2L}, \ldots n_{9L})^T \leftrightarrow n_R \equiv (n_L)^C$$
$$= \left((n_{1L})^C,\ (n_{2L})^C, \ldots (n_{9L})^C\right)^T. \tag{42}$$

The total neutrino mixing matrix are written in the popular ISS form

$$U^{\nu} = \begin{pmatrix} (I_3 - \frac{1}{2}RR^{\dagger})U_{\text{PMNS}} & RV \\ -R^{\dagger}U_{\text{PMNS}} & (I_K - \frac{1}{2}R^{\dagger}R)V \end{pmatrix} + \mathcal{O}(R^3). \tag{43}$$

This matrix is also identified with the general form given in Eq. (8) to determine the relevant couplings relating to the gauge boson Z.

Defining $M' = M_R\mu_L^{-1}M_R^T \sim M^2\mu_L^{-1} \gg m_D$, The ISS relations are:

$$R = M_D^{\dagger}M_N'^{*-1} = \left(-m_D^{\dagger}M'^{*-1},\quad m_D^{\dagger}\left(M^{\dagger}\right)^{-1}\right),$$
$$m_{\nu} = -M_D^T M_N'^{-1} M_D = m_D^T\left(M^T\right)^{-1}\mu_L M^{-1} m_D,$$
$$V^*\hat{M}_N V^{\dagger} \simeq M_N + \frac{1}{2}R^T R^* M_N + \frac{1}{2}M_N R^{\dagger} R. \tag{44}$$

We will apply the following simple ISS framework in numerical investigation [85]:

$$M_R \equiv M_0 I_3,\ V \simeq \frac{1}{\sqrt{2}}\begin{pmatrix} -iI_3 & I_3 \\ iI_3 & I_3 \end{pmatrix},\ m_D = M_0\hat{x}_{\nu}^{1/2}U_{\text{PMNS}}^{\dagger},$$
$$R = \left(-U_{\text{PMNS}}\frac{\sqrt{\mu_L\hat{m}_{\nu}}}{M_0},\ U_{\text{PMNS}}\hat{x}_{\nu}^{1/2}\right)$$
$$\simeq \left(\mathcal{O}_{3\times 3},\ U_{\text{PMNS}}\hat{x}_{\nu}^{1/2}\right), \tag{45}$$

where $\hat{x}_{\nu} \equiv \frac{\hat{m}_{\nu}}{\mu_0}$ satisfying the ISS condition $\max[\left(|\hat{x}_{\nu}|\right)_{ab}] \ll 1$ with all $a, b = 1, 2, 3$. The precise form of U^{ν} in terms of $\hat{x}_{\nu}$ used here was given in Ref. [86]. Consequently, all six neutrino masses are nearly degenerate, $m_{n_i} \simeq M_0\ \forall i = \overline{4, 9}$. Also, the total neutrino mixing matrix U^{ν} will be determined from the formulas given in Eq. (45).

A detailed calculation was shown in Appendix D to derive all physical Higgs states including masses and mixing parameters. The Yukawa couplings of Higgs and two leptons are derived from Eq. (35). Defining Higgs boson couplings with leptons that

$$\lambda_{ij}^h = \sum_{c=1}^{3}\left(U_{cj}^{\nu}U_{ci}^{\nu *}m_{n_i} + U_{ci}^{\nu}U_{cj}^{\nu *}m_{n_j}\right),$$
$$\lambda_{ai}^{L,G} = -\sum_{b=1}^{3}U_{(b+3)i}^{\nu}(m_D)_{ba},\quad \lambda_{ai}^{R,G} = U_{ai}^{\nu *}m_a,$$
$$\lambda_{ai}^{L,1} = -c_{\phi}t_{\beta}^{-1}\sum_{b=1}^{3}U_{(b+3)i}^{\nu}(m_D)_{ba},$$

Table 3 Feynman rules for SM-like Higgs couplings giving one-loop contributions to $h \to e_a e_b$ in the 2HDM$N_{L,R}$, where $p_{0,\pm\mu}$ denotes the incoming momenta of neutral and charged scalars

Vertex	Coupling	Vertex	Coupling
$h\overline{n_i}n_j$	$-\frac{igc_\alpha}{2m_W s_\beta}\left[\lambda^h_{ij}P_L+\lambda^{h*}_{ij}P_R\right]$	$h\overline{e_a}e_a$	$\frac{igm_a s_\alpha}{2m_W c_\beta}$
$c_k\overline{n_i}e_a$	$\frac{-ig}{\sqrt{2}m_W}\left[\lambda^{L,k}_{ai}P_L+\lambda^{R,k}_{ai}P_R\right]$	$c_k^-\overline{e_a}n_i$	$\frac{-ig}{\sqrt{2}m_W}\left[\lambda^{L,k*}_{ai}P_R+\lambda^{R,k*}_{ai}P_L\right]$
$hW^+_\mu W^-_\nu$	$ig^{\mu\nu}m_W c_\delta$	hG^+G^-	$-i\frac{c_\delta m_h^2}{v_H^2}$
$hG^+W^-_\mu$	$-\frac{ig}{2}c_\delta(p_0-p_+)^\mu$	$hG^-W^-_\mu$	$\frac{ig}{2}c_\delta(p_0-p_-)^\mu$
$hc_1^+W^-_\mu$	$-\frac{ig}{2}s_\delta c_\phi(p_0-p_+)^\mu$	$hc_1^-W^+_\mu$	$\frac{ig}{2}s_\delta c_\phi(p_0-p_-)^\mu$
$hc_2^+W^-_\mu$	$\frac{ig}{2}s_\delta s_\phi(p_0-p_+)^\mu$	$hc_2^-W^+_\mu$	$-\frac{ig}{2}s_\delta s_\phi(p_0-p_-)^\mu$
$hc_1^+c_1^-$	$i\lambda^{hcc}_{11}$	$hc_2^+c_2^-$	$i\lambda^{hcc}_{22}$
$hc_1^+c_2^-$	$i\lambda^{hcc}_{12}$	$hc_2^+c_1^-$	$i\lambda^{hcc}_{21}=i\lambda^{hcc}_{12}$

$$\lambda^{R,1}_{ai}=\left(-U^{\nu*}_{ai}m_a t_\beta c_\phi+\frac{\sqrt{2}m_W s_\phi}{g}\sum_{b=1}^{3}y^\chi_{ba}U^{\nu*}_{(b+6)i}\right),$$
$$\lambda^{L,2}_{ai}=s_\phi t_\beta^{-1}\sum_{b=1}^{3}U^{\nu}_{(b+3)i}(m_D)_{ba},$$
$$\lambda^{R,2}_{ai}=U^{\nu*}_{ai}m_a t_\beta s_\phi+\frac{\sqrt{2}m_W c_\phi}{g}\sum_{b=1}^{3}y^\chi_{ba}U^{\nu*}_{(b+6)i}, \tag{46}$$

leading to the following coupling of scalars and leptons:

$$\begin{aligned}\mathcal{L}^{hll}_Y=&\,h\sum_{a=1}^{3}\frac{s_\alpha}{c_\beta}\times\frac{gm_a}{\sqrt{2}m_W}-\frac{gc_\alpha}{4m_W s_\beta}\\&\times h\sum_{i,j}\overline{n_i}\left[\lambda^h_{ij}P_L+\lambda^{h*}_{ij}P_R\right]n_j\\&-\frac{g}{\sqrt{2}m_W}\sum_{k=0}^{2}\sum_{a=1}^{3}\sum_{i}\left[c_k\overline{n_i}\left(\lambda^{L,k}_{ai}P_L+\lambda^{R,k}_{ai}P_R\right)e_a\right.\\&\left.+\text{h.c.}\right],\end{aligned} \tag{47}$$

where $c_0^\pm=G_W^\pm$ is the Goldstone boson absorbed by $W^\pm$. We note that $\lambda^h_{ij}=\lambda^h_{ji}$, i.e., the coupling $h\overline{n_i}n_j$ is symmetric following the rules defined in Ref. [77] and consistent with previous works [17,87].

In the numerical investigation, we use the parameter

$$\delta\equiv\frac{\pi}{2}+\alpha-\beta \tag{48}$$

so that in the limit $\delta\to 0$ leads to the consistency with the SM for couplings of the SM-like Higgs boson h appearing in the model under consideration, namely $s_{\beta-\alpha}=c_\delta\to 1$, $c_{\beta-\alpha}=s_\delta\to 0$, $s_\alpha/s_\beta=-\left(c_\delta t_\beta^{-1}-s_\delta\right)\to -t_\beta^{-1}$, and $s_\alpha/c_\beta=-\left(c_\delta-t_\beta s_\delta\right)\to -1$. The Feynman rules for couplings of the SM-like Higgs boson relating to the decay $h\to e_b^+e_a^-$ considered in this work are listed in Table 3, where

$$\begin{aligned}\lambda^{hcc}_{11}=&\left[\frac{s_{2\beta}}{2}c_\phi^2(s_\alpha s_\beta\lambda_1-c_\alpha c_\beta\lambda_2)-c_\delta c_\phi^2\lambda_3\right.\\&\left.+\frac{s_{2\beta}}{2}c_\phi^2c_{(\beta+\alpha)}\,\lambda_{345}+s_\phi^2(c_\beta s_\alpha\lambda_{1\chi}-c_\alpha s_\beta\lambda_{2\chi})\right]v_H\\&+\frac{c_\delta s_{2\phi}^2\left(m_{c_2}^2-m_{c_1}^2\right)}{2v_H},\\\lambda^{hcc}_{22}=&\left[\frac{s_{2\beta}}{2}s_\phi^2(s_\alpha s_\beta\lambda_1-c_\alpha c_\beta\lambda_2)-c_\delta s_\phi^2\lambda_3\right.\\&\left.+\frac{s_{2\beta}}{2}s_\phi^2c_{(\beta+\alpha)}\lambda_{345}+c_\phi^2(c_\beta s_\alpha\lambda_{1\chi}-c_\alpha s_\beta\lambda_{2\chi})\right]v_H\\&-\frac{c_\delta s_{2\phi}^2\left(m_{c_2}^2-m_{c_1}^2\right)}{2v_H},\\\lambda^{hcc}_{12}=&\,\frac{s_{2\phi}}{2}\left[\frac{s_{2\beta}}{2}\left(-s_\alpha s_\beta\lambda_1+c_\alpha c_\beta\lambda_2\right)+c_\delta\lambda_3\right.\\&\left.-\frac{s_{2\beta}}{2}c_{(\beta+\alpha)}\lambda_{345}+(c_\beta s_\alpha\lambda_{1\chi}-c_\alpha s_\beta\lambda_{2\chi})\right]v_H\\&+\frac{c_\delta s_{4\phi}\left(m_{c_2}^2-m_{c_1}^2\right)}{4v_H},\end{aligned} \tag{49}$$

where the coupling λ appearing in λ^{hcc}_{ij} was replaced with the expression given in Eq. (D23).

The Feynman rules for couplings of the gauge boson Z relating to the decay $Z\to e_b^+e_a^-$ are listed in Table 4, where $W^3_\mu=s_W A_\mu+c_W Z_\mu$ and $B_\mu=c_W A_\mu-s_W Z_\mu$, resulting the couplings of Z being consistent with those given in Eqs. (10), (12), and (13) for the 2HDM without the singlet scalar $\chi^\pm$.

3.2 Decays $h\to e_a e_b$

The effective Lagrangian of the LFVh decay $h\to e_a^\pm e_b^\mp$ is

$$\mathcal{L}^{\text{LFV}h}=h\left(\Delta^{(ab)}_L\overline{e_a}P_L e_b+\Delta^{(ab)}_R\overline{e_a}P_R e_b\right)+\text{H.c.},$$

where scalar factors $\Delta_{(ab)L,R}$ arise from the loop contributions. The one-loop diagrams of the decays $h\to e_a^-e_b^+$ in the unitary gauge are shown in Fig. 4.

Table 4 Feynman rules for Z couplings giving one-loop contributions to $Z \to e_b^+ e_a^-$ in the 2HDM$N_{L,R}$, where $p_{0,\pm\mu}$ denotes the incoming momenta of neutral and charged scalars

Vertex	Coupling	Vertex	Coupling
$Z_\mu \overline{n_i} n_j$	$\frac{ie}{2s_W c_W}\gamma^\mu \left[q_{ij} P_L - q_{ji} P_R\right]$	$Z_\mu \overline{e_a} e_a$	$ie\gamma^\mu \left(t_L P_L + t_R P_R\right)$
$Z_\mu W_\nu^+ W_\alpha^-$	$-\frac{ie}{t_r}\Gamma^{\mu\nu\alpha}(p_0, p_+, p_-)$	$Z_\mu G^+ G^-$	$-iet_L(p_+ - p_-)^\mu$
$Z_\mu G^+ W_\nu^-$	$-iem_W t_R g^{\mu\nu}$	$Z_\mu G^- W_\nu^+$	$-iem_W t_R g^{\mu\nu}$
$Z c_1^+ c_1^-$	$\frac{ie\left(c_\phi^2 - 2s_W^2\right)}{2c_W s_W}(p_+ - p_-)^\mu$	$Z c_2^+ c_2^-$	$\frac{ie\left(s_\phi^2 - 2s_W^2\right)}{2c_W s_W}(p_+ - p_-)^\mu$
$Z c_1^+ c_2^-$	$-\frac{ies_{2\phi}}{4c_W s_W}(p_+ - p_-)^\mu$	$Z c_2^+ c_1^-$	$-\frac{ies_{2\phi}}{4c_W s_W}(p_+ - p_-)^\mu$

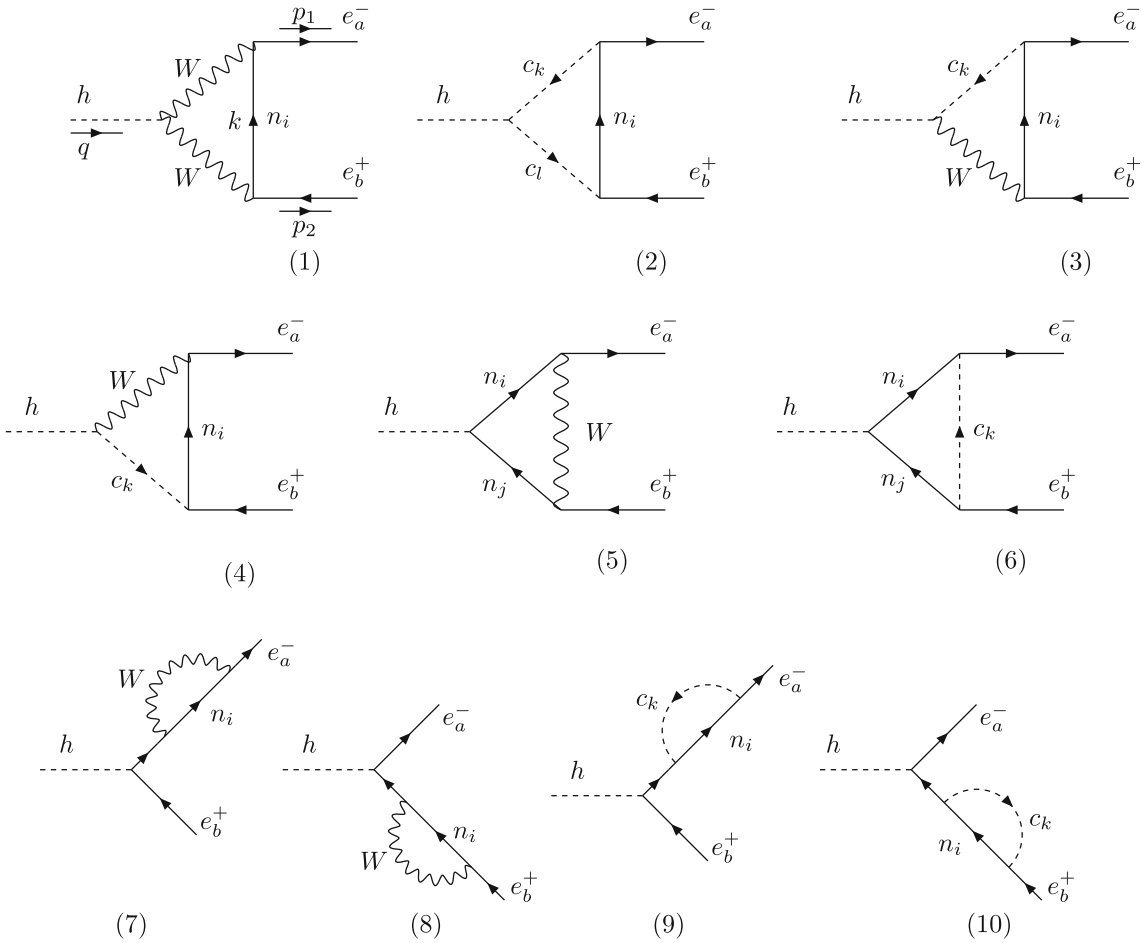

Fig. 4 One-loop Feynman diagrams of the decays $h \to e_b^+ e_a^-$ in the 2HDM$N_{L,R}$

The partial width of the decay is [88]

$$\Gamma(h \to e_a e_b) \equiv \Gamma(h \to e_a^- e_b^+) + \Gamma(h \to e_a^+ e_b^-) \simeq \frac{m_h}{8\pi}\left(|\Delta_L^{(ab)}|^2 + |\Delta_R^{(ab)}|^2\right), \tag{50}$$

with the condition $m_h \gg m_{a,b}$ being masses of charged leptons. The on-shell conditions for external particles are $p_{1,2}^2 = m_{e_a,e_b}^2$ and $q^2 \equiv (p_1 + p_2)^2 = m_h^2$. The corresponding branching ratio is $\mathrm{Br}(h \to e_a e_b) = \Gamma(h \to e_a e_b)/\,\Gamma_h^{\mathrm{total}}$ where $\Gamma_h^{\mathrm{total}} \simeq 4.1 \times 10^{-3}$ GeV [89]. Formulas of $\Delta_{(ab)L,R}$ are given as follows

$$\Delta_{L,R}^{(ab)} = \Delta_{L,R}^{(ab)W} + \Delta_{L,R}^{(ab)c} + \Delta_{L,R}^{(ab)Wc},$$
$$\Delta_{L,R}^{(ab)W} = \Delta_{L,R}^{(ab)nWW} + \Delta_{L,R}^{(ab)Wnn} + \Delta_{(ab)L,R}^{nW},$$
$$\Delta_{L,R}^{(ab)c} = \sum_{k,l=1,2} \Delta_{L,R}^{(ab)nc_k c_l} + \sum_{k=1}^{2}\left(\Delta_{L,R}^{(ab)c_k nn} + \Delta_{L,R}^{(ab)nc_k}\right),$$

$$\Delta_{L,R}^{(ab)Wc} = \sum_{k=1}^{2}\left(\Delta_{L,R}^{(ab)c_kWn} + \Delta_{L,R}^{(ab)nWc_k}\right), \tag{51}$$

where detailed analytic forms are given in Appendix C.

3.3 Decays $Z \to e_b^+ e_a^-$

In this model, the one-loop contributions to the LFVZ decays $Z \to e_b^+ e_a^-$ consists of the two parts originated from exchanges of $W^\pm$ and singly charged Higgs bosons $c_k^\pm$ with Feynman rules listed in Table 4. Analytic formulas of one-loop contributions from these Higgs were listed in Appendix B, consistent with previous results [76]. The partial decay widths are given in Eq. (15), where the form factors are

$$\begin{aligned}
&\bar{a}_{L,R} = a_{l,r}^W + a_{l,r}^{c^\pm},\ \bar{b}_{L,R} = b_{l,r}^W + b_{l,r}^{c^\pm},\\
&\bar{a}_{l,r}^W = \bar{a}_{l,r}^{nWW} + \bar{a}_{l,r}^{Wnn} + \bar{a}_{l,r}^{nW},\\
&\bar{b}_{l,r}^W = \bar{b}_{l,r}^{nWW} + \bar{b}_{l,r}^{Wnn} + \bar{b}_{l,r}^{nW},\\
&\bar{a}_{l,r}^{c^\pm} = \sum_{p,q=1}^{2}\bar{a}_{l,r}^{nc_pc_q} + \sum_{k}^{2}\left(\bar{a}_{l,r}^{c_knn} + \bar{a}_{l,r}^{nc_k}\right),\\
&\bar{b}_{l,r}^{c^\pm} = \sum_{p,q=1}^{2}\bar{b}_{l,r}^{nc_pc_q} + \sum_{k}^{2}\left(\bar{b}_{l,r}^{c_knn} + \bar{b}_{l,r}^{nc_k}\right).
\end{aligned} \tag{52}$$

3.4 $(g-2)_{e,\mu}$ and decays $e_b \to e_a\gamma$

The branching ratios of the cLFV decays are formulated as follows [7,90,91]:

$$\begin{aligned}
\mathrm{Br}(e_b \to e_a\gamma) = \frac{48\pi^2}{G_F^2 m_b^2}&\left(\left|c_{(ab)R}\right|^2 + \left|c_{(ba)R}\right|^2\right)\\
&\times \mathrm{Br}(e_b \to e_a\overline{\nu_a}\nu_b),
\end{aligned} \tag{53}$$

where $G_F = g^2/(4\sqrt{2}m_W^2)$, $\mathrm{Br}(\mu \to e\overline{\nu_e}\nu_\mu) \simeq 1$, $\mathrm{Br}(\tau \to e\overline{\nu_e}\nu_\tau) \simeq 0.1782$, $\mathrm{Br}(\tau \to \mu\overline{\nu_\mu}\nu_\tau) \simeq 0.1739$ [84], and

$$\begin{aligned}
c_{(ab)R} &= c_{(ab)R}^{c^\pm}\left(h^\pm\right) + c_{(ab)R}^{W},\\
c_{(ba)R} &= c_{(ab)R}[a \to b,\ b \to a],\\
c_{(ab)R}^{c^\pm} &= \sum_{k=1}^{2} c_{(ab)R}\left(c_k^\pm\right),\\
c_{(ab)R}\left(c_k^\pm\right) &= \frac{g^2 e}{32\pi^2 m_W^2 m_{c_k}^2}\\
&\times \sum_{i=1}^{9}\left[\lambda_{ia}^{L,k*}\lambda_{ib}^{R,k} m_{n_i} f_\Phi(x_{i,k})\right.\\
&\left.+\left(m_b\lambda_{ia}^{L,k*}\lambda_{ib}^{L,k} + m_a\lambda_{ia}^{R,k*}\lambda_{ib}^{R,k}\right)\tilde{f}_\Phi(x_{i,k})\right],
\end{aligned}$$

$$\begin{aligned}
c_{(ab)R}(W) \simeq \frac{eG_F m_{e_b}}{4\sqrt{2}\pi^2}&\left[-\frac{5\delta_{ab}}{12} + \left(U_{\mathrm{PMNS}}\hat{x}_\nu U_{\mathrm{PMNS}}^\dagger\right)_{ab}\right.\\
&\left.\times\left(\tilde{f}_V(x_W) + \frac{5}{12}\right)\right]
\end{aligned} \tag{54}$$

with $x_{i,k} \equiv m_{n_i}^2/m_{c_k}^2$, $x_W = M_0^2/m_W^2$, and [7]

$$\begin{aligned}
f_\Phi(x) &= 2\tilde{g}_\Phi(x) = \frac{x^2 - 1 - 2x\ln x}{4(x-1)^3},\\
g_\Phi &= \frac{x - 1 - \ln x}{2(x-1)^2},\\
\tilde{f}_\Phi(x) &= \frac{2x^3 + 3x^2 - 6x + 1 - 6x^2\ln x}{24(x-1)^4},\\
\tilde{f}_V(x) &= \frac{-4x^4 + 49x^3 - 78x^2 + 43x - 10 - 18x^3\ln x}{24(x-1)^4}.
\end{aligned} \tag{55}$$

The one-loop contributions from the singly charged Higgs boson $c_{1,2}^\pm$ and $W^\pm$ exchanges to a_{e_a} are:

$$a_{e_a}^{c^\pm} = -\frac{4m_a}{e}\left(\sum_{k=1}^{2}\mathrm{Re}[c_{(aa)R}(c_k^\pm)] + \Delta c_{(aa)R}(W)\right), \tag{56}$$

where $\Delta c_{(aa)R}(W) = \left(U_{\mathrm{PMNS}}\hat{x}_\nu U_{\mathrm{PMNS}}^\dagger\right)_{aa} \times\left(\tilde{f}_V(x_W) + \frac{5}{12}\right)$ is the deviation between the 2HDM$N_{L,R}$ and the SM.

Up to the order $\mathcal{O}(R^2)$ of the neutrino mixing matrix, the non-zero one-loop contributions relating to $c_{1,2}^\pm$ were determined precisely, see Refs. [86,92]. Accordingly, the main contribution to $a_{e_a}(c^\pm)$ is

$$\begin{aligned}
a_{e_a,0}(c^\pm) = \frac{G_F m_a^2}{\sqrt{2}\pi^2} \times \mathrm{Re}\left\{\left[\frac{vt_\beta^{-1}c_\alpha s_\alpha}{\sqrt{2}m_a}U_{\mathrm{PMNS}}\hat{x}_\nu^{1/2}y^\chi\right]_{aa}\right.\\
\left.\times\left[x_1 f_\Phi(x_1) - x_2 f_\Phi(x_2)\right]\right\},
\end{aligned} \tag{57}$$

where $x_k = M_0^2/m_{c_k}^2$. In numerical calculation, the following diagonal form of $c_{(ab)R,0}$ will be chosen for discussing the Yukawa coupling matrix y^χ at the beginning

$$c_{(ab)R,0} \propto \left[U_{\mathrm{PMNS}}\hat{x}_\nu^{1/2}y^\chi\right]_{ab} \propto \delta_{ab}. \tag{58}$$

The non-zero values of $c_{(ab)R}$ and $c_{(ba)R}$ with $b \neq a$ may give large contributions to the cLFV rates, see a detailed discussion in Ref. [93]. Correspondingly, the formula of $a_{e_a,0}$ is proportional to a diagonal matrix y^d satisfying:

$$\begin{aligned}
&U_{\mathrm{PMNS}} \times \mathrm{diag}\left(\frac{m_{n_1}}{m_{n_3}},\ \frac{m_{n_2}}{m_{n_3}},\ 1\right)^{1/2} y^\chi\\
&\quad = y^d \equiv \mathrm{diag}\left(y_{11}^d,\ y_{22}^d,\ y_{33}^d\right),
\end{aligned} \tag{59}$$

where $m_{n_3} > m_{n_2} > m_{n_1}$ corresponding to the normal order of the neutrino oscillation data will be chosen in the numerical investigation. Then, the main contributions from charged Higgs bosons to a_{e_a} was shown to be [92]

$$a_{e_a,0} = \frac{G_F m_a^2 \sqrt{x_0}}{\sqrt{2}\pi^2} \times \text{Re}\left[\frac{v t_\beta^{-1} c_\alpha s_\alpha}{\sqrt{2} m_a} y^d\right]_{aa} \times [x_1 f_\Phi(x_1) - x_2 f_\Phi(x_2)], \tag{60}$$

where $x_k \equiv M_0^2/m_{c_k}^2$ $(k = 1, 2)$, and

$$x_0 \equiv \frac{m_{n_3}}{\mu_0}. \tag{61}$$

Note that $c_{(ab)R,0}$ vanishes with $a \neq b$, therefore do not affect the $\text{Br}(e_b \to e_a\gamma)$. The values of entries y^χ will be scanned around the diagonal forms of y^d to guarantee the cLFV constraints of experiments.

3.5 Numerical discussion

We will use the best-fit values of the neutrino osculation data [84] corresponding to the normal order (NO) scheme with $m_{n_1} < m_{n_2} < m_{n_3}$, namely

$$s_{12}^2 = 0.318,\ s_{23}^2 = 0.574,\ s_{13}^2 = 0.022,\ \delta = 194\ [\text{Deg}],$$
$$\Delta m_{21}^2 = 7.5 \times 10^{-5}[\text{eV}^2],\ \Delta m_{32}^2 = 2.47 \times 10^{-3}[\text{eV}^2]. \tag{62}$$

The active mixing matrix and neutrino masses are determined as follows

$$\hat{m}_\nu = \left(\hat{m}_\nu^2\right)^{1/2} = \text{diag}\left(m_{n_1},\ \sqrt{m_{n_1}^2 + \Delta m_{21}^2},\ \sqrt{m_{n_1}^2 + \Delta m_{21}^2 + \Delta m_{32}^2}\right),$$
$$U_{\text{PMNS}} = \begin{pmatrix} c_{12}c_{13} & c_{13}s_{12} & s_{13}e^{-i\delta} \\ -c_{23}s_{12} - c_{12}s_{13}s_{23}e^{i\delta} & c_{12}c_{23} - s_{12}s_{13}s_{23}e^{i\delta} & c_{13}s_{23} \\ s_{12}s_{23} - c_{12}c_{23}s_{13}e^{i\delta} & -c_{23}s_{12}e^{i\delta}s_{13} - c_{12}s_{23} & c_{13}c_{23} \end{pmatrix}. \tag{63}$$

We fix $m_{n_1} = 0.01$ eV for simplicity in numerical investigation. This choice of active neutrino masses satisfies the constraint from Plank2018 [94], $\sum_{i=a}^3 m_{n_a} \leq 0.12$ eV.

The non-unitary of the active neutrino mixing matrix $\left(I_3 - \frac{1}{2}RR^\dagger\right) U_{\text{PMNS}}$ is constrained by other phenomenology such as electroweak precision [95,96], leading to a very strict constraint of $\eta \equiv \frac{1}{2}\left|RR^\dagger\right| \propto \hat{x}_\nu \propto x_0$ in the ISS framework [5,97,98].

The well-known numerical parameters are [84]

$$g = 0.652,\ G_F = 1.1664 \times 10^{-5}\ \text{GeV},$$
$$s_W^2 = 0.231,\ \alpha_e = 1/137,\ e = \sqrt{4\pi\alpha_e},$$
$$m_W = 80.377\ \text{GeV}, m_Z = 91.1876\ \text{GeV},$$
$$m_h = 125.25\ \text{GeV},$$
$$\Gamma_h = 4.07 \times 10^{-3}\ \text{GeV},\ \Gamma_Z = 2.4955\ \text{GeV},$$
$$m_e = 5 \times 10^{-4}\ \text{GeV},\ m_\mu = 0.105\ \text{GeV},$$
$$m_\tau = 1.776\ \text{GeV}. \tag{64}$$

For the free parameters of the 2HD$N_{L,R}$ model, the numerical scanning ranges are

$$M_0, m_{c_{1,2}} \in [1,\ 10]\ \text{TeV};\ \lambda_1, |\lambda_4|, |\lambda_5| \in [0,\ 4\pi];$$
$$t_\beta \in [5, 30];\ x_0 \in \left[10^{-6}, 5 \times 10^{-4}\right];\ \phi \in [0, \pi];$$
$$|y_{ab}^d| \leq 3.5\ \forall a, b = 1, 2, 3. \tag{65}$$

The matching condition with SM requires small $|s_\delta|$. Therefore, we fix $s_\delta = 0$ in the numerical investigation. The Higgs self-couplings and Higgs masses appearing in Eq. (49) are $\lambda_1, \lambda_4, \lambda_5, \lambda_{1\chi}$, and $\lambda_{2\chi}$, in which some of them are given in Eq. (D23). The related independent parameters are chosen as $\lambda_{1\chi}$, and $\lambda_{2\chi}$, apart from those given in Eq. (65). For simplicity, we will fix $\lambda_{1\chi} = \lambda_{2\chi} = 0$. In the numerical investigation we take lower bounds that $m_H, m_A \geq 500$ GeV. The couplings $hc_k^+ c_l^-$ given in (49) are determined after confirming numerically that all Higgs couplings must satisfy the two conditions of bounded from below and unitarity limits mentioned in Appendix D. All Yukawa couplings of the matrices y^χ and f must satisfy the perturbative limits, therefore we choose the safe upped bounds that $|y_{ab}^\chi|, |f_{ab}| \leq 3 < \sqrt{4\pi}$.

In the following discussion on numerical results, we just collect allowed points in the scanning ranges given in Eq. (65), in which they satisfy all experimental LFV constraints listed in Eqs. (3), (4), and (5). In addition the $(g-2)_{e,\mu}$ data is chosen at 1σ deviations derived from two Eqs. (1) and (2).

Firstly, we focus on the simplest case of $\delta = 0$, and only $y_{11}^d, y_{22}^d \neq 0$, while $y_{ab}^d = 0$ for $(ab) = (33)$ and $a \neq b$. The correlations between $\Delta a_{e,\mu}$ with t_β, ϕ, and x_0 are shown in Fig. 5.

The allowed ranges of these three parameters are: $5 \leq t_\beta < 20$, $0.2 < \phi < 2.93$ and $10^{-5} < x_0 < 4 \times 10^{-4}$. The import property is that $s_\phi c_\phi$ always non-zero.

The correlations between $\Delta a_{e,\mu}$ with y_{11}^d, and y_{22}^d are shown in Fig. 6.

The allowed regions are $0.03 \leq |y_{11}^d| \leq 0.15$ and $1 \leq |y_{22}^d| \leq 3$.

The correlations between $\Delta a_{e,\mu}$ with neutrinos and charged Higgs masses are shown in Fig. 7.

There are not constraints of M_0 and charged Higgs boson masses in the scanning regions given in Eq. (65).

The correlations between $\Delta a_{e,\mu}$ with cLFV decays $\text{Br}(e_b \to e_a\gamma)$ are shown in Fig. 8.

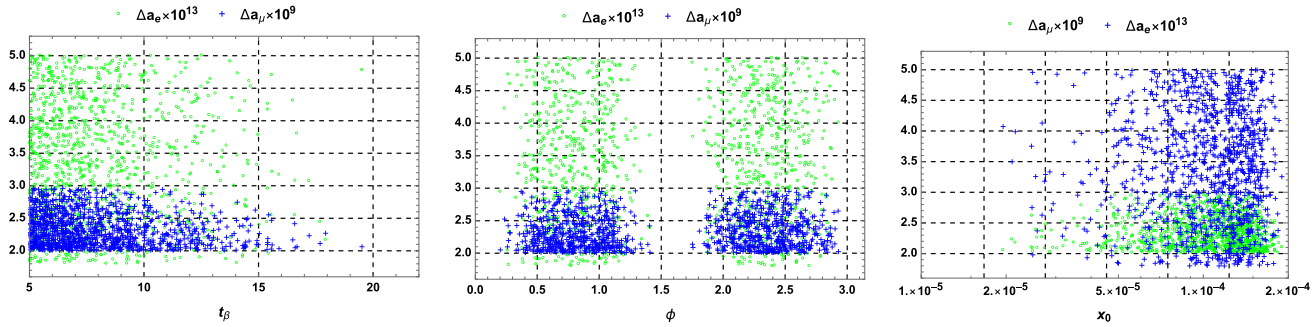

Fig. 5 The correlations between $\Delta a_{e,\mu}$ and t_β (left), ϕ (center), and x_0 (right) in the limits of $\delta = 0$ and $y^d_{11}, y^d_{22} \neq 0$

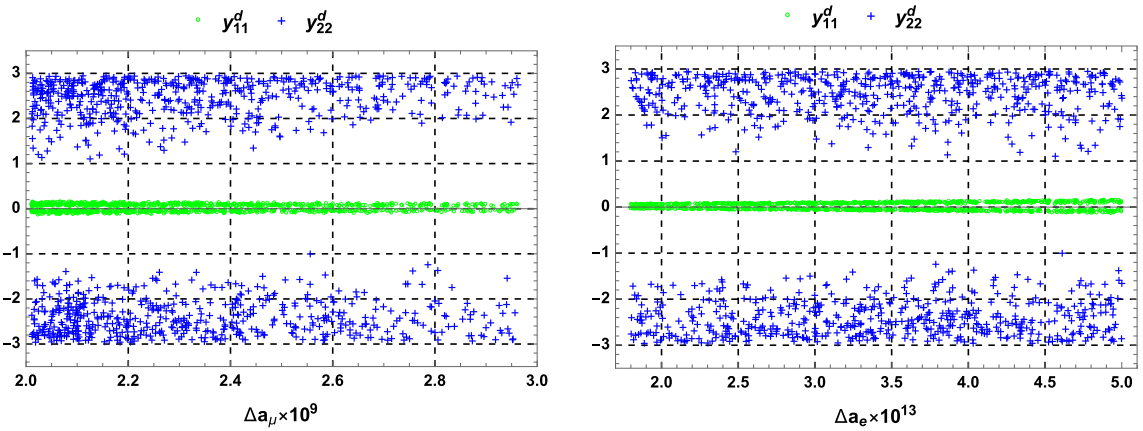

Fig. 6 The correlations between $\Delta a_{e,\mu}$ vs y^d_{11} and y^d_{22} in the limits of $\delta = 0$ and $y^d_{11}, y^d_{22} \neq 0$

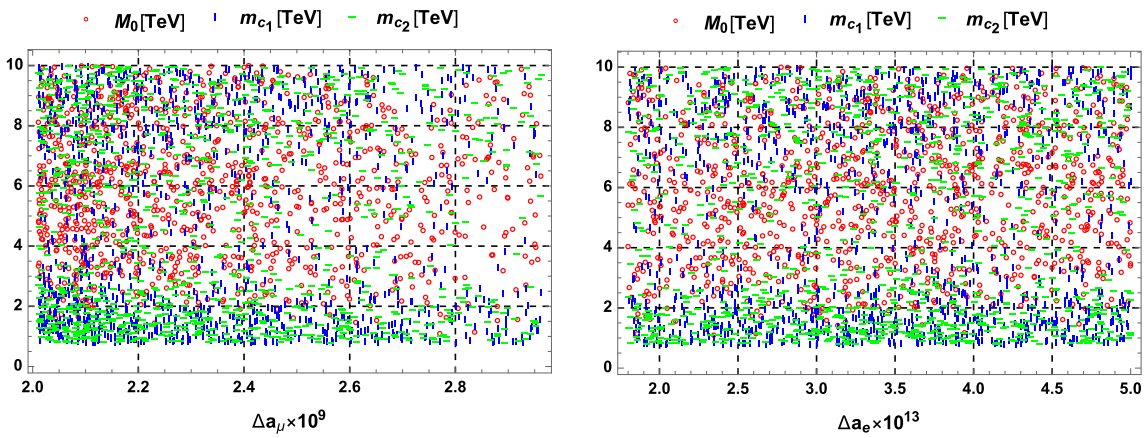

Fig. 7 The correlations between $\Delta a_{e,\mu}$ vs neutrinos and charged Higgs masses in the limits of $\delta = 0$ and $y^d_{11}, y^d_{22} \neq 0$

The decay $\mu \to e\gamma$ can reach the experimental bound, but two decay modes are much smaller than the near future experimental sensitivities, namely Fig. 8 shows two upper values of $\text{Br}(\tau \to e\gamma) < 10^{-13}$ and $\text{Br}(\tau \to \mu\gamma) < 1.5 \times 10^{-12}$.

The correlations between $\Delta a_{e,\mu}$ with LFV decays $\text{Br}(Z \to e^+_b e^-_a)$ are shown in Fig. 9.

These three decays can reach the future sensitivities. The upper bound are found as follows: $\max[\text{Br}(Z \to \mu^+ e^-)] \simeq 2.75 \times 10^{-8}$, $\max[\text{Br}(Z \to \tau^+ e^-)] \simeq 2.43 \times 10^{-8}$, and $\max[\text{Br}(Z \to \tau^+ \mu^-)] \simeq 3.53 \times 10^{-7}$. Although these three decays rates are smaller than the recent experimental upper bounds, they all reach the near future sensitivities of experiments. This property in the 2HDM$N_{L,R}$ is different from the model discussed in Ref. [1], where all LFV Z decay rates are predicted to be suppressed. Also, $\text{Br}(Z \to \mu^\pm e^\mp) < 10^{-9}$ was confirmed in Ref. [23].

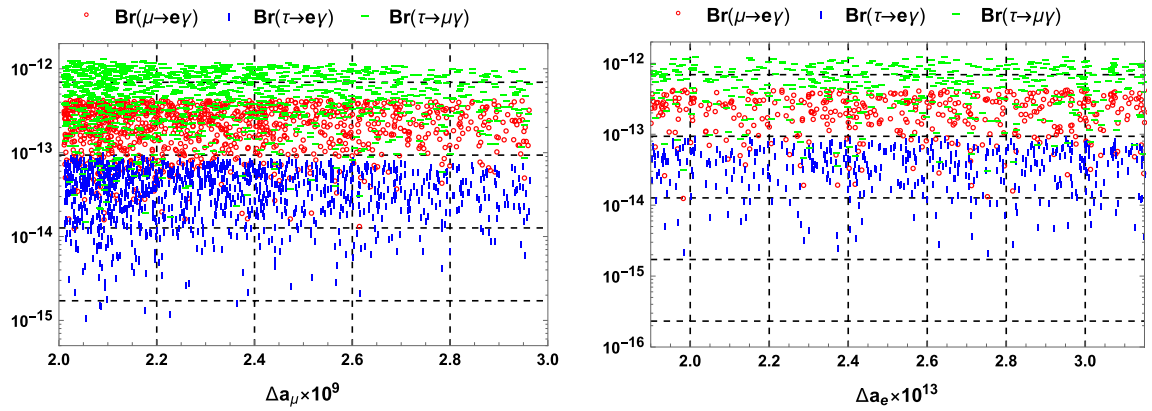

Fig. 8 The correlations between $\Delta a_{e,\mu}$ vs cLFV decays $\mathrm{Br}(e_b \to e_a\gamma)$ in the limits of $\delta = 0$ and $y^d_{11}, y^d_{22} \neq 0$

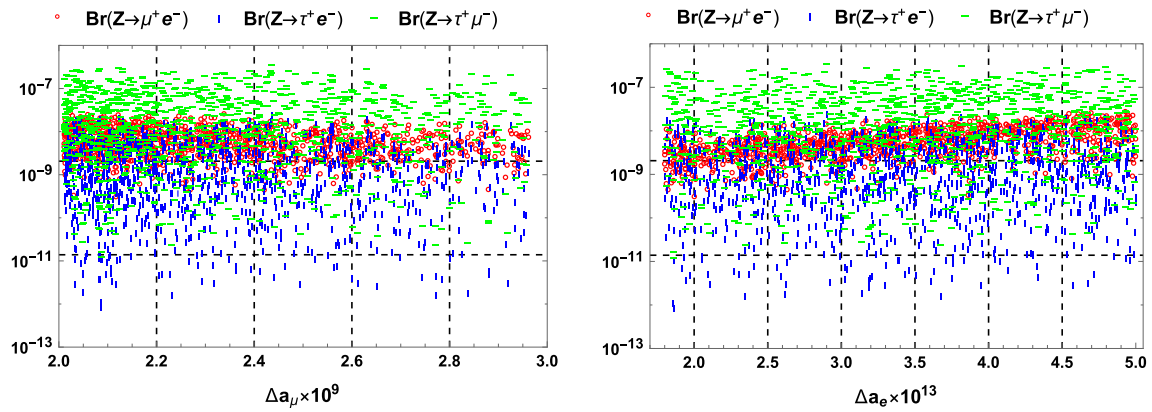

Fig. 9 The correlations between $\Delta a_{e,\mu}$ vs $\mathrm{Br}(Z \to e^+_b e^-_a)$ in the limits of $\delta = 0$ and $y^d_{11}, y^d_{22} \neq 0$

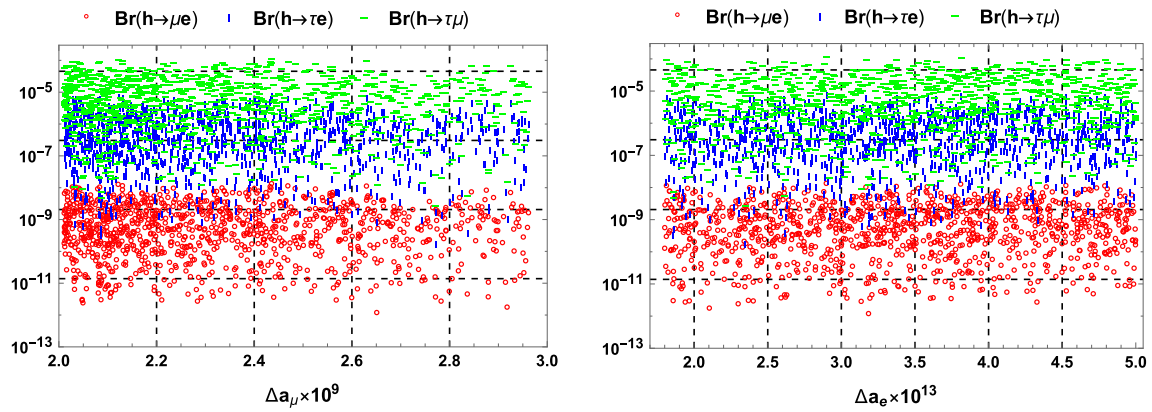

Fig. 10 The correlations between $\Delta a_{e,\mu}$ vs $\mathrm{Br}(h \to e_b e_a)$ in the limits of $\delta = 0$ and $y^d_{11}, y^d_{22} \neq 0$

The correlations between $\Delta a_{e,\mu}$ with LFV decays $\mathrm{Br}(h \to e_b e_a)$ are shown in Fig. 10.

The upper bounds of these decays are $\mathrm{Br}(h \to \mu^+ e^-) < 1.4 \times 10^{-8}$, $\mathrm{Br}(h \to \tau^+ e^-) < 8 \times 10^{-6}$, and $\mathrm{Br}(h \to \tau^+ \mu^-) < 1.2 \times 10^{-4}$. Only $\mathrm{Br}(h \to \tau^+ \mu^-)$ can reach the near future experimental sensitivities.

In the more general conditions of numerical investigations, the allowed regions of the parameters such as heavy neutrinos and charged Higgs boson masses, and $y^d_{11,22}$ do not change significantly. Therefore, we will not pay attention to them. The two entries $|y^d_{12}|, |y^d_{21}| < 10^{-3}$ because of the strict constraint from $\mathrm{Br}(e_b \to e_a\gamma)$. As a consequence, they give suppressed contributions to the remaining LFV decay rates, therefore we will fix $y^d_{12} = y^d_{21} = 0$ in the numerical investigation. In addition, the allowed regions prefer the small $|y_{31}| < 0.05$, we therefore consider the following con-

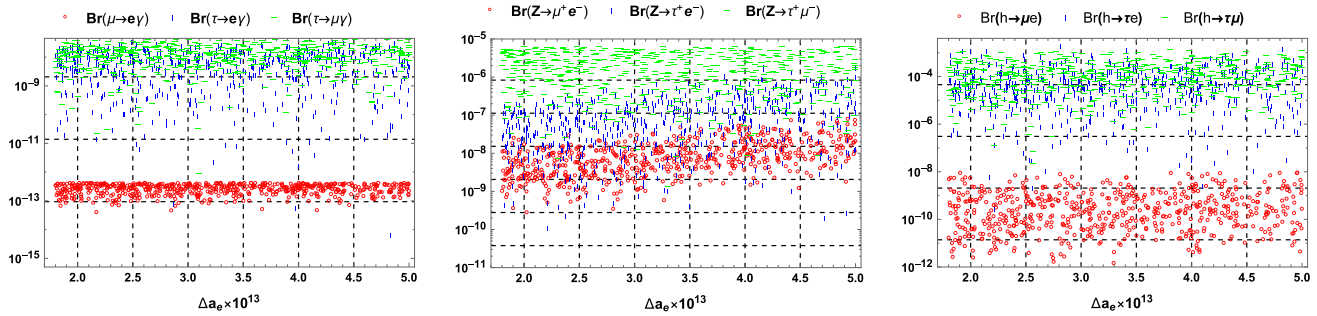

Fig. 11 The correlations between $\Delta a_{e,\mu}$ vs LFV decays in the limits given by Eq. (66)

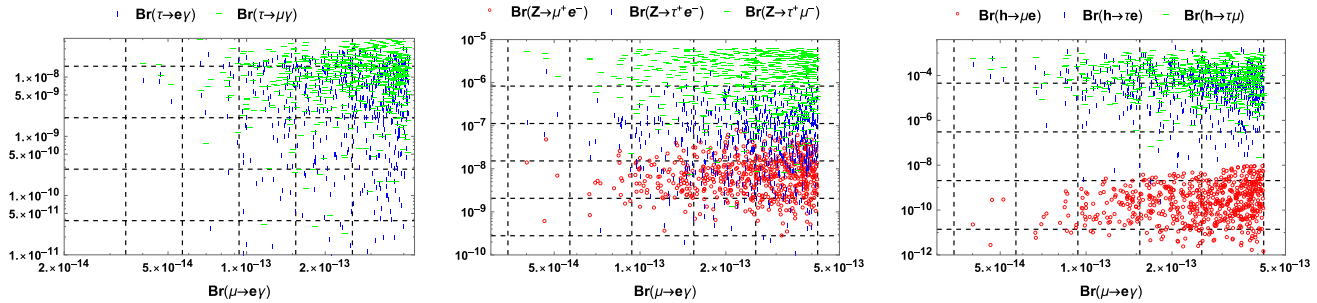

Fig. 12 The correlations between $\mathrm{Br}(\mu \to e\gamma)$ vs LFV decays in the limits given by Eq. (66)

straints:

$$y_{31} = 0,\ |y_{33}| < 1,\ |y_{13}|, |y_{23}|, |y_{32}| \leq 0.5. \tag{66}$$

The allowed ranges of y^d_{11}, y^d_{22} do not change significantly with the case 1. In contrast the upper bounds of the LFV decays enhance strongly, namely:

$$\begin{aligned}
\mathrm{Br}(\mu \to e\gamma) &\leq 4.2 \times 10^{-13},\\
\mathrm{Br}(\tau \to e\gamma) &\leq 3.3 \times 10^{-8},\\
\mathrm{Br}(\tau \to \mu\gamma) &\leq 4.4 \times 10^{-8},\\
\mathrm{Br}(Z \to \mu^+ e^-) &\leq 7.9 \times 10^{-8},\\
\mathrm{Br}(Z \to \tau^+ e^-) &\leq 1.9 \times 10^{-6},\\
\mathrm{Br}(Z \to \tau^+ \mu^-) &\leq 6.5 \times 10^{-6},\\
\mathrm{Br}(h \to \mu e) &\leq 9.1 \times 10^{-9},\\
\mathrm{Br}(h \to \tau e) &\leq 2 \times 10^{-3},\\
\mathrm{Br}(h \to \tau \mu) &\leq 1.4 \times 10^{-3}.
\end{aligned} \tag{67}$$

Therefore, five decays rates, including three cLFV decay $e_b \to e_a\gamma$, one $Z \to \tau^+\mu^-$, and two LFVh decays $h \to \tau\mu, \tau e$ have upper bounds coinciding with recent experimental constraints. Only $\mathrm{Br}(h \to \mu e)$ is much smaller than the near future experimental sensitivities. In contrast, $\mathrm{Br}(Z \to \mu^\pm e^\mp)$ can reach large values close to 10^{-7}, which are different from previous discussions.

The correlations between a_e with different LFV decays are shown in Fig. 11.

It shows that all allowed values of a_e support small LFV decays rates corresponding to the future sensitivities, hence the model will not be excluded if any of LFV decays are detected. All LFV decay rates depend weakly on a_μ, we therefore do not present here.

The dependence of the LFV decay rates vs $\mathrm{Br}(e_b \to e_a\gamma)$ are given in Fig. 12.

Although, $\mathrm{Br}(e_b \to e_a\gamma)$ is the most stringent from experiments, the future sensitivities of $\mathcal{O}(10^{-9})$ still support all other decays rates reaching the respective expected sensitivities, except $\mathrm{Br}(h \to \mu e)$, which is always invisible for future experimental searches.

There are significant dependence between $\mathrm{Br}(\tau \to e\gamma)$ and two decay rates $\mathrm{Br}(h \to e_b e_a)$ and $\mathrm{Br}(Z \to e_b^+ e_a^-)$, see illustrations in Fig. 13.

Here large $\mathrm{Br}(\tau \to e\gamma)$ predicts large $\mathrm{Br}(Z \to \tau^+ e^-)$ and $\mathrm{Br}(h \to \tau e)$. Therefore, if one of these decays are detected, there are some clues to predict the values of the two remaining ones.

4 Conclusions

We have explored the LFV decays in the allowed regions of the parameter space accommodating the $(g-2)_{\mu,e}$ in the 2HDM$N_{L,R}$ framework. We obtained some following interesting results that distinguish the 2HDM$N_{L,R}$ from other

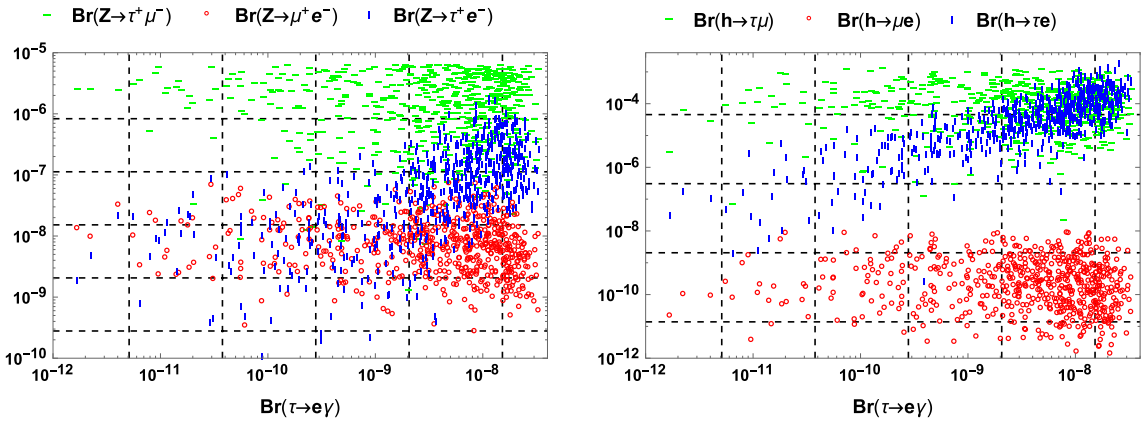

Fig. 13 The correlations between Br($\tau \to e\gamma$) vs LFV decays in the limits given by Eq. (66)

available BSM. Firstly, there exist allowed regions predicting the large values of Br($e_b \to e_a\gamma$), Br($h \to \tau\mu, \tau e$), and Br($Z \to \tau^{\pm}\mu^{\mp}, \tau^{\pm}e^{\mp}$) close to the recent experimental constraints. Furthermore, significant correlations among Br($\tau \to e\gamma$), Br($Z \to \tau^{\pm}e^{\mp}$), and Br($h \to \tau e$) were found, which will be interesting for testing the model if at least one of these decay channels is detected experimentally. Secondly, the 2HDM$N_{L,R}$ model predicts large max[Br($Z \to \mu^{\pm}e^{\mp}$)] $\simeq 7.9 \times 10^{-8}$, but suppressed Br($h \to \mu e$) $< 10^{-8}$ which is invisible for the near future experimental sensitivity. This is in contrast with the prediction from the 2HDM model discussed in Ref. [1], which predicts large LFVh but very small LFVZ decay rates. On the other hand, some BSM discussed in Ref. [23] for example, support large LFVZ but small LFVh decay rates. Therefore, if future experiments confirm the existence of any LFV signals, they will be used to determine the reality of many available models or constrain the model parameter space we have studied in this work.

Acknowledgements We are grateful Dr. Navin McGinnis for the interesting comments. This research is funded by Vietnam National University HoChiMinh City (VNU-HCM) under grant number "C2022-16-06".

Data Availability Statement This manuscript has no associated data or the data will not be deposited. [Authors' comment: All the related data has been mentioned in the manuscript.]

Code availability Code/software will be made available on reasonable request. [Author's comment: The code/software generated during and/or analysed during the current study is available from the corresponding author on reasonable request.]

Open Access This article is licensed under a Creative Commons Attribution 4.0 International License, which permits use, sharing, adaptation, distribution and reproduction in any medium or format, as long as you give appropriate credit to the original author(s) and the source, provide a link to the Creative Commons licence, and indicate if changes were made. The images or other third party material in this article are included in the article's Creative Commons licence, unless indicated otherwise in a credit line to the material. If material is not included in the article's Creative Commons licence and your intended use is not permitted by statutory regulation or exceeds the permitted use, you will need to obtain permission directly from the copyright holder. To view a copy of this licence, visit http://creativecommons.org/licenses/by/4.0/.
Funded by SCOAP[3].

Appendix A: PV functions for one loop contributions defined by LoopTools

A.1 General notations

The PV-functions used here were listed in Ref. [91], namely

$$A_0(m) = \frac{(2\pi\mu)^{4-d}}{i\pi^2}\int \frac{d^dk}{k^2-m^2+i\delta},$$
$$B_{\{0,\mu,\mu\nu\}}(p_i^2, M_0^2, M_i^2) = \frac{(2\pi\mu)^{4-d}}{i\pi^2}\int \frac{d^dk \times \{1, k_\mu, k_\mu k_\nu\}}{D_0 D_i},$$
$$i = 1, 2,$$
$$C_{0,\mu,\mu\nu} = \frac{(2\pi\mu)^{4-d}}{i\pi^2}\int \frac{d^dk\{1, k_\mu, k_\mu k_\nu\}}{D_0 D_1 D_2}, \tag{A1}$$

where $D_0 \equiv k^2 - M_0^2 + i\delta$, $D_1 \equiv (k-p_1)^2 - M_1^2 + i\delta$, $D_2 \equiv (k+p_2)^2 - M_2^2 + i\delta$, $C_{0,\mu,\mu\nu} = C_{0,\mu,\mu\nu}(p_1^2, (p_1+p_2)^2, p_2^2; M_0^2, M_1^2, M_2^2)$, δ is an real positive quantity, and μ is an arbitrary mass parameter introduced via dimensional regularization [99]. The scalar PV-functions are defined as follows:

$$B_\mu(p_1^2, M_0^2, m_a^2) = (-p_{1\mu})B_1(p_1^2, M_0^2, M_1^2) \equiv (-p_{1\mu})B_1^{(1)},$$
$$B_\mu(p_2^2, M_0^2, M_2^2) = p_{2\mu}B_1(p_2^2, M_0^2, M_2^2) \equiv p_{2\mu}B_1^{(2)},$$
$$B_{\mu\nu}(q_i^2, M_0^2, M_i^2) = B_{00}(q_i^2, M_0^2, M_i^2)g_{\mu\nu} + B_{11}(q_i^2, M_0^2, M_i^2)p_{i\mu}p_{i\nu} \equiv B_{00}^{(i)}g_{\mu\nu} + B_{11}^{(i)}p_{i\mu}p_{i\nu},$$
$$C_\mu = (-p_{1\mu})C_1 + p_{2\mu}C_2,$$
$$C_{\mu\nu} = g_{\mu\nu}C_{00} + p_{1\mu}p_{1\nu}C_{11} + p_{2\mu}p_{2\nu}C_{22}$$

$$+ (p_{1\mu}p_{2\nu} + p_{2\mu}p_{1\nu})C_{12}. \tag{A2}$$

The external momentum $q^2 = (p_2 + p_1)^2 = m_Z^2$ and m_h^2 for the LFVZ and LFVh processes, respectively. As a result, the scalar functions A_0, B_0, C_0, C_{00}, C_i, C_{ij} $(k, l = 1, 2)$ are well-known PV functions consistent with those in LoopTools [100]. Useful well-known relations used in this work are:

$$\begin{aligned}
&A_0(m)p_\mu = \frac{(2\pi\mu)^{4-d}}{i\pi^2}\int \frac{d^dk k_\mu}{(k+p)^2 - m^2 + i\delta},\\
&B_0^{(i)} \equiv B_0(p_i^2; M_0^2, M_i^2) = B_0(p_i^2; M_i^2, M_0^2),\\
&B_1^{(i)} \equiv B_1(p_i^2; M_0^2, M_i^2)\\
&\quad = -\frac{1}{2p_i^2}\left[A_0(M_i^2) - A_0(M_0^2) + f_i B_0^{(i)}\right],\\
&B_0^{(12)} = \frac{(2\pi\mu)^{4-d}}{i\pi^2}\int \frac{d^dk}{D_0' D_1'} = B_0(q^2; M_1^2, M_2^2),\\
&B_\mu^{(12)} \equiv B_\mu(q^2; M_1^2, M_2^2) = \frac{(2\pi\mu)^{4-d}}{i\pi^2}\\
&\quad \int \frac{d^dk \times (k+p_1)_\mu}{D_0' D_1'}\\
&\quad \equiv B_1^{(12)} q_\mu + B_0^{(12)} p_{1\mu},
\end{aligned} \tag{A3}$$

where $f_i = p_i^2 + M_i^2 - M_0^2, q = p_1 + p_2, D_0' \equiv k^2 - M_1^2 + i\delta$, $D_1' = (k+q)^2 - M_2^2 + i\delta$, and $B_{0,1}^{(12)} \equiv B_{0,1}(q^2; M_1^2, M_2^2)$. The scalar functions A_0, B_0, C_0 can be calculated using the techniques given in Ref. [78]. For simplicity, we define new notations appearing in many important formulas:

$$\begin{aligned}
&X_0 \equiv C_0 + C_1 + C_2,\\
&X_1 \equiv C_{11} + C_{21} + C_1\\
&X_2 \equiv C_{12} + C_{22} + C_2,\\
&X_3 \equiv C_1 + C_2 = X_0 - C_0,\\
&X_{012} \equiv X_0 + X_1 + X_2,\ X_{ij} = X_i + X_j.
\end{aligned} \tag{A4}$$

For the decays $h \to e_b^\pm e_a^\mp$ and $Z \to e_b^+ e_a^-$, we can derive all formulas of C_i, and C_{ij} as functions of A_0, $B_0^{(i)}$, and C_0 consistent with Ref. [91], using the following relations:

$$\begin{aligned}
&2m_a^2 C_1 + (m_a^2 + m_b^2 - q^2)C_2 = -f_1 C_0 - B_0^{(12)} + B_0^{(2)},\\
&(m_a^2 + m_b^2 - q^2)C_1 + 2m_b^2 C_2 = -f_2 C_0 - B_0^{(12)} + B_0^{(1)},\\
&2C_{00} + 2m_a^2 C_{11} + (m_a^2 + m_b^2 - q^2)C_{12} = B_1^{(12)} + B_0^{(12)} - f_1 C_1,\\
&2m_a^2 C_{12} + (m_a^2 + m_b^2 - q^2)C_{22}\\
&= -B_1^{(12)} + B_1^{(2)} - f_1 C_2\\
&2C_{00} + (m_a^2 + m_b^2 - q^2)C_{12} + 2m_b^2 C_{22}\\
&= B_1^{(12)} - f_2 C_2,\\
&(m_a^2 + m_b^2 - q^2)C_{11} + 2m_b^2 C_{12}\\
&= B_0^{(12)} + B_1^{(12)} + B_1^{(1)} - f_2 C_1,\\
&4C_{00} - \frac{1}{2} + m_a^2 C_{11} + (m_a^2 + m_b^2 - q^2)C_{12} + m_b^2 C_{22}\\
&= B_0^{(12)} + M_0^2 C_0,
\end{aligned} \tag{A5}$$

where $f_i = M_i^2 - M_0^2 + m_i^2$, $q^2 = m_Z^2, m_h^2$, and $C_{12} = C_{21}$ is used.

Appendix B: One-loop contributions to $Z \to e_b^+ e_a^-$

B.1 Calculation for V^μ exchanges in the unitary gauge

Before going to the details of the calculation. We list here important well-known results such as the on-shell conditions gives $p_1^2 = m_a^2$, $p_2^2 = m_b^2$, and $q^2 = m_Z^2$, where m_a, m_b, and m_Z are the masses of leptons a, b $(a, b = 1, 2, 3)$, and gauge boson Z. The momentum conservation gives $q = p_1 + p_2$. Two internal momenta $k_1 \equiv k - p_1$ and $k_2 \equiv k + p_2$ with $i = 1, 2$ are denoted in Fig. 1.

When solving the Dirac matrices in the general dimension d, we will use the following identities [101]:

$$\begin{aligned}
&\gamma^\mu\gamma_\mu = d,\ \gamma^\mu\gamma^\nu\gamma_\mu = (2-d)\gamma^\nu \to \gamma^\mu \not{p}\gamma^\mu = (2-d)\not{p},\\
&\gamma^\mu\gamma^\nu\gamma^\rho\gamma_\mu = 4g^{\nu\rho} + (d-4)\gamma^\nu\gamma^\rho \to \gamma^\mu \not{p}_1\not{p}_2\gamma^\mu\\
&\quad = 4p_1.p_2 + (d-4)\not{p}_1\not{p}_2,\\
&\gamma^\mu\gamma^\nu\gamma^\rho\gamma^\sigma\gamma_\mu = -2\gamma^\sigma\gamma^\rho\gamma^\nu - (d-4)\gamma^\nu\gamma^\rho\gamma^\sigma\\
&\quad \to \gamma^\mu \not{p}_1\not{p}_2\not{p}_3\gamma_\mu = -2\not{p}_3\not{p}_2\not{p}_1 - (d-4)\not{p}_1\not{p}_2\not{p}_3.
\end{aligned}$$

Then we take $d = 4$ for all finite integrals. For all divergent integrals, after changing into the expressions in terms of the PV-functions, we take $d = 4 - 2\epsilon$, then determining the final finite results before fixing $\epsilon = 0$. In addition, we will use the following transformation to change from integral to the notations of the PV-functions:

$$\begin{aligned}
&\int \frac{d^4k}{(2\pi)^4} \to \frac{i}{16\pi^2} \times \frac{(2\pi\mu)^{4-d}}{i\pi^2}\int d^dk = \frac{i}{16\pi^2}\\
&\times (\text{PV-functions})\,.
\end{aligned}$$

In practice, the overall factor $i/(16\pi^2)$ will be added in the final results.

The diagram (1) in Fig. 1 corresponding to the following amplitude:

$$\begin{aligned}
i\mathcal{M}_1^{(U)} &= i\mathcal{M}_{nWW}^{(U)}\\
&= \int \frac{d^4k}{(2\pi)^4}\overline{u_a}\left[\frac{ie}{\sqrt{2}s_W}U_{ai}^{\nu}\gamma^{\beta'}P_L\right]\frac{i\left(m_{n_i} + \not{k}\right)}{D_0}\\
&\times \left[\frac{ie}{\sqrt{2}s_W}U_{bi}^{\nu*}\gamma^{\alpha'}P_L\right]v_b \times \frac{-i}{D_1}\left(g_{\beta\beta'} - \frac{k_{1\beta}k_{1\beta'}}{m_W^2}\right)\\
&\times \left[-ig_{ZWW}\Gamma^{\mu\beta\alpha}(q, k_1, -k_2)\varepsilon_\mu\right]\frac{-i}{D_2}\left(g_{\alpha\alpha'} - \frac{k_{2\alpha}k_{2\alpha'}}{m_W^2}\right)
\end{aligned}$$

$$= \frac{e^3 U^v_{ai} U^{v*}_{bi}}{2 s^2_W t_R} \int \frac{d^4k}{(2\pi)^4} \times \frac{\overline{u_a}\left[\gamma^{\beta'} \not{k} \gamma^{\alpha'} P_L\right] v_b}{D_0 D_1 D_2} \times \left(g_{\beta\beta'} - \frac{k_{1\beta} k_{1\beta'}}{m^2_W}\right)\left(g_{\alpha\alpha'} - \frac{k_{2\alpha} k_{2\alpha'}}{m^2_W}\right) \times \left[\varepsilon^\beta (q-k_1)^\alpha + g^{\beta\alpha}\varepsilon (k_1+k_2) + \varepsilon^\alpha (-k_2-q)^\beta\right] = \frac{e^3 U^v_{ai} U^{v*}_{bi}}{2 s^2_W t_R} [I_1 + I_2 + I_3]. \quad \text{(B1)}$$

For simplicity, we omit the sum over all neutrino masses m_{n_i} for $i = 1, \ldots, K+3$. The final results must taken into account this sum for all diagrams, in order to simplify many intermediate steps of calculation. The first integral I_1 contains only the highest order of variable $k_\mu k_\nu$ in the integrand, hence it is easily to write in terms of PV-function given in Appendix A, namely

$$\begin{aligned}
I_1 &= \int \frac{d^4k}{(2\pi)^4} \frac{\overline{u_a}\left\{\gamma^{\beta'} \not{k} \gamma^{\alpha'} P_L \times g_{\beta\beta'} g_{\alpha\alpha'}\right\} P_L v_b}{D_0 D_1 D_2} \\
&\quad \times \left[\varepsilon^\beta (q-k_1)^\alpha + g^{\beta\alpha}\varepsilon (k_1+k_2) + \varepsilon^\alpha (-k_2-q)^\beta\right] \\
&= \int \frac{d^4k}{(2\pi)^4} \times \frac{\overline{u_a}}{D_0 D_1 D_2} \left\{\not{\varepsilon}\not{k}(2\not{p}_1 + \not{p}_2) - \left(D_0 + m^2_{n_i}\right) \not{\varepsilon} \right. \\
&\quad + (4-2d)\varepsilon.k \not{k} - (4-2d) p_1.\varepsilon \not{k} \\
&\quad \left. - \left(D_0 + m^2_{n_i} + \not{p}_1\not{k} + 2\not{p}_2\not{k}\right)\not{\varepsilon} \right\} P_L v_b \\
&= \overline{u_a}\left\{\left[-2m^2_{n_i} C_0 + (4-2d) C_{00} - m^2_a C_1 - m^2_b C_2 \right.\right. \\
&\quad \left.\left. + 2\left(m^2_Z - m^2_a - m^2_b\right)(C_1 + C_2)\right]\not{\varepsilon} \right. \\
&\quad - 4(p_1.\varepsilon) C_2 \not{p}_2 + 2\not{p}_1\not{\varepsilon}\not{p}_2 C_2 \\
&\quad - 2(p_1.\varepsilon) C_1 \not{p}_2 + 2(p_1.\varepsilon) C_2 \not{p}_1 + (C_1 + C_2)\not{p}_1\not{\varepsilon}\not{p}_2 \\
&\quad - 4(p_1.\varepsilon) C_1 \not{p}_2 + 2\not{p}_1\not{\varepsilon}\not{p}_2 C_1 \\
&\quad \left. + (4-2d)(p_1.\varepsilon)\left[X_1 \not{p}_1 - X_2 \not{p}_2\right] \right\} P_L v_b \\
&= \overline{u_a}\left\{\left[-2m^2_{n_i} C_0 - 4C_{00} - m^2_a C_1 - m^2_b C_2 \right.\right. \\
&\quad \left.\left. + 2\left(m^2_Z - m^2_a - m^2_b\right)(C_1 + C_2)\right]\not{\varepsilon} \right. \\
&\quad \left. + m_a (p_1.\varepsilon)\left[4C_1 + 2C_2 - 4X_1\right] \right\} P_L v_b \\
&\quad + m_b \times \overline{u_a}\left\{ - 3m_a (C_1 + C_2)\not{\varepsilon} + (p_1.\varepsilon) \right. \\
&\quad \left. \times \left[4C_2 + 2C_1 - 4X_2\right] \right\} P_R v_b. \quad \text{(B2)}
\end{aligned}$$

In the above calculation, all terms proportional to $\frac{1}{D_1 D_2}$ without any factors m_{n_i} will vanish after taking the sum $\sum_{i=1}^{K+3} U^v_{ai} U^{v*}_{bi} = \delta_{ab} = 0$. In addition, all PV-functions $C_{0,k,kl}$ with $k, l = 1, 2$ are finite, hence we will take $d = 4$ for the relevant factors. Finally, all divergent parts of the PV-functions C_{00} and $B^{(k)}_{0,1}$ are independent to m_{n_i}, therefore vanish after the summation. We also apply $d = 4$. These comments will be applied to our calculation from now on. The second integral I_2 contains dangerous terms like $\not{k}_2\not{k}\not{k}_2$ in the integrand, resulting in the PV functions originated from higher tensor ranks such as $C_{\mu\nu\alpha}, \ldots$, which were not defined in appendix A, namely

$$\begin{aligned}
I_2 &= -\frac{1}{m^2_W} \int \frac{d^4k}{(2\pi)^4} \\
&\quad \times \frac{\overline{u_a}}{D_0 D_1 D_2} \left\{\not{\varepsilon}\not{k}\not{k}_2 [k_2.(q-k_1)] + \not{k}_2\not{k}\not{k}_2 [\varepsilon.(k_1+k_2)] \right. \\
&\quad - (\not{k}_2 + \not{q})\not{k}\not{k}_2 (\varepsilon k_2) \\
&\quad + \not{k}_1\not{k}(\not{q} - \not{k}_1)(\varepsilon k_1) + \not{k}_1\not{k}\not{k}_1 [\varepsilon (k_1+k_2)] \\
&\quad \left. - \not{k}_1\not{k}\not{\varepsilon}[k_1 (k_2+q)] \right\} P_L v_b \\
&= -\frac{1}{m^2_W} \int \frac{d^4k}{(2\pi)^4} \times \frac{\overline{u_a}}{D_0 D_1 D_2} \times \left\{\not{\varepsilon}\left(k^2 + \not{k}\not{p}_2\right)\right. \\
&\quad \times \left(2k.p_1 + p^2_2 - k^2 + 2p_1.p_2\right) \\
&\quad + \left(k^2 + \not{p}_2\not{k}\right)(\not{k} + \not{p}_2)\,\varepsilon.(2k - 2p_1) \\
&\quad - \left(k^2 + \not{p}_1\not{k} + 2\not{p}_2\not{k}\right)(\not{k} + \not{p}_2)\,\varepsilon\,(k + p_2) \\
&\quad + \left(k^2 - \not{p}_1\not{k}\right)(-\not{k} + 2\not{p}_1 + \not{p}_2)\,\varepsilon\,(k - p_1) \\
&\quad + \left(k^2 - \not{p}_1\not{k}\right)(\not{k} - \not{p}_1)\,\varepsilon\,(2k - 2p_1) \\
&\quad \left. - \left(k^2 - \not{p}_1\not{k}\right)\not{\varepsilon}\left(k^2 + 2kp_2 - 2p_1 p_2 - p^2_1\right)\right\} P_L v_b.
\end{aligned}$$

Using the property of the polarization of external gauge boson Z gives $q.\varepsilon = 0 \Longleftrightarrow \varepsilon.k_1 = \varepsilon.k_2 \Longleftrightarrow \varepsilon.(k - p_1) = \varepsilon(k + p_2)$, we can show that all terms with higher orders of k^2 in the numerators will vanish. Namely,

$$\begin{aligned}
I_2 &= -\frac{1}{m^2_W} \int \frac{d^4k}{(2\pi)^4} \times \frac{\overline{u_a}}{D_0 D_1 D_2} \left\{\not{\varepsilon}\left(D_0 + m^2_{n_i} + \not{k}\not{p}_2\right)\right. \\
&\quad \times \left(-D_1 - m^2_W + m^2_Z\right) \\
&\quad - \left(D_0 + m^2_{n_i} - \not{p}_1\not{k}\right)\not{\varepsilon}\left(D_2 + m^2_W - m^2_Z\right) \\
&\quad + \left[2D_0\not{k} + 2m^2_{n_i}\not{k} + 2D_0\not{p}_2 + 2m^2_{n_i}\not{p}_2 \right. \\
&\quad + 2D_0\not{p}_2 + 2m^2_{n_i}\not{p}_2 + 2\not{p}_2\not{k}\not{p}_2 - D_0\not{k} \\
&\quad - m^2_{n_i}\not{k} - D_0\not{p}_1 - m^2_{n_i}\not{p}_1 - 2D_0\not{p}_2 - 2m^2_{n_i}\not{p}_2 \\
&\quad - D_0\not{p}_2 - m^2_{n_i}\not{p}_2 - \not{p}_1\not{k}\not{p}_2 - 2\not{p}_2\not{k}\not{p}_2 - D_0\not{k} \\
&\quad - m^2_{n_i}\not{k} + 2D_0\not{p}_1 + 2m^2_{n_i}\not{p}_1 + D_0\not{p}_2 \\
&\quad + m^2_{n_i}\not{p}_2 + D_0\not{p}_1 + m^2_{n_i}\not{p}_1 - 2\not{p}_1\not{k}\not{p}_1 - \not{p}_1\not{k}\not{p}_2 \\
&\quad + 2D_0\not{k} + 2m^2_{n_i}\not{k} - 2D_0\not{p}_1 - 2m^2_{n_i}\not{p}_1 \\
&\quad \left. \left. - 2D_0\not{p}_1 - 2m^2_{n_i}\not{p}_1 + 2\not{p}_1\not{k}\not{p}_1\right](\varepsilon k - p_1.\varepsilon)\right\} P_L v_b \\
&= -\frac{1}{m^2_W}\overline{u_a}\left\{\not{\varepsilon}\left[-m^2_{n_i}\left(B^{(1)}_0 + B^{(2)}_0\right) - m^2_a B^{(1)}_1 \right.\right. \\
&\quad \left.\left. + 2m^2_{n_i}\left(-m^2_W + m^2_Z\right) C_0 - m^2_b B^{(2)}_1\right]\right.
\end{aligned}$$

$$
\begin{aligned}
&+\left(-m_W^2+m_Z^2\right)\left(-C_1\not{\varepsilon}\not{p}_1\not{p}_2+m_b^2C_2\not{\varepsilon}\right.\\
&\left.+m_a^2C_1\not{\varepsilon}-C_2\not{p}_1\not{p}_2\not{\varepsilon}\right)\\
&-2\left[m_{n_i}^2(-C_1\not{p}_1+C_2\not{p}_2)+m_{n_i}^2C_0\not{p}_2-m_{n_i}^2C_0\not{p}_1\right.\\
&\left.+m_a^2C_1\not{p}_2-m_b^2C_2\not{p}_1\right](p_1.\varepsilon)\\
&+2\left[\frac{m_{n_i}^2\gamma^\mu k_\mu k_\nu}{D_0D_1D_2}+\frac{m_{n_i}^2\not{p}_2k_\nu}{D_0D_1D_2}-\frac{m_{n_i}^2\not{p}_1k_\nu}{D_0D_1D_2}\right.\\
&\left.-\frac{\not{p}_1\gamma^\mu\not{p}_2k_\mu k_\nu}{D_0D_1D_2}\right]\varepsilon_\nu\Big\}P_Lv_b\\
=&-\frac{1}{m_W^2}\overline{u_a}\left\{\not{\varepsilon}\left[\left(m_Z^2-m_W^2\right)\left(2m_{n_i}^2C_0+m_a^2C_1+m_b^2C_2\right)\right.\right.\\
&\left.-m_{n_i}^2\left(B_0^{(1)}+B_0^{(2)}\right)-m_a^2B_1^{(1)}-m_b^2B_1^{(2)}+2m_{n_i}^2C_{00}\right]\\
&+2m_a(p_1.\varepsilon)\left[\left(m_Z^2-m_W^2+m_{n_i}^2+m_b^2\right)C_2\right.\\
&+m_{n_i}^2(C_0+2C_1+C_{11})\\
&\left.+m_b^2C_{22}+(m_{n_i}^2+m_b^2)C_{12}\right]\Big\}P_Lv_b\\
&-\frac{m_b}{m_W^2}\overline{u_a}\left\{\not{\varepsilon}m_a\left[2C_{00}-(m_Z^2-m_W^2)(C_1+C_2)\right]\right.\\
&+2(p_1.\varepsilon)\left[(m_Z^2-m_W^2+m_{n_i}^2+m_a^2)C_1\right.\\
&+m_{n_i}^2(C_0+2C_2+C_{22})+m_a^2C_{11}\\
&\left.\left.+(m_{n_i}^2+m_a^2)C_{12}\right]\right\}P_Rv_b. \qquad \text{(B3)}
\end{aligned}
$$

We can see that the higher tensor ranks of PV-functions vanish because the relevant terms in numerators were changed into the factor D_0, resulting in many terms of the form $1/(D_1D_2)$ independent to neutrinos masses m_{n_i}. They are proportional to the sum $\sum_{i=1}^{K+3}U_{ai}^vU_{bi}^{v*}=0$ with $a\neq b$.

Using above tricks to calculate I_3, we have

$$
\begin{aligned}
I_3=&\frac{1}{m_W^4}\int\frac{d^4k}{(2\pi)^4}\frac{\overline{u_a}}{D_0D_1D_2}\\
&\times\not{k}_1\not{k}\not{k}_2\Big\{k_1.\varepsilon\left[k_2.(q-k_1)\right]+(k_1.k_2)(k_1+k_2).\varepsilon\\
&-k_2.\varepsilon\left[k_1.(k_2+q)\right]\Big\}P_Lv_b\\
=&\frac{1}{m_W^4}\int\frac{d^4k}{(2\pi)^4}\times\frac{\overline{u_a}}{D_0D_1D_2}\left(k^2-\not{p}_1\not{k}\right)(\not{k}+\not{p}_2)\\
&\times\Big\{\varepsilon.k_1\,(k+p_2).(-k+2p_1+p_2)\;+2\,(k_1.k_2)\,\varepsilon.k_1\\
&-\varepsilon.k_2\,(k_1.(k+p_1+2p_2))\Big\}P_Lv_b\\
=&\frac{1}{m_W^4}\int\frac{d^4k}{(2\pi)^4}\times\frac{\overline{u_a}}{D_0D_1D_2}\left(D_0\not{k}+m_{n_i}^2\not{k}-D_0\not{p}_1-m_{n_i}^2\not{p}_1\right.\\
&\left.+D_0\not{p}_2+m_{n_i}^2\not{p}_2-\not{p}_1\not{k}\not{p}_2\right)\\
&\times(\varepsilon.k_1)\left[-k.k_2+2k_2.p_1-k.k_1-2k.p_2+k_1.p_1\right.\\
&\left.+2k_1.k_2\right]P_Lv_b\\
=&\frac{1}{m_W^4}\int\frac{d^4k}{(2\pi)^4}\times\overline{u_a}\left(\frac{m_{n_i}^2\not{k}}{D_0D_1D_2}-\frac{m_{n_i}^2\not{p}_1}{D_0D_1D_2}\right.\\
&\left.+\frac{m_{n_i}^2\not{p}_2}{D_0D_1D_2}-\frac{\not{p}_1\not{k}\not{p}_2}{D_0D_1D_2}\right)\\
&\times\left[\varepsilon.(k-p_1)\right]\left[k_2.(q-k_1)-k_1.(q+k_2)+2k_1.k_2\right]\\
&P_Lv_b. \qquad \text{(B4)}
\end{aligned}
$$

Note that: $k_2\,(q-k_1)-k_1\,(q+k_2)+2k_1k_2=(k_2-k_1)\,.q=(p_2+p_1)\,q=p_0^2=m_Z^2$. Therefore

$$
\begin{aligned}
I_3=&\frac{m_Z^2}{m_W^4}\int\frac{d^4k}{(2\pi)^4}\\
&\times\overline{u_a}\left\{\left[\frac{m_{n_i}^2\gamma^\mu\varepsilon^\nu k_\mu k_\nu}{D_0D_1D_2}+\frac{m_{n_i}^2\varepsilon^\mu k_\mu}{D_0D_1D_2}(-\not{p}_1+\not{p}_2)\right.\right.\\
&\left.-\frac{2p_2^\mu\varepsilon^\nu k_\mu k_\nu}{D_0D_1D_2}\not{p}_1+\not{p}_1\not{p}_2\frac{\gamma^\mu\varepsilon^\nu k_\mu k_\nu}{D_0D_1D_2}\right]\\
&-(p_1.\varepsilon)\left[m_{n_i}^2\,(-C_1\not{p}_1+C_2\not{p}_2)+m_{n_i}^2C_0\,(-\not{p}_1+\not{p}_2)\right.\\
&\left.\left.+m_a^2C_1\not{p}_2-m_b^2C_2\not{p}_1\right]\right\}P_Lv_b\\
=&\frac{m_Z^2}{m_W^4}\times\overline{u_a}\left\{m_{n_i}^2C_{00}\not{\varepsilon}+m_a(p_1.\varepsilon)\left[m_{n_i}^2X_{01}+m_b^2X_2\right]\right\}P_Lv_b\\
&+\frac{m_Z^2m_b}{m_W^4}\times\overline{u_a}\left\{m_aC_{00}\not{\varepsilon}+(p_1.\varepsilon)\left[m_{n_i}^2X_{02}+m_a^2X_1\right]\right\}P_Rv_b.
\end{aligned}
\qquad \text{(B5)}
$$

The final result of $\mathcal{M}_1^{(U)}$ is derived in terms of the PV-functions as follows:

$$
\begin{aligned}
i\mathcal{M}_1^{(U)}=&\frac{e^3U_{ai}^vU_{bi}^{v*}}{2s_W^2t_R}\\
&\times\overline{u_a}\Big\{\left[-2m_{n_i}^2C_0-4C_{00}-m_a^2C_1-m_b^2C_2\right.\\
&\left.+2\left(m_Z^2-m_a^2-m_b^2\right)X_3\right]\not{\varepsilon}\\
&+m_a(p_1.\varepsilon)\left[4C_1+2C_2-4X_1\right]\Big\}P_Lv_b+\overline{u_a}\times m_b\\
&\left\{-3m_aX_3\not{\varepsilon}+(p_1.\varepsilon)\left[4C_2+2C_1-4X_2\right]\right\}P_Rv_b\\
&-\frac{1}{m_W^2}\overline{u_a}\left\{\not{\varepsilon}\left[\left(m_Z^2-m_W^2\right)\left(2m_{n_i}^2C_0+m_a^2C_1+m_b^2C_2\right)\right.\right.\\
&\left.-m_{n_i}^2\left(B_0^{(1)}+B_0^{(2)}\right)-m_a^2B_1^{(1)}-m_b^2B_1^{(2)}+2m_{n_i}^2C_{00}\right]\\
&\left.+2m_a(p_1.\varepsilon)\left[\left(m_Z^2-m_W^2\right)C_2+m_{n_i}^2X_{01}+m_b^2X_2\right]\right\}P_Lv_b\\
&-\frac{m_b}{m_W^2}\overline{u_a}\left\{\not{\varepsilon}m_a\left[2C_{00}-(m_Z^2-m_W^2)X_3\right]\right.\\
&\left.+2(p_1.\varepsilon)\left[(m_Z^2-m_W^2)C_1+m_{n_i}^2X_{02}+m_a^2X_1\right]\right\}P_Rv_b\\
&+\frac{m_Z^2}{m_W^4}\overline{u_a}\left\{\not{\varepsilon}m_{n_i}^2C_{00}+m_a(p_1.\varepsilon)\left[m_{n_i}^2X_{01}+m_b^2X_2\right]\right\}P_Lv_b
\end{aligned}
$$

$$+\frac{m_Z^2 m_b}{m_W^4}\overline{u_a}\left\{m_a C_{00}\not{\varepsilon}+(p_1.\varepsilon)\left[m_{n_i}^2 X_{02}+m_a^2 X_1\right]\right\}P_R v_b. \tag{B6}$$

Equation (B6) results in the form factors given in Eqs. (17), (18), (19), and (20).

The amplitude originated from diagram (2) in Fig. 1 is

$$\begin{aligned}
i\mathcal{M}_2^{(U)} &= \int \frac{d^4k}{(2\pi)^4}\times\overline{u_a}\times\left[\frac{ie}{\sqrt{2}s_W}U_{ai}^{v}\gamma^{\alpha}P_L\right]\\
&\times\frac{i\left(-\not{k}_1+m_{n_i}\right)}{D_1}\left[\frac{ie}{2s_W c_W}\not{\varepsilon}\left(q_{ij}P_L-q_{ji}P_R\right)\right]\\
&\times\frac{i\left(-\not{k}_2+m_{n_j}\right)}{D_2}\times\left[\frac{ie}{\sqrt{2}s_W}U_{bj}^{v*}\gamma^{\beta}P_L\right]\times v_b\\
&\times\frac{-i}{D_0}\left(g_{\alpha\beta}-\frac{k_\alpha k_\beta}{m_W^2}\right)\\
&=\frac{e^3U_{ai}^{v}U_{bj}^{v*}}{4s_W^3c_W}\int\frac{d^4k}{(2\pi)^4}\frac{\overline{u_a}}{D_0D_1D_2}\left\{q_{ij}\gamma^{\alpha}\not{k}_1\not{\varepsilon}\not{k}_2\gamma^{\beta}\right.\\
&\left.-q_{ji}m_{n_i}m_{n_j}\gamma^{\alpha}\not{\varepsilon}\gamma^{\beta}\right\}\left(g_{\alpha\beta}-\frac{k_\alpha k_\beta}{m_W^2}\right)P_L v_b\\
&=\frac{e^3U_{ai}^{v}U_{bj}^{v*}}{4m_W^2s_W^3c_W}\int\frac{d^4k}{(2\pi)^4}\times\frac{\overline{u_a}}{D_0D_1D_2}\\
&\times\left\{q_{ij}\left[(-2\not{k}_2\not{\varepsilon}\not{k}_1+(4-d)\not{k}_1\not{\varepsilon}\not{k}_2)\,m_W^2-\not{k}\not{k}_1\not{\varepsilon}\not{k}_2\not{k}\right]\right.\\
&\left.-q_{ji}m_{n_i}m_{n_j}\left[(2-d)\not{\varepsilon}m_W^2-\not{k}\not{\varepsilon}\not{k}\right]\right\}P_L v_b\\
&=\frac{e^3U_{ai}^{v}U_{bj}^{v*}}{4m_W^2s_W^3c_W}\int\frac{d^4k}{(2\pi)^4}\times\overline{u_a}\\
&\times\left\{q_{ij}\left[m_W^2\left(\frac{-2\gamma^{\mu}\not{\varepsilon}\gamma^{\nu}k_\mu k_\nu}{D_0D_1D_2}\right.\right.\right.\\
&-2C_1\not{p}_1\not{\varepsilon}\not{p}_1+2C_2\not{p}_2\not{\varepsilon}\not{p}_1\\
&+\;2C_1\not{p}_2\not{\varepsilon}\not{p}_1-2C_2\not{p}_2\not{\varepsilon}\not{p}_2\\
&+2C_0\Big(2p_1.\varepsilon(-\not{p}_1+\not{p}_2)\\
&\left.-\left(m_Z^2-m_a^2-m_b^2\right)\not{\varepsilon}-\not{p}_1\not{\varepsilon}\not{p}_2\right)\\
&+\;(4-d)\Big(\frac{\gamma^{\mu}\not{\varepsilon}\gamma^{\nu}k_\mu k_\nu}{D_0D_1D_2}-C_1\not{p}_1\not{\varepsilon}\not{p}_2+C_2\not{p}_2\not{\varepsilon}\not{p}_2\\
&+C_1\not{p}_1\not{\varepsilon}\not{p}_1-C_2\not{p}_1\not{\varepsilon}\not{p}_2-C_0\not{p}_1\not{\varepsilon}\not{p}_2\Big)\Big)\\
&\left.-\frac{\left(k^2-\not{k}\not{p}_1\right)\not{\varepsilon}\left(k^2+\not{p}_2\not{k}\right)}{D_0D_1D_2}\right]+q_{ji}m_{n_i}m_{n_j}\\
&\left[2C_0m_W^2\not{\varepsilon}+\gamma^{\mu}\not{\varepsilon}\gamma^{\nu}\Big(C_{00}g_{\mu\nu}+C_{11}p_{1\mu}p_{1\nu}\right.\\
&\left.\left.+\;C_{22}p_{2\mu}p_{2\nu}-C_{12}\left(p_{1\mu}p_{2\nu}+p_{1\nu}p_{2\mu}\right)\Big)\right]\right\}P_L v_b.
\end{aligned}\tag{B7}$$

Using a relation that

$$\left(k^2-\not{k}\not{p}_1\right)\not{\varepsilon}\left(k^2+\not{p}_2\not{k}\right)=\left(D_1+m_{n_i}^2-m_a^2+\not{p}_1\not{k}\right)\not{\varepsilon}\times\left(D_2+m_{n_j}^2-m_b^2-\not{k}\not{p}_2\right)$$

we will derive $\mathcal{M}_2^{(U)}$ in terms of PV-functions defined in Appendix A as follows

$$\begin{aligned}
i\mathcal{M}_2^{(U)} &= \frac{e^3U_{ai}^{v}U_{bj}^{v*}}{4m_W^2s_W^3c_W}\\
&\times\overline{u_a}\left\{q_{ij}\left[m_W^2\left((2-d)^2C_{00}+2m_a^2X_{01}\right.\right.\right.\\
&+2m_b^2X_{02}+2m_Z^2(C_{12}-X_0)\Big)\not{\varepsilon}\\
&-(2p_1.\varepsilon)m_a\left(m_W^2\left(4X_1+2C_0+2C_2\right)\right.\\
&\left.-m_{n_j}^2C_2+m_b^2X_2\right)\\
&-\Big((m_{n_i}^2-m_a^2)B_0^{(1)}+(m_{n_j}^2-m_b^2)B_0^{(2)}\\
&+(m_{n_i}^2-m_a^2)(m_{n_j}^2-m_b^2)C_0\\
&-m_a^2B_1^{(1)}-m_b^2B_1^{(2)}-(m_{n_j}^2-m_b^2)m_a^2C_1\\
&\left.-(m_{n_i}^2-m_a^2)m_b^2C_2\Big)\right]\\
&+q_{ji}m_{n_i}m_{n_j}\left[\Big(4m_W^2C_0+(2-d)C_{00}\right.\\
&-C_{11}m_a^2-C_{22}m_b^2\\
&\left.+C_{12}\left(m_Z^2-m_a^2-m_b^2\right)\Big)\not{\varepsilon}\right.\\
&\left.+2\varepsilon.p_1m_a(C_{11}+C_{12})\right]\Big\}P_L v_b\\
&+\frac{e^3U_{ai}^{v}U_{bj}^{v*}m_b}{4m_W^2s_W^3c_W}\overline{u_a}\left\{q_{ij}\left[\not{\varepsilon}m_a\left(-(2-d)C_{00}\right.\right.\right.\\
&+2m_W^2X_0+m_a^2X_1+m_b^2X_2\\
&\left.-m_{n_j}^2C_2-m_{n_i}^2C_1-m_Z^2C_{12}\right)\\
&\left.+2(p_1.\varepsilon)\left(-2m_W^2X_{02}+m_{n_i}^2C_1-m_a^2X_1\right)\right]\\
&\left.+q_{ji}m_{n_i}m_{n_j}\left[2\varepsilon.p_1(C_{22}+C_{12})\right]\right\}P_R v_b.
\end{aligned}\tag{B8}$$

From Eq. (B8) results in four form factors listed in Eqs. (21), (22), (23), and (24).

For diagram (3) in Fig. 1:

$$\begin{aligned}
i\mathcal{M}_3^{(U)} &= \int\frac{d^4k}{(2\pi)^4}\times\overline{u_a}\left[\frac{ie}{\sqrt{2}s_W}U_{ai}^{v}\gamma^{\alpha}P_L\right]\frac{i\left(m_{n_i}+\not{k}\right)}{D_0}\\
&\times\left[\frac{ie}{\sqrt{2}s_W}U_{bi}^{v*}\gamma^{\beta}P_L\right]\\
&\times\frac{i\left(m_b+\not{p}_1\right)}{p_1^2-m_b^2}\times\left[ie\not{\varepsilon}\left(t_LP_L+t_RP_R\right)\right]v_b
\end{aligned}$$

$$
\begin{aligned}
&\times \frac{-i}{D_1}\left(g_{\alpha\beta}-\frac{k_{1\alpha}k_{1\beta}}{m_W^2}\right)\\
&=\frac{e^3U_{ai}^{\nu}U_{bi}^{\nu*}}{2s_W^2(m_a^2-m_b^2)}\int\frac{d^4k}{(2\pi)^4}\\
&\times\frac{\overline{u_a}\gamma^{\alpha}\not{k}\gamma^{\beta}P_L\left(m_b+\not{p}_1\right)\not{\epsilon}(t_LP_L+t_RP_R)}{D_0D_1}\\
&\left(g_{\alpha\beta}-\frac{k_{1\alpha}k_{1\beta}}{m_W^2}\right)\\
&=\frac{e^3U_{ai}^{\nu}U_{bi}^{\nu*}}{2s_W^2(m_a^2-m_b^2)}\int\frac{d^4k}{(2\pi)^4}\\
&\times\frac{\overline{u_a}}{D_0D_1}\left[(2-d)\not{k}-\frac{\not{k}_1\not{k}\not{k}_1}{m_W^2}\right]\\
&\left(t_L\not{p}_1\not{\epsilon}P_L+t_Rm_b\not{\epsilon}P_R\right)v_b\\
&=\frac{e^3U_{ai}^{\nu}U_{bi}^{\nu*}m_a^2t_L}{2m_W^2s_W^2(m_a^2-m_b^2)}\overline{u_a}\left\{2m_{n_i}^2B_0^{(1)}\right.\\
&\left.-\left[(2-d)m_W^2-m_{n_i}^2-m_a^2\right]B_1^{(1)}\right\}\not{\epsilon}P_Lv_b\\
&+\frac{e^3U_{ai}^{\nu}U_{bi}^{\nu*}m_am_bt_R}{2m_W^2s_W^2(m_a^2-m_b^2)}\overline{u_a}\left\{2m_{n_i}^2B_0^{(1)}\right.\\
&\left.-\left[(2-d)m_W^2-m_{n_i}^2-m_a^2\right]B_1^{(1)}\right\}\not{\epsilon}P_Rv_b. \qquad \text{(B9)}
\end{aligned}
$$

Similarly for the diagram (4) of Fig. 1, we get

$$
\begin{aligned}
i\mathcal{M}_4^{(U)}&=\frac{e^3U_{bi}^{\nu*}U_{ai}^{\nu}}{2s_W^2(m_b^2-m_a^2)}\\
&\times\int\frac{d^4k}{(2\pi)^4}\times\frac{\overline{u_a}}{D_0D_2}\times\not{\epsilon}(t_LP_L+t_RP_R)\left(m_a-\not{p}_2\right)\\
&\times\gamma^{\alpha}\not{k}\gamma^{\beta}\left(g_{\alpha\beta}-\frac{k_{2\alpha}k_{2\beta}}{m_W^2}\right)P_Lv_b\\
&=\frac{U_{ai}^{\nu}e^3U_{bi}^{\nu*}t_L}{2m_W^2s_W^2(m_b^2-m_a^2)}\overline{u_a}\left\{2m_{n_i}^2B_0^{(2)}\right.\\
&\left.-\left[(2-d)m_W^2-m_{n_i}^2-m_b^2\right]B_1^{(2)}\right\}\not{\epsilon}P_Lv_b\\
&+\frac{U_{ai}^{\nu}e^3U_{bi}^{\nu*}t_R}{2m_W^2s_W^2(m_b^2-m_a^2)}\overline{u_a}\left\{2m_{n_i}^2B_0^{(2)}\right.\\
&\left.-\left[(2-d)m_W^2-m_{n_i}^2-m_b^2\right]B_1^{(2)}\right\}\not{\epsilon}P_Rv_b. \qquad \text{(B10)}
\end{aligned}
$$

Combining two results of $\mathcal{M}_3^{(U)}$ and $\mathcal{M}_4^{(U)}$, we obtain four form factors listed in Eqs. (25), (26), and (27).

B.2 Divergent cancellation in $Z\to e_b^+e_a^-$ amplitude

The divergence cancellation in the total form factor $\bar{a}_{l,r}$ and $\bar{b}_{l,r}$ is proved below.

$$
\begin{aligned}
\mathrm{div}\left[\bar{a}_l^{nWW}\right]&=\frac{e^3}{2s_W^2t_R}\left\{\frac{1}{m_W^2}\left(2-\frac{1}{2}\right)+\frac{m_Z^2}{4m_W^4}\right\}\\
&\sum_{i=1}^{6}U_{ai}^{\nu}U_{bi}^{\nu*}m_{n_i}^2\Delta_{\epsilon}\\
&=\frac{e^3}{4m_W^2s_W^3c_W}\left\{3c_W^2+\frac{1}{2}\right\}\sum_{i=1}^{6}U_{ai}^{\nu}U_{bi}^{\nu*}m_{n_i}^2\Delta_{\epsilon},\\
\mathrm{div}\left[\bar{a}_l^{Wnn}\right]&=\frac{e^3}{4m_W^2s_W^3c_W}\sum_{i,j=1}^{6}U_{ai}^{\nu}U_{bj}^{\nu*}q_{ij}(-m_{n_i}^2-m_{n_j}^2)\Delta_{\epsilon}\\
&=\frac{e^3}{4m_W^2s_W^3c_W}(-2)\sum_{i=1}^{6}U_{ai}^{\nu}U_{bi}^{\nu*}m_{n_i}^2\Delta_{\epsilon},\\
\mathrm{div}\left[\bar{a}_l^{nW}\right]&=\frac{e^3t_L}{2m_W^2s_W^2}\left(2-\frac{1}{2}\right)\sum_{i=1}^{6}U_{ai}^{\nu}U_{bi}^{\nu*}m_{n_i}^2\Delta_{\epsilon}\\
&=\frac{e^3}{4m_W^2s_W^3c_W}\left(\frac{3}{2}s_W^2-\frac{3}{2}c_W^2\right)\sum_{i=1}^{6}U_{ai}^{\nu}U_{bi}^{\nu*}m_{n_i}^2\Delta_{\epsilon},
\end{aligned}
\qquad \text{(B11)}
$$

where $\mathrm{div}\left[B_0^{(1)}\right]=\mathrm{div}\left[B_0^{(2)}\right]=-2\mathrm{div}\left[B_1^{(1)}\right]=-2\mathrm{div}\left[B_1^{(2)}\right]=4\mathrm{div}\left[C_{00}\right]\equiv\Delta_{\epsilon}$ and $t_R=\frac{s_W}{c_W}$; $t_L=\frac{s_W^2-c_W^2}{2s_Wc_W}$; $m_Z=\frac{m_W}{c_W}$; $q_{ij}=\left(U^{\dagger}U\right)_{ij}$.

Because $\left(3c_W^2+\frac{1}{2}-2+\frac{3}{2}s_W^2-\frac{3}{2}c_W^2\right)=0$, the sum of all divergent parts of $\bar{a}_{l,r}$ and $\bar{b}_{l,r}$ is zero. Also, we see easily that $\mathrm{div}\left[\bar{a}_r^{nWW}\right]=\mathrm{div}\left[\bar{a}_r^{Wnn}\right]=\mathrm{div}\left[\bar{a}_r^{nW}\right]=\mathrm{div}\left[\bar{b}_l^{nWW}\right]=\mathrm{div}\left[\bar{b}_r^{nWW}\right]=\mathrm{div}\left[\bar{b}_l^{Wnn}\right]=\mathrm{div}\left[\bar{b}_r^{Wnn}\right]=0$.

B.3 The results in the 't Hoof–Feynman gauge

The form factors calculated in the 't Hooft–Feynman corresponding to 10 diagrams including 6 diagrams in Fig. 2 and 4 diagrams in Fig. 1 are denoted respectively as follows. Two diagrams (1) and (2) in Fig. 2 give

$$
\begin{aligned}
\bar{a}'_{l,1+2}\equiv\ \bar{a}'_{nWG,l}&=\frac{-e^2t_R}{2s_W^2}\sum_{i=1}^{K+3}U_{ai}^{\nu}U_{bi}^{\nu*}\\
&\left(2m_{n_i}^2C_0+m_a^2C_1+m_b^2C_2\right),\\
\bar{a}'_{r,1+2}\equiv\ \bar{a}'_{nWG,r}&=\frac{e^2t_R}{2s_W^2}\times m_am_b\sum_{i=1}^{K+3}U_{ai}^{\nu}U_{bi}^{\nu*}X_3,
\end{aligned}
$$

$$\bar{b}'_l \equiv \bar{b}'_{nWG,l} = \frac{-e^2 t_R}{2s_W^2} \sum_{i=1}^{K+3} U^{\nu}_{ai} U^{\nu *}_{bi} \left[2m_a C_2\right],$$
$$\bar{b}'_r \equiv \bar{a}'_{nWG,r} = \frac{-e^2 t_R}{2s_W^2} \sum_{i=1}^{K+3} U^{\nu}_{ai} U^{\nu *}_{bi} \left[2m_b C_1\right], \quad \text{(B12)}$$

where $C_{0,1,2} = C_{0,1,2}(m_a^2, m_Z^2, m_b^2; m_i^2, m_W^2, m_W^2)$ and $X_3 = X_3(m_a^2, m_Z^2, m_b^2; m_i^2, m_W^2, m_W^2)$. Diagrams (3) in Fig. 2 gives

$$\bar{a}'_{l,3} \equiv \bar{a}'_{nGG,l} = \frac{e^2 t_L}{s_W^2 m_W^2} \sum_{i=1}^{K+3} U^{\nu}_{ai} U^{\nu *}_{bi} m_{n_i}^2 C_{00},$$
$$\bar{a}'_{r,3} \equiv \bar{a}'_{nGG,r} = \frac{e^2 t_L m_a m_b}{s_W^2 m_W^2} \sum_{i=1}^{K+3} U^{\nu}_{ai} U^{\nu *}_{bi} C_{00},$$
$$\bar{b}'_{l,3} \equiv \bar{b}'_{nGG,l} = \frac{e^2 t_L m_a}{s_W^2 m_W^2} \sum_{i=1}^{K+3} U^{\nu}_{ai} U^{\nu *}_{bi} \left[m_b^2 X_2 + m_{n_i}^2 X_{01}\right],$$
$$\bar{b}'_{r,3} \equiv \bar{a}'_{nGG,r} = \frac{e^2 t_L m_b}{s_W^2 m_W^2} \sum_{i=1}^{K+3} U^{\nu}_{ai} U^{\nu *}_{bi} \left[m_a^2 X_1 + m_{n_i}^2 X_{02}\right], \quad \text{(B13)}$$

where $X_{0,1,2} = X_{0,1,2}(m_a^2, m_Z^2, m_b^2; m_i^2, m_W^2, m_W^2)$ and $C_{00} = C_{00}(p_1^2, q^2, p_2^2; m_i^2, m_W^2, m_W^2)$.

Diagram (4) in Fig. 2 gives:

$$\begin{aligned}
\bar{a}'_{l,4} &\equiv \bar{a}'_{Gnn,l} \\
&= \frac{e^2}{4s_W^3 c_W m_W^2} \\
&\quad \times \sum_{i,j=1}^{K+3} U^{\nu}_{ai} U^{\nu *}_{bj} \left\{ q_{ij} \left[\left(m_a^2 m_j^2 + m_b^2 m_i^2 - m_a^2 m_b^2 \right) X_0 \right.\right. \\
&\quad \left. - m_i^2 m_j^2 C_0 - m_b^2 m_i^2 C_1 - m_a^2 m_j^2 C_2 \right] \\
&\quad \left. - q_{ji} m_{n_i} m_{n_j} \left[B_0^{(12)} - 2C_{00} + m_W^2 C_0 \right] \right\}, \\
\bar{a}'_{r,4} &\equiv \bar{a}'_{Gnn,r} \\
&= \frac{e^2 m_a m_b}{4s_W^3 c_W m_W^2} \sum_{i=1}^{K+3} U^{\nu}_{ai} U^{\nu *}_{bj} q_{ij} \left[B_0^{(12)} + m_W^2 C_0 \right. \\
&\quad \left. - 2C_{00} - (m_{n_i}^2 - m_a^2) C_1 - (m_{n_j}^2 - m_b^2) C_2 \right], \\
\bar{b}'_{l,4} &\equiv \bar{b}'_{Gnn,l} \\
&= \frac{e^2 m_a}{4s_W^3 c_W m_W^2} \sum_{i=1}^{K+3} U^{\nu}_{ai} U^{\nu *}_{bj} \left[2q_{ij} \left(m_{n_j}^2 C_2 - m_b^2 X_2 \right) \right. \\
&\quad \left. + 2q_{ji} m_{n_i} m_{n_j} (X_1 - C_1) \right], \\
\bar{b}'_{r,4} &\equiv \bar{b}'_{Gnn,r} \\
&= \frac{e^2 m_b}{4s_W^3 c_W m_W^2} \sum_{i=1}^{K+3} U^{\nu}_{ai} U^{\nu *}_{bj} \left\{ 2q_{ij} \left[m_{n_i}^2 C_1 - m_a^2 X_1 \right] \right. \\
&\quad \left. + 2q_{ji} m_{n_i} m_{n_j} (X_2 - C_2) \right\}, \quad \text{(B14)}
\end{aligned}$$

where $X_{0,1,2} = X_{0,1,2}(m_a^2, m_Z^2, m_b^2; m_i^2, m_j^2, m_W^2)$ and $C_{00} = C_{00}(m_a^2, m_Z^2, m_b^2; m_i^2, m_j^2, m_W^2)$.

Two diagrams (5) and (6) in Fig. 2 give

$$\begin{aligned}
\bar{a}'_{l,5+6} &\equiv \bar{a}'_{nG,l} \\
&= \frac{e^2 t_L}{2m_W^2 s_W^2 \left(m_a^2 - m_b^2\right)} \sum_{i=1}^{K+3} U^{\nu}_{ai} U^{\nu *}_{bi} \left[m_{n_i}^2 \left(m_a^2 + m_b^2 \right) \right. \\
&\quad \times \left(B_0^{(1)} - B_0^{(2)} \right) + m_a^2 m_b^2 \left(B_1^{(1)} - B_1^{(2)} \right) \\
&\quad \left. + m_{n_i}^2 \left(m_a^2 B_1^{(1)} - m_b^2 B_1^{(2)} \right) \right], \\
\bar{a}'_{r,5+6} &\equiv \bar{a}'_{nG,r} \\
&= \frac{e^2 m_a m_b t_R}{2m_W^2 s_W^2 \left(m_a^2 - m_b^2\right)} \sum_{i=1}^{K+3} U^{\nu}_{ai} U^{\nu *}_{bi} \\
&\quad \left[2m_{n_i}^2 \left(B_0^{(1)} - B_0^{(2)} \right) \right. \\
&\quad \left. + m_{n_i}^2 \left(B_1^{(1)} - B_1^{(2)} \right) + \left(m_a^2 B_1^{(1)} - m_b^2 B_1^{(2)} \right) \right], \\
\bar{b}'_{l,5+6} &= \bar{b}'_{r,5+6} = 0, \quad \text{(B15)}
\end{aligned}$$

where $B_{0,1}^{(k)} = B_{0,1}^{(k)}(p_k^2; m_{n_i}^2, m_W^2)$.

Form factors corresponding to diagram (1) in Fig. 1, calculated in the HF gauge:

$$\begin{aligned}
\bar{a}'_{nWW,l} &= \frac{e^2}{2s_W^2 t_r} \sum_{i=1}^{K+3} U^{\nu}_{ai} U^{\nu *}_{bi} \\
&\quad \left[-2 \left(B_0^{(12)} + m_{n_i}^2 C_0 \right) + (4 - 2d) C_{00} \right. \\
&\quad \left. - \left(m_a^2 C_1 + m_b^2 C_2 \right) + 2 \left(m_Z^2 - m_a^2 - m_b^2 \right) X_3 \right], \\
\bar{a}'_{nWW,r} &= \frac{e^2}{2s_W^2 t_r} \sum_{i=1}^{K+3} U^{\nu}_{ai} U^{\nu *}_{bi} \left(-3m_a m_b X_3 \right), \\
\bar{b}'_{nWW,l} &= \frac{e^2 m_a}{2s_W^2 t_r} \sum_{i=1}^{K+3} U^{\nu}_{ai} U^{\nu *}_{bi} \left[4C_1 + 2C_2 - 4X_1 \right], \\
\bar{b}'_{nWW,r} &= \frac{e^2 m_b}{2s_W^2 t_r} \sum_{i=1}^{K+3} U^{\nu}_{ai} U^{\nu *}_{bi} \left[4C_2 + 2C_1 - 4X_2 \right], \quad \text{(B16)}
\end{aligned}$$

where $X_{0,1,2} = X_{0,1,2}(m_a^2, m_Z^2, m_b^2; m_i^2, m_W, m_W^2)$ and $C_{00} = C_{00}(m_a^2, m_Z^2, m_b^2; m_i^2, m_W^2, m_W^2)$. Form factors corresponding to diagram (2) in Fig. 1, calculated in the HF

gauge:

$$\begin{aligned}
\bar{a}'_{Wnn,l} &= \frac{e^2}{4s_W^3 c_W}\sum_{i=1}^{K+3} U^{\nu}_{ai}U^{\nu *}_{bj}\Big\{q_{ij}\Big[4C_{00}+2\Big(m_a^2 X_{01}\\
&\quad +m_b^2 X_{02}-m_Z^2 X_0-m_Z^2 C_{12}\Big)\Big]\\
&\quad +2q_{ji}m_{n_i}m_{n_j}C_0\Big\},\\
\bar{a}'_{Wnn,r} &= \frac{e^2 m_a m_b}{4s_W^3 c_W}\sum_{i=1}^{K+3} U^{\nu}_{ai}U^{\nu *}_{bj}\left[2q_{ij}X_0\right],\\
\bar{b}'_{Wnn,l} &= \frac{e^2 m_a}{4s_W^3 c_W}\sum_{i=1}^{K+3} U^{\nu}_{ai}U^{\nu *}_{bj}\left[-4q_{ij}X_{01}\right],\\
\bar{b}'_{Wnn,r} &= \frac{e^2 m_b}{4s_W^3 c_W}\sum_{i=1}^{K+3} U^{\nu}_{ai}U^{\nu *}_{bj}\left[-4q_{ij}X_{02}\right],
\end{aligned} \tag{B17}$$

where $X_{0,1,2} = X_{0,1,2}(m_a^2, m_Z^2, m_b^2; m_i^2, m_j^2, m_W^2)$ and $C_{00} = C_{00}(m_a^2, m_Z^2, m_b^2; m_i^2, m_j^2, m_W^2)$.

Form factors corresponding to diagram (3) and (4) in Fig. 1, calculated in the HF gauge:

$$\begin{aligned}
\bar{a}'_{nW,l} &= \frac{2e^2}{2s_W^2(m_a^2-m_b^2)}\sum_{i=1}^{K+3} U^{\nu}_{ai}U^{\nu *}_{bi}\\
&\quad \left[t_L\left(m_a^2 B_1^{(1)}-m_b^2 B_1^{(2)}\right)\right],\\
\bar{a}'_{nW,r} &= \frac{2e^2 U^{\nu}_{ai}U^{\nu *}_{bi}}{2s_W^2(m_a^2-m_b^2)}\sum_{i=1}^{K+3} U^{\nu}_{ai}U^{\nu *}_{bi}\\
&\quad \left[t_R m_a m_b\left(B_1^{(1)}-B_1^{(2)}\right)\right],\\
\bar{b}'_{nW,l} &= \bar{b}'_{nW,r} = 0.
\end{aligned} \tag{B18}$$

We note that the PV-functions A, B, and C defined in this work are consistent with notations used LoopTools and Ref. [1]. The equivalences between two final lepton states defined in our work and Ref. [1] are $e_b \equiv \ell_1$ and $e_a \equiv \ell_2$, which implies that $p_{1\mu} = p_{a\mu} \equiv p_{\ell_2\mu} = p_{2\mu}$ and $p_{2\mu} = p_{b\mu} \equiv p_{\ell_1\mu} = p_{1\mu}$, i.e., $\{p_{1\mu}, p_{2\mu}\} \leftrightarrow \{p_{2\mu}, p_{1\mu}\} = \{-q_\mu, p_\mu\}$ corresponding to the definitions in Appendix A of Ref. [1]. In addition, there is a change that $(ij) \equiv (ji)$ for diagrams containing two different lepton propagators. As a consequence, the following identifications is needed in order to check the consistence of the results between our work and Ref. [1]:

$$\begin{aligned}
&m_a^2 = m_a^2 \leftrightarrow m_{\ell_2}^2, \quad m_b^2 = m_b^2 \leftrightarrow m_{\ell_1}^2,\\
&\left\{q_{ij}, m_i, m_j\right\} = \left\{q_{ji}, m_j, m_i\right\},\\
&\{C_0, C_{12}, X_0, X_3, X_{12}\} \leftrightarrow \{C_0, C_{12}, X_0, X_3, X_{12}\},\\
&\left\{B^{(1)}_{0,1,11,00}, B^{(2)}_{0,1,11,00}, C_{1,2,11,22}, X_{01,02}\right\}\\
&\leftrightarrow \left\{B^{(2)}_{0,1,11,00}, B^{(1)}_{0,1,11,00}, C_{2,1,22,11}, X_{02,01}\right\}.
\end{aligned} \tag{B19}$$

The above relations are realized from the properties that the C-functions relating to the cLFV Z decays are derived in the different orders of the propagators in the numerators $\{D_0, D_1, D_2\} \leftrightarrow \left\{k^2 - A, (k+p)^2 - B, (k+q)^2 - C\right\}$ with $-p_{1\mu} = p_\mu = p_{\ell_1}$ and $p_{2\mu} = q_\mu = -p_{\ell_2}$, for example

$$\begin{aligned}
h_0 &= C_0(m_{\ell_1}^2, q^2, m_{\ell_2}^2; m_W^2, m_i^2, m_j^2)\\
&= C_0(m_b^2, q^2, m_a^2; m_W^2, m_i^2, m_j^2)\\
&= C_0(m_a^2, q^2, m_b^2; m_W^2, m_j^2, m_i^2),\\
h_1 &= C_1(m_{\ell_1}^2, q^2, m_{\ell_2}^2; m_W^2, m_i^2, m_j^2)\\
&= C_1(m_b^2, q^2, m_a^2; m_W^2, m_i^2, m_j^2)\\
&= C_2(m_a^2, q^2, m_b^2; m_W^2, m_j^2, m_i^2), \ldots
\end{aligned}$$

The transformations between our results with those given in Ref. [23] are done through the following relations:

$$\begin{aligned}
-\frac{e}{16\pi^2}\bar{a}_l &= F_V^L - i\left(m_a F_T^L + m_b F_T^R\right),\\
-\frac{e}{16\pi^2}\bar{a}_r &= F_V^R - i\left(m_a F_T^R + m_b F_T^L\right),\\
-\frac{e}{16\pi^2}\bar{b}_{l,r} &= 2i F_T^{L,R},
\end{aligned}$$

where $m_a \equiv m_\alpha$, $m_b \equiv m_\beta$, $q_{ij} \equiv C_{ij}$, and $q_{ji} \equiv C^*_{ij}$. The redundant relations given in appendix A were used to check the consistence. There appears an overall sign because of the different sign conventions in Lagrangians. Regarding analytic formulas computed in the unitary gauge, we realize that all form factors $F_T^{L,R}$ and F_V^R, and $F_V^{L(c+d)}$ in Ref. [23] are totally consistent with ours, while the remaining $F_V^{L(a)}$ and $F_V^{L(b)}$ result in two deviations as follows:

$$\begin{aligned}
&\frac{e}{16\pi^2}\bar{a}_l^{Wnn} + \left[F_V^{L(b)} - i\left(m_a F_T^{L(b)} + m_b F_T^{R(b)}\right)\right]\\
&= \frac{g^3}{32 c_W \pi^2}\sum_{i,j=1}^{K+3} q_{ij}\Big[-B_0^{(1)} - B_0^{(2)} + 2B_0^{(12)}\\
&\quad +m_a^2(3C_1 + C_2 + C_0) + m_b^2(C_1 + 3C_2 + C_0)\\
&\quad +C_0(m_{n_i}^2 - m_{n_j}^2) - (C_1 + C_2)m_Z^2\Big],
\end{aligned} \tag{B20}$$

where $B_0^{(1)} = B_0(m_a^2; m_W^2, m_i^2)$, $B_0^{(2)} = B_0(m_b^2; m_W^2, m_j^2)$, $C_k = C_k(m_a^2, m_Z^2, m_b^2, m_W^2, m_i^2, m_j^2)$, and

$$\begin{aligned}
&\frac{e}{16\pi^2}\bar{a}_l^{nWW} + \left[F_V^{L(b)} - i\left(m_a F_T^{L(b)} + m_b F_T^{R(b)}\right)\right]\\
&= .\frac{g^3 c_W}{16\pi^2}\sum_{i=1}^{K+3}\Big[B_0^{(1)} + B_0^{(2)} - m_a^2(3C_1 + C_2 + C_0)\\
&\quad -m_b^2(C_1 + 3C_2 + C_0)
\end{aligned}$$

$$-2C_0(m_{n_i}^2 - m_W^2) + (C_1 + C_2)m_Z^2\Big]$$

with $B_0^{(k)} = B_0(p_k^2; m_i^2, m_W^2)$, $C_k = C_k(m_a^2, m_Z^2, m_b^2, m_i^2, m_W^2, m_W^2)$.

B.4 Scalar one-loop contributions to the $Z \to e_b^+ e_a^-$ amplitude

For contributions from Higgs mediations, similar to the diagrams in Fig. 1, but the gauge boson propagators W are replaced with scalars c, namely diagram (1), (2), and (3+4) are denoted as ns_1s_2, s_knn, and ns_k. They are also 4 diagrams (3), (4), and (5+6) in Fig. 2. The Lagrangian consisting of relevant scalar couplings is

$$\begin{aligned}\mathcal{L}_S = &\sum_{a=1}^{3}\sum_{i=1}^{K+3}\sum_{k}\overline{n_i}(L_{ai}^k P_L + R_{ai}^k P_R)e_a s_k \\ &+ (-eg_{Zs_1s_2})Z_\mu s_1^- s_2^+ (p_+ - p_-)^\mu + \text{h.c.}\end{aligned} \tag{B21}$$

The results are listed as follows. The diagram with three propagators ns_1s_2:

$$\begin{aligned}\bar{a}_{ns_1s_2,l} &= 2g_{Zs_1s_2}\sum_{i=1}^{K+3} L_{ai}^{1*}L_{bi}^2 C_{00} \\ &= 2g_{Zs_1s_2}\sum_{i=1}^{K+3}\frac{L_{ai}^{1*}L_{bi}^2}{2}\Big[m_{n_i}^2 C_0 - m_a^2 C_1 - m_b^2 C_2 \\ &\quad - \left(m_a^2 + m_b^2 - m_Z^2\right)C_{12}\Big], \\ \bar{a}_{ns_1s_2,r} &= 2g_{Zs_1s_2}\sum_{i=1}^{K+3} R_{ai}^{1*}R_{bi}^2 C_{00} \\ &= 2g_{Zs_1s_2}\sum_{i=1}^{K+3} R_{ai}^{1*}R_{bi}^2\Big[m_{n_i}^2 C_0 - m_a^2 C_1 - m_b^2 C_2 \\ &\quad - \left(m_a^2 + m_b^2 - m_Z^2\right)C_{12}\Big], \\ \bar{b}_{ns_1s_2,l} &= 2g_{Zs_1s_2}\sum_{i=1}^{K+3}\Big[L_{ai}^{1*}L_{bi}^2 m_a X_1 + R_{ai}^{1*}R_{bi}^2 m_b X_2 \\ &\quad - R_{ai}^{1*}L_{bi}^2 m_{n_i} X_0\Big], \\ \bar{b}_{ns_1s_2,r} &= 2g_{Zs_1s_2}\sum_{i=1}^{K+3}\Big[R_{ai}^{1*}R_{bi}^2 m_a X_1 + L_{ai}^{1*}L_{bi}^2 m_b X_2 \\ &\quad - L_{ai}^{1*}R_{bi}^2 m_{n_i} X_0\Big],\end{aligned} \tag{B22}$$

where $C_{0,00,k,kl} = C_{0,00,k,kl}(p_1^2, m_Z^2, p_2^2; m_{n_i^2}, m_{s_1}^2, m_{s_2}^2)$.

The diagram with three propagators snn:

$$\begin{aligned}\bar{a}_{s_knn,l} = &-\frac{1}{2s_W c_W}\sum_{i,j=1}^{K+3}\Big\{q_{ij}\Big[\lambda_{ai}^{L,k*}\lambda_{bj}^{L,k} m_{n_i}m_{n_j}C_0 \\ &+\lambda_{ai}^{R,k*}\lambda_{bj}^{L,k} m_{n_j}m_a(C_0 + C_1) \\ &+\lambda_{ai}^{L,k*}\lambda_{bj}^{R,k} m_{n_i}m_b(C_0 + C_2) + \lambda_{ai}^{R,k*}\lambda_{bj}^{R,k} m_a m_b X_0\Big] \\ &-q_{ji}\Big[\lambda_{ai}^{L,k*}\lambda_{bj}^{L,k}\Big(2C_{00} - B_0^{(12)} - m_{s_k}^2 \\ &C_0 - m_a^2 C_1 - m_b^2 C_2\Big) \\ &-\lambda_{ai}^{R,k*}\lambda_{bj}^{L,k} m_{n_i}m_a C_1 + \lambda_{ai}^{L,k*}\lambda_{bj}^{R,k} m_{nj}m_b C_2\Big]\Big\}, \\ \bar{a}_{s_knn,r} = &-\frac{1}{2s_W c_W}\sum_{i,j=1}^{K+3}\Big\{q_{ij}\Big[-\lambda_{ai}^{L,k*}\lambda_{bj}^{R,k} m_{n_i}m_a C_1 \\ &+\lambda_{ai}^{R,k*}\lambda_{bj}^{L,k} m_{n_j}m_b C_2 \\ &+\lambda_{ai}^{R,k*}\lambda_{bj}^{R,k}\Big((2-d)C_{00} - \left(m_Z^2 - m_a^2 - m_b^2\right) \\ &C_{12} - m_a^2 C_1 - m_b^2 C_2\Big)\Big] \\ &-q_{ji}\Big[\lambda_{ai}^{R,k*}\lambda_{bj}^{R,k} m_{n_i}m_{n_j}C_0 \\ &+\lambda_{ai}^{L,k*}\lambda_{bj}^{R,k} m_{n_j}m_a(C_0 + C_1) \\ &+\lambda_{ai}^{R,k*}\lambda_{bj}^{L,k} m_{n_i}m_b(C_0 + C_2) + \lambda_{ai}^{L,k*}\lambda_{bj}^{L,k} m_a m_b X_0\Big]\Big\}, \\ \bar{b}_{s_knn,l} = &-\frac{1}{s_W c_W}\sum_{i,j=1}^{K+3}\Big\{q_{ij}\lambda_{ai}^{R,k*}\lambda_{bj}^{R,k} m_b X_2 \\ &-q_{ji}\Big[\lambda_{ai}^{L,k*}\lambda_{bj}^{L,k} m_a X_1 + \lambda_{ai}^{R,k*}\lambda_{bj}^{L,k} m_{n_i} C_1\Big]\Big\}, \\ \bar{b}_{s_knn,r} = &-\frac{1}{s_W c_W}\sum_{i,j=1}^{K+3}\Big\{q_{ij}\lambda_{ai}^{R,k*}\lambda_{bj}^{R,k} m_a X_1 \\ &-q_{ji}\Big[\lambda_{ai}^{L,k*}\lambda_{bj}^{L,k} m_b X_2 + \lambda_{ai}^{L,k*}\lambda_{bj}^{R,k} m_{n_j} C_2\Big]\Big\},\end{aligned} \tag{B23}$$

where $C_{0,00,k,kl} = C_{0,00,k,kl}(p_1^2, m_Z^2, p_2^2; m_{s_k}^2, m_{n_i^2}, m_{n_j^2})$.

The two one-loop-two-point diagrams with two propagators nc:

$$\begin{aligned}\bar{a}_{ns_k,l} = &\frac{-t_L}{(m_a^2 - m_b^2)}\sum_{i=1}^{K+3}\Big[m_{n_i}\left(\lambda_{ai}^{L,k*}\lambda_{bi}^{R,k} m_b + \lambda_{ai}^{R,k*}\lambda_{bi}^{L,k} m_a\right) \\ &\left(B_0^{(1)} - B_0^{(2)}\right) \\ &-\left(\lambda_{ai}^{L,k*}\lambda_{bi}^{L,k} m_b^2 + \lambda_{ai}^{R,k*}\lambda_{bi}^{R,k} m_a m_b\right)\left(B_1^{(1)} - B_1^{(2)}\right)\Big], \\ \bar{a}_{ns_k,r} = &\frac{-t_R}{(m_a^2 - m_b^2)}\sum_{i=1}^{K+3}\Big[m_{n_i}\left(\lambda_{ai}^{L,k*}\lambda_{bi}^{R,k} m_a + \lambda_{ai}^{R,k*}\lambda_{bi}^{L,k} m_b\right) \\ &\left(B_0^{(1)} - B_0^{(2)}\right) \\ &-\left(\lambda_{ai}^{L,k*}\lambda_{bi}^{L,k} m_a m_b + \lambda_{ai}^{R,k*}\lambda_{bi}^{R,k} m_b^2\right)\left(B_1^{(1)} - B_1^{(2)}\right)\Big], \\ \bar{b}_{ns_k,l} = &\bar{b}_{ns_k,r} = 0.\end{aligned} \tag{B24}$$

Appendix C: Form factors for the LFVh decays $h \to e_a e_b$

Denoting that $\Delta_{L,R}^{(i)} \equiv \Delta_{L,R}^{(ab)(i)}$ for short, the private contributions of all diagrams in Fig. 4 to the LFVh decay amplitude are as follows [8,102,103]. The first class consists of only

gauge boson, namely four diagrams (1), (5), (7), and (8). The diagram (1) nWW:

$$\begin{aligned}\Delta_L^{(1)} &= \Delta_L^{nWW}\\ &= \frac{g^3 m_a}{64\pi^2 m_W^3} c_\delta\\ &\times \sum_{i=1}^{9} U_{ai}^{\nu} U_{bi}^{\nu *} \Big\{ m_{n_i}^2 \left(B_0^{(1)} + B_0^{(2)} + B_1^{(1)} \right) + m_b^2 B_1^{(2)}\\ &- \left(2m_W^2 + m_h^2\right) m_{n_i}^2 C_0\\ &- \left[m_{n_i}^2 \left(2m_W^2 + m_h^2\right) + 2m_W^2 \left(2m_W^2 + m_a^2 - m_b^2\right) \right] C_1\\ &- \left[2m_W^2 \left(m_a^2 - m_h^2\right) + m_b^2 m_h^2 \right] C_2 \Big\}, \end{aligned} \tag{C1}$$

$$\begin{aligned}\Delta_R^{(1)} &= \Delta_R^{nWW}\\ &= \frac{g^3 m_b}{64\pi^2 m_W^3} c_\delta\\ &\times \sum_{i=1}^{9} U_{ai}^{\nu} U_{bi}^{\nu *} \Big\{ m_{n_i}^2 \left(B_0^{(1)} + B_0^{(2)} + B_1^{(2)} \right) + m_a^2 B_1^{(1)}\\ &- \left(2m_W^2 + m_h^2\right) m_{n_i}^2 C_0\\ &- \left[2m_W^2 \left(m_b^2 - m_h^2\right) + m_a^2 m_h^2 \right] C_1\\ &- \left[m_{n_i}^2 \left(2m_W^2 + m_h^2\right) + 2m_W^2 \left(2m_W^2 - m_a^2 + m_b^2\right) \right] C_2 \Big\}, \end{aligned} \tag{C2}$$

where $B_{0,1}^{(i)} = B_{0,1}(p_i^2; m_{n_i}^2, m_W^2)$ and $C_{0,1,2} = C_{0,1,2}(p_1^2, m_h^2, p_2^2; m_{n_i}^2, m_W^2, m_W^2)$.

The diagrams (5) with three propagators Wnn:

$$\begin{aligned}\Delta_L^{(5)} &= \Delta_L^{(Wnn)}\\ &= \frac{g^3 m_a}{64\pi^2 m_W^3} \times \frac{c_\alpha}{s_\beta} \sum_{i,j=1}^{9} U_{ai}^{\nu} U_{bj}^{\nu *} \Big\{ \lambda_{ij}^{0*} m_{n_j}\\ &\times \left[-B_0^{(12)} + m_W^2 C_0 + \left(2m_W^2 + m_{n_i}^2 - m_a^2\right) C_1 \right]\\ &+ \lambda_{ij}^0 m_{n_i} \left[B_1^{(1)} + \left(2m_W^2 + m_{n_j}^2 - m_b^2\right) C_1 \right] \Big\},\\ \Delta_R^{(5)W} &= \Delta_R^{(Wnn)}\\ &= \frac{g^3 m_b}{64\pi^2 m_W^3} \times \frac{c_\alpha}{s_\beta} \sum_{i=1}^{9} U_{ai}^{\nu} U_{bj}^{\nu *} \Big\{ \lambda_{ij}^0 m_{n_i}\\ &\times \left[-B_0^{(12)} + m_W^2 C_0 + \left(2m_W^2 + m_{n_j}^2 - m_b^2\right) C_2 \right]\\ &+ \lambda_{ij}^{0*} m_{n_j} \left[B_1^{(2)} + \left(2m_W^2 + m_{n_i}^2 - m_a^2\right) C_2 \right] \Big\}, \end{aligned} \tag{C3}$$

where λ_{ij}^h is given in Eq. (46), $B_0^{(12)} = B_0(m_h^2; m_{n_i}^2, m_{n_j}^2)$, $B_1^{(k)} = B_1(p_k^2; m_W^2, m_{n_i}^2)$, and $C_{0,1,2} = C_{0,1,2}(p_1^2, m_h^2, p_2^2; m_W^2, m_{n_i}^2, m_{n_j}^2)$ with $k = 1, 2$.

The diagrams (7+8) with two propagators nW:

$$\begin{aligned}\Delta_L^{(7+8)} &= \Delta_L^{nW}\\ &= \frac{g^3 m_a}{64\pi^2 m_W^3} \times \frac{s_\alpha}{c_\beta} \times \frac{m_b^2}{m_b^2 - m_a^2} \sum_{i=1}^{9} U_{ai}^{\nu} U_{bi}^{\nu *}\\ &\times \left[\left(2m_W^2 + m_{n_i}^2\right) \left(B_1^{(2)} - B_1^{(1)} \right) \right.\\ &\left. + m_b^2 B_1^{(2)} - m_a^2 B_1^{(1)} + 2m_{n_i}^2 \left(B_0^{(2)} - B_0^{(1)} \right) \right],\\ \Delta_R^{(7+8)} &= \Delta_R^{nW} = \frac{m_a}{m_b} \Delta_L^{(7+8)}, \end{aligned} \tag{C4}$$

where $\Delta_{L,R}^{(7+8)} \equiv \Delta_{L,R}^{(7)} + \Delta_{L,R}^{(8)}$, and $B_{0,1}^{(i)} \equiv B_{0,1}(p_i^2; m_{n_i}^2, m_W^2)$.

There are 4 diagrams relating with only scalar mediation, namely diagrams (2), (6), (9), and (10). The diagrams (2) with three propagators ncc:

$$\begin{aligned}\Delta_L^{(2)} &= \Delta_L^{(ncc)}\\ &= \frac{g^2}{32\pi^2 m_W^2} \sum_{k,l=1}^{2} \lambda_{kl}^h \sum_{i=1}^{9} \Big[-\lambda_{ai}^{R,k*} \lambda_{bi}^{L,l} m_{n_i} C_0\\ &+ \lambda_{ai}^{L,k*} \lambda_{bi}^{L,l} m_a C_1 + \lambda_{ai}^{R,k*} \lambda_{bi}^{R,l} m_b C_2 \Big],\\ \Delta_R^{(2)} &= \Delta_R^{(ncc)}\\ &= \frac{g^2}{32\pi^2 m_W^2} \sum_{k,l=1}^{2} \lambda_{kl}^h \sum_{i=1}^{9} \Big[-\lambda_{ai}^{L,k*} \lambda_{bi}^{R,l} m_{n_i} C_0\\ &+ \lambda_{ai}^{R,k*} \lambda_{bi}^{R,l} m_a C_1 + \lambda_{ai}^{L,k*} \lambda_{bi}^{L,l} m_b C_2 \Big], \end{aligned} \tag{C5}$$

where $C_{0,1,2} = C_{0,1,2}(p_1^2, m_h^2, p_2^2; m_{n_i}^2, m_{c_k}^2, m_{c_l}^2)$, and λ_{kl}^h are given in Eq (49).

The diagrams (6) with cnn:

$$\begin{aligned}\Delta_L^{(6)} &= \Delta_L^{(cnn)}\\ &= \frac{g^3 c_\alpha}{64\pi^2 m_W^3 s_\beta} \sum_{k=1}^{2} \sum_{i,j=1}^{9} \Big\{ \lambda_{ij}^{0*} \Big[\lambda_{ai}^{R,k*} \lambda_{bj}^{L,k}\\ &\left(B_0^{(12)} + m_{c_k}^2 C_0 + m_a^2 C_1 + m_b^2 C_2 \right)\\ &+ \lambda_{ai}^{R,k*} \lambda_{bj}^{R,k} m_b m_{n_j} C_2 + \lambda_{ai}^{L,k*} \lambda_{bj}^{L,k} m_a m_{n_i} C_1 \Big]\\ &+ \lambda_{ij}^0 \Big[\lambda_{ai}^{R,k*} \lambda_{bj}^{L,k} m_{n_i} m_{n_j} C_0 + \lambda_{ai}^{R,k*} \lambda_{bj}^{R,k} m_{n_i} m_b (C_0 + C_2)\\ &+ \lambda_{ai}^{L,k*} \lambda_{bj}^{L,k} m_a m_{n_j} (C_0 + C_1)\\ &+ \lambda_{ai}^{L,k*} \lambda_{bj}^{R,k} m_a m_b (C_0 + C_1 + C_2) \Big] \Big\}, \end{aligned} \tag{C6}$$

$$\begin{aligned}\Delta_R^{(6)} &= \Delta_R^{(cnn)}\\ &= \frac{g^3 c_\alpha}{64\pi^2 m_W^3 s_\beta} \sum_{k=1}^{2} \sum_{i,j=1}^{9} \Big\{ \lambda_{ij}^{0} \Big[\lambda_{ai}^{L,k*} \lambda_{bj}^{R,k}\\ &\left(B_0^{(12)} + m_{c_k}^2 C_0 + m_a^2 C_1 + m_b^2 C_2 \right)\\ &+ \lambda_{ai}^{L,k*} \lambda_{bj}^{L,k} m_b m_{n_j} C_2 + \lambda_{ai}^{R,k*} \lambda_{bj}^{R,k} m_a m_{n_i} C_1 \Big]\\ &+ \lambda_{ij}^{0*} \Big[\lambda_{ai}^{L,k*} \lambda_{bj}^{R,k} m_{n_i} m_{n_j} C_0 + \lambda_{ai}^{L,k*} \lambda_{bj}^{L,k} m_{n_i} m_b (C_0 + C_2) \end{aligned}$$

$$+\lambda_{ai}^{R,k*}\lambda_{bj}^{R,k}m_a m_{n_j}(C_0+C_1) +\lambda_{ai}^{R,k*}\lambda_{bj}^{L,k}m_a m_b(C_0+C_1+C_2)\Big]\Big\}, \tag{C7}$$

where $B_0^{(12)} = B_0(m_h^2; m_{n_i}^2, m_{n_j}^2)$, and $C_{0,1,2} = C_{0,1,2}(p_1^2, m_h^2, p_2^2; m_{c_k}^2, m_{n_i}^2, m_{n_j}^2)$,

The diagrams (9+10) with $nc_l^{\pm}$:

$$\begin{aligned}
\Delta_L^{(9+10)} &= \Delta_L^{(nc)} \\
&= \frac{g^3 s_\alpha}{64\pi^2 c_\beta m_W^3 \left(m_a^2 - m_b^2\right)} \\
&\times \sum_{k=1}^{2}\sum_{i=1}^{9}\Big[m_a m_b m_{n_i}\lambda_{ai}^{L,k*}\lambda_{bi}^{R,k}\left(B_0^{(1)} - B_0^{(2)}\right) \\
&+m_{n_i}\lambda_{ai}^{R,k*}\lambda_{bi}^{L,k}\left(m_b^2 B_0^{(1)} - m_a^2 B_0^{(2)}\right) \\
&+m_a m_b\left(\lambda_{ai}^{L,k*}\lambda_{bi}^{L,k}m_b + \lambda_{ai}^{R,k*}\lambda_{bi}^{R,k}m_a\right)\left(-B_1^{(1)} + B_1^{(2)}\right)\Big], \\
\Delta_R^{(9+10)} &= \Delta_R^{(nc)} \\
&= \frac{g^3 s_\alpha}{64\pi^2 c_\beta m_W^3 \left(m_a^2 - m_b^2\right)} \\
&\times \sum_{k=1}^{2}\sum_{i=1}^{9}\Big[m_a m_b m_{n_i}\lambda_{ai}^{R,k*}\lambda_{bi}^{L,k}\left(B_0^{(1)} - B_0^{(2)}\right) \\
&+m_{n_i}\lambda_{ai}^{L,k*}\lambda_{bi}^{R,k}\left(m_b^2 B_0^{(1)} - m_a^2 B_0^{(2)}\right) \\
&+m_a m_b\left(\lambda_{ai}^{R,k*}\lambda_{bi}^{R,k}m_b + \lambda_{ai}^{L,k*}\lambda_{bi}^{L,k}m_a\right)\left(-B_1^{(1)} + B_1^{(2)}\right)\Big],
\end{aligned} \tag{C8}$$

where $\Delta_{L,R}^{(9+10)} \equiv \Delta_{L,R}^{(9)} + \Delta_{L,R}^{(10)}$, and $B_{0,1}^{(i)} \equiv B_{0,1}(p_i^2; m_{n_i}^2, m_{c_k}^2)$. The analytic forms of $\Delta_{L,R}^{(i)}$ given here were also cross-checked using the FORM package [79,80].

There are 2 diagrams consisting of both scalar and vector mediation, namely diagrams (3) and (4). The diagrams (3) ncW:

$$\begin{aligned}
\Delta_L^{(3)} &= \Delta_L^{(ncW)} \\
&= \frac{e g^2 s_\delta f_k}{64\pi^2 s_W m_W^3} \\
&\times \sum_{i=1}^{9} U_{bi}^{v*}\Big\{\lambda_{ai}^{L,k*}m_a m_{n_i}\left[2m_W^2 C_0 + \left(m_W^2 - m_{c_k}^2 + m_h^2\right)C_1\right] \\
&+\lambda_{ai}^{R,k*}\Big[m_{n_i}^2 B_0^{(2)} + m_b^2 B_1^{(2)} - m_{n_i}^2\left(m_W^2 - m_{c_k}^2 + m_h^2\right)C_0 \\
&-2m_a^2 m_W^2 C_1 + \left[2m_W^2\left(m_h^2 - m_a^2\right) - m_b^2\left(m_W^2 - m_{c_k}^2 + m_h^2\right)\right]C_2\Big]\Big\},
\end{aligned} \tag{C9}$$

$$\begin{aligned}
\Delta_R^{(3)} &= \Delta_R^{(ncW)} \\
&= -\frac{g^3 m_b s_\delta f_k}{64\pi^2 m_W^3} \\
&\times \sum_{i=1}^{9} U_{bi}^{v*}\Big\{\lambda_{ai}^{L,k*}m_{n_i}\left[B_0^{(2)} + B_1^{(2)} + \left(m_W^2 + m_{c_k}^2 - m_h^2\right)C_0\right. \\
&\left.-\left(m_W^2 - m_{c_k}^2 + m_h^2\right)C_2\right] \\
&-\lambda_{ai}^{R,k*}m_a\left[\left(m_W^2 + m_{c_k}^2 - m_h^2\right)C_1 + 2m_W^2 C_2\right]\Big\},
\end{aligned} \tag{C10}$$

where

$f_1 = c_\phi, \quad f_2 = -s_\phi,$

$B_{0,1}^{(2)} = B_{0,1}(p_2^2; m_{n_i}^2, m_W^2)$, and $C_{0,1,2} = C_{0,1,2}(p_1^2, m_h^2, p_2^2; m_{n_i}^2, m_{c_k}^2, m_W^2)$.

The diagrams (4) with nWc:

$$\begin{aligned}
\Delta_L^{(4)} &= \Delta_L^{(nWc)} \\
&= -\frac{e g^2 m_a s_\delta f_k}{64\pi^2 s_W m_W^3}\sum_{i=1}^{9} U_{ai}^{v} \\
&\times \Big\{\lambda_{bi}^{L,k}m_{n_i}\Big[B_0^{(1)} + B_1^{(1)} + \left(m_W^2 + m_{c_k}^2 - m_h^2\right)C_0 \\
&-\left(m_W^2 - m_{c_k}^2 + m_h^2\right)C_1\Big] \\
&-\lambda_{bi}^{R,1}m_b\left[2m_W^2 C_1 + \left(m_W^2 + m_{c_k}^2 - m_h^2\right)C_2\right]\Big\},
\end{aligned} \tag{C11}$$

$$\begin{aligned}
\Delta_R^{(4)} &= \Delta_R^{(nWc)} \\
&= \frac{g^3 s_\delta f_k}{64\pi^2 m_W^3}\sum_{i=1}^{9} U_{ai}^{v} \\
&\times \Big\{\lambda_{bi}^{L,k}m_b m_{n_i}\left[2m_W^2 C_0 + \left(m_W^2 - m_{c_k}^2 + m_h^2\right)C_2\right] \\
&+\lambda_{bi}^{R,k}\Big[m_{n_i}^2 B_0^{(1)} + m_a^2 B_1^{(1)} - m_{n_i}^2\left(m_W^2 - m_{c_k}^2 + m_h^2\right)C_0 \\
&+\left[2m_W^2\left(m_h^2 - m_b^2\right) - m_a^2\left(m_W^2 - m_{c_k}^2 + m_h^2\right)\right]C_1 \\
&-2m_b^2 m_W^2 C_2\Big]\Big\},
\end{aligned} \tag{C12}$$

where $B_{0,1}^{(1)} = B_{0,1}(p_1^2; m_{n_i}^2, m_W^2)$ and $C_{0,1,2} = C_{0,1,2}(p_1^2, m_h^2, p_2^2; m_{n_i}^2, m_W^2, m_{c_k}^2)$.

The divergent cancellation of the decay amplitudes are proved following Refs. [102–104].

Appendix D: The Higgs sector of the 2HDM$N_{L,R}$

The Higgs potential of the model

$$\mathcal{V} = \mathcal{V}_\varphi + \mathcal{V}_{\rm 2HDM}, \tag{D1}$$

$$\begin{aligned}
\mathcal{V}_\varphi &= \mu_\varphi^2\varphi^*\varphi + \mu_\chi^2\chi^+\chi^- + \lambda_\varphi\left(\varphi^*\varphi\right)^2 \\
&+\lambda_\chi\left(\chi^+\chi^-\right)^2 + \lambda_{\varphi\chi}\left(\varphi^*\varphi\right)\left(\chi^+\chi^-\right) \\
&+\sum_{i=1}^{2}\left[\lambda_{i\varphi}(\varphi^*\varphi) + \lambda_{i\chi}(\chi^+\chi^-)\right]\left(H_i^\dagger H_i\right) \\
&+\left\{\lambda\left(H_1^T i\sigma_2 H_2\right)\chi^-\varphi + \text{h.c.}\right\},
\end{aligned} \tag{D2}$$

$$\begin{aligned}
\mathcal{V}_{\rm 2HDM} &= \mu_{11}^2 H_1^\dagger H_1 + \mu_{22}^2 H_2^\dagger H_2 - \left(\mu_{12}^2 H_1^\dagger H_2 + \text{h.c.}\right) \\
&+\frac{1}{2}\lambda_1\left(H_1^\dagger H_1\right)^2 + \frac{1}{2}\lambda_2\left(H_2^\dagger H_2\right)^2 \\
&+\lambda_3\left(H_1^\dagger H_1\right)\left(H_2^\dagger H_2\right) + \lambda_4\left(H_1^\dagger H_2\right)\left(H_2^\dagger H_1\right) \\
&+\frac{\lambda_5}{2}\left[\left(H_1^\dagger H_2\right)^2 + \left(H_2^\dagger H_1\right)^2\right].
\end{aligned} \tag{D3}$$

The minima conditions of the Higgs potential:

$$\begin{aligned} r_1: \quad \mu_{11}^2 &= -\frac{1}{2}c_\beta^2\lambda_1 v_H^2 - \frac{1}{2}\lambda_{345}s_\beta^2 v_H^2 + t_\beta\mu_{12}^2 - \frac{\lambda_{1\varphi}v_\varphi^2}{2}, \\ r_2: \quad \mu_{22}^2 &= -\frac{1}{2}c_\beta^2\lambda_{345} v_H^2 - \frac{1}{2}\lambda_2 s_\beta^2 v_H^2 + \frac{\mu_{12}^2}{t_\beta} - \frac{\lambda_{2\varphi}v_\varphi^2}{2}, \\ r': \quad \mu_\varphi^2 &= -\frac{1}{2}c_\beta^2\lambda_{1\varphi} v_H^2 - \frac{1}{2}\lambda_{2\varphi}s_\beta^2 v_H^2 - \lambda_\varphi v_\varphi^2, \end{aligned} \tag{D4}$$

where $\lambda_{345} = \lambda_3 + \lambda_4 + \lambda_5$.

Neutral CP-odd Higgs bosons. We find that z' is one massless eigenstate corresponding the Goldstone of B'_μ. The squared mass matrix in the basis (z_1, z_2) is:

$$\mathcal{M}_A^2 = \begin{pmatrix} t_\beta\mu_{12}^2 - s_\beta^2 v_H^2\lambda_5 & c_\beta s_\beta v_H^2\lambda_5 - \mu_{12}^2 \\ c_\beta s_\beta v_H^2\lambda_5 - \mu_{12}^2 & \frac{\mu_{12}^2}{t_\beta} - c_\beta^2 v_H^2\lambda_5 \end{pmatrix}. \tag{D5}$$

The mixing matrix $R(\beta)$ diagonalizing $\mathcal{M}_A^2$:

$$R(\beta) = \begin{pmatrix} c_\beta & s_\beta \\ -s_\beta & c_\beta \end{pmatrix} \Rightarrow R(\beta)\mathcal{M}_A^2 R^T(\beta)$$

$$= \text{diag}\left(0,\ \frac{\mu_{12}^2}{c_\beta s_\beta} - \lambda_5 v_H^2\right), \tag{D6}$$

where $R(x)$ is a real 2×2 rotation matrix of angle x satisfying $R^T(x)R(x) = R(x)R^T(x) = I_2$. This gives

$$\begin{aligned} &m_{G_Z} = 0,\ m_A^2 = \frac{\mu_{12}^2}{c_\beta s_\beta} - \lambda_5 v_H^2, \\ &\begin{pmatrix} z_1 \\ z_2 \end{pmatrix} = R^T(\beta)\begin{pmatrix} G_Z \\ A \end{pmatrix} = \begin{pmatrix} c_\beta G_Z - s_\beta A \\ G_Z s_\beta + c_\beta A \end{pmatrix}. \end{aligned} \tag{D7}$$

Neutral CP-even Higgs bosons. In the original basis (r_1, r_2, r'), the squared mass matrix is:

$$\mathcal{M}_h^2 = \begin{pmatrix} c_\beta^2\lambda_1 v_H^2 + t_\beta\mu_{12}^2 & c_\beta s_\beta v_H^2\lambda_{345} - \mu_{12}^2 & c_\beta v_H v_\varphi\lambda_{1\varphi} \\ c_\beta s_\beta v_H^2\lambda_{345} - \mu_{12}^2 & s_\beta^2\lambda_2 v_H^2 + \frac{\mu_{12}^2}{t_\beta} & s_\beta v_H v_\varphi\lambda_{2\varphi} \\ c_\beta v_H v_\varphi\lambda_{1\varphi} & s_\beta v_H v_\varphi\lambda_{2\varphi} & 2v_\varphi^2\lambda_\varphi \end{pmatrix}. \tag{D8}$$

Because $\det\mathcal{M}_h^2\big|_{v_H=0} = 0$, there are at least one Higgs boson having mass at the electroweak scale, which will be identified with the real one found experimentally. In this work we limit $\lambda_{1\varphi} = \lambda_{2\varphi} = 0$, leading to the consequence that $\mathcal{M}_h^2$ has one physical state r' with very heavy mass $m_{r'}^2 = 2v_\varphi^2\lambda_\varphi \propto v_\varphi^2$. The remaining 2×2 matrix, $\mathcal{M}_h'^2$, is diagonalized by a transformation $O(\alpha)$[3]:

$$O(\alpha) = \begin{pmatrix} -s_\alpha & c_\alpha \\ c_\alpha & s_\alpha \end{pmatrix} \Rightarrow O(\alpha)\mathcal{M}_h'^2 O^T(\alpha) = \text{diag}\left(m_h^2, m_H^2\right), \tag{D9}$$

$$\begin{pmatrix} r_1 \\ r_2 \end{pmatrix} = O^T(\alpha)\begin{pmatrix} h \\ H \end{pmatrix} = \begin{pmatrix} -s_\alpha h + c_\alpha H \\ c_\alpha h + s_\alpha H \end{pmatrix}, \tag{D10}$$

where h and H are SM-like Higgs and new heavy Higgs boson. Their masses and mixing parameter α are determined as follows

$$\begin{aligned} m_h^2 &= M_{11}^2 s_{\beta-\alpha}^2 + M_{22}^2 c_{\beta-\alpha}^2 + M_{12}^2 s_{2(\beta-\alpha)}, \\ m_H^2 &= M_{11}^2 c_{\beta-\alpha}^2 + M_{22}^2 s_{\beta-\alpha}^2 - M_{12}^2 s_{2(\beta-\alpha)}, \end{aligned} \tag{D11}$$

$$\tan 2(\beta-\alpha) = \frac{2c_\beta^2 s_\beta^2 v_H^2\left[c_\beta^2\lambda_1 - s_\beta^2\lambda_2 + \lambda_{345}(s_\beta^2 - c_\beta^2)\right]}{c_\beta s_\beta v_H^2\left(c_\beta^4\lambda_1 - c_\beta^2 s_\beta^2(\lambda_1 + \lambda_2 - 4\lambda_{345}) + \lambda_2 s_\beta^4\right) - \mu_{12}^2} \tag{D12}$$

where the entries M_{ij}^2 are:

$$M^2 = \begin{pmatrix} v_H^2\left(c_\beta^4\lambda_1 + \frac{1}{2}s_{2\beta}^2\lambda_{345} + \lambda_2 s_\beta^4\right) & \frac{1}{2}s_{2\beta}v_H^2\left(c_{2\beta}\lambda_{345} - c_\beta^2\lambda_1 + s_\beta^2\lambda_2\right) \\ \star & c_\beta^2 s_\beta^2 v_H^2(\lambda_1 + \lambda_2 - 2\lambda_{345}) + \frac{\mu_{12}^2}{c_\beta s_\beta} \end{pmatrix}. \tag{D13}$$

It is noted that $O(\alpha-\beta)M^2 O^T(\alpha-\beta) = \text{diag}\left(m_h^2, m_H^2\right)$. The final results are

$$\begin{aligned} h &= \frac{1}{\sqrt{2}}\left[v_H c_\beta + c_\alpha H - s_\alpha h + i c_\beta G_Z - i s_\beta A\right], \\ H &= \frac{1}{\sqrt{2}}\left[v_H s_\beta + s_\alpha H + c_\alpha h + i s_\beta G_Z + i c_\beta A\right]. \end{aligned} \tag{D14}$$

Singly charged Higgs bosons. The basis (H_1^-, H_2^-, χ^-) gives the following squared mass matrix:

$$\mathcal{M}_C^2 = \frac{1}{2}\begin{pmatrix} 2t_\beta\mu_{12}^2 - \lambda_{45}s_\beta^2 v_H^2 & c_\beta s_\beta\lambda_{45}v_H^2 - 2\mu_{12}^2 & \lambda s_\beta v_H v_\varphi \\ \star & \frac{2\mu_{12}^2}{t_\beta} - c_\beta^2\lambda_{45}v_H^2 & -\lambda c_\beta v_H v_\varphi \\ \star & \star & 2\mathcal{M}_{+33}^2 \end{pmatrix}, \tag{D15}$$

where

$$\lambda_{45} = \lambda_4 + \lambda_5, \tag{D16}$$

$$\mathcal{M}_{+33}^2 = (c_\beta^2\lambda_{1\chi} + \lambda_{2\chi}s_\beta^2)v_H^2 + \lambda_{\varphi\chi}v_\varphi^2 + 2\mu_\chi^2. \tag{D17}$$

[3] This definition give the popular forms of the SM-like Higgs couplings

The mixing matrix O_C is defined as:

$$O_C \mathcal{M}_C^2 O_C^T = \text{diag}\left(0,\ m_{c_1}^2,\ m_{c_2}^2\right),\ O_C O_C^T = O_C^T O_C = I_3. \tag{D18}$$

where $(c_0^\pm, c_1^\pm, c_2^\pm)$ are mass eigenstates with $c_0^\pm$ being the Goldstone bosons of $W^\pm$:

$$\begin{pmatrix} H_1^\pm \\ H_2^\pm \\ \chi^\pm \end{pmatrix} = O_C^T \begin{pmatrix} c_0^\pm \\ c_1^\pm \\ c_2^\pm \end{pmatrix} = \begin{pmatrix} c_\beta & -c_\phi s_\beta & s_\beta s_\phi \\ s_\beta & c_\beta c_\phi & -c_\beta s_\phi \\ 0 & s_\phi & c_\phi \end{pmatrix} \begin{pmatrix} c_0^\pm \\ c_1^\pm \\ c_2^\pm \end{pmatrix}, \tag{D19}$$

where

$$t_{2\phi} \equiv \tan(2\phi) = \frac{2\lambda s_{2\beta} v_H v_\varphi}{s_{2\beta}\lambda_{45} v_H^2 + 2 s_{2\beta} M_{+33}^2 - 4\mu_{12}^2}. \tag{D20}$$

This gives

$$\begin{aligned} m_{c_1}^2 &= c_\phi^2 \left[\frac{2\mu_{12}^2}{s_{2\beta}} - \frac{\lambda_{45} v_H^2}{2}\right] + s_\phi^2 \left[\mathcal{M}_{+33}^2\right] + s_{2\phi}\left[-\frac{1}{2}\lambda v_H v_\varphi\right], \\ m_{c_2}^2 &= s_\phi^2 \left[\frac{2\mu_{12}^2}{s_{2\beta}} - \frac{\lambda_{45} v_H^2}{2}\right] + c_\phi^2 \left[\mathcal{M}_{+33}^2\right] - s_{2\phi}\left[-\frac{1}{2}\lambda v_H v_\varphi\right]. \end{aligned} \tag{D21}$$

In the numerical calculation, the following quantities relating to the Higgs potential are independent inputs:

$$\lambda_1,\ \lambda_4,\ \lambda_5,\ m_h,\ m_H,\ m_{c_1},\ m_{c_2},\ \delta,\ \phi, \tag{D22}$$

where δ was defined in Eq. (48) for accommodating the SM results. The dependent parameters are:

$$\begin{aligned} m_A^2 &= c_\phi^2 m_{c_1}^2 + s_\phi^2 m_{c_2}^2 + \frac{1}{2}\left(\lambda_4 - \lambda_5\right) v_H^2, \\ \lambda_2 &= \frac{c_\beta^2 \lambda_1 s_\alpha^2}{c_\alpha^2 s_\beta^2} + \frac{c_{2\alpha} m_h^2 + \left(\lambda_5 v_H^2 + m_A^2\right) s_\delta \left(s_\alpha s_\beta - c_\alpha c_\beta\right)}{c_\alpha^2 s_\beta^2 v_H^2}, \\ \lambda_3 &= \frac{c_\beta \lambda_1 s_\alpha}{c_\alpha s_\beta} + \frac{s_\delta s_\beta \left(\lambda_5 v_H^2 + m_A^2\right) - s_\alpha m_h^2}{c_\alpha c_\beta s_\beta v_H^2} - \lambda_4 - \lambda_5, \\ m_H^2 &= \frac{v_H^2 \left(c_\beta^2 \lambda_1 + \lambda_5 s_\beta^2\right) - s_\alpha^2 m_h^2 + s_\beta^2 m_A^2}{c_\alpha^2}. \end{aligned} \tag{D23}$$

We note that the following intermediate parameters are absorbed in the Higgs potential:

$$\begin{aligned} \mu_{12}^2 &= c_\beta s_\beta \left(\lambda_5 v_H^2 + m_A^2\right), \\ \lambda &= \frac{s_{2\phi}(m_{c_2}^2 - m_{c_1}^2)}{v_H v_\varphi}, \\ \mathcal{M}_{+33}^2 &= s_\phi^2 m_{c_1}^2 + c_\phi^2 m_{c_2}^2, \end{aligned}$$

In the numerical discussions, all Higgs couplings were checked to satisfy the two conditions of bounded from below and the unitarity limits [81], namely

$$\begin{aligned} &4\pi \geq \lambda_1, \lambda_2 \geq 0, \\ &\lambda_3 + \sqrt{\lambda_1 \lambda_2} \geq 0,\ \lambda_3 + \lambda_4 + \sqrt{\lambda_1 \lambda_2} - |\lambda_5| \geq 0, \\ &\left|\frac{3}{2}\left(\lambda_1 + \lambda_2\right) + \sqrt{\frac{9}{4}(\lambda_1 - \lambda_2)^2 + (2\lambda_3 + \lambda_4)^2}\right| < 8\pi, \\ &\left|\frac{1}{2}\left(\lambda_1 + \lambda_2\right) + \frac{1}{2}\sqrt{(\lambda_1 - \lambda_2)^2 + 4\lambda_4^2}\right| < 8\pi, \\ &\left|\frac{1}{2}\left(\lambda_1 + \lambda_2\right) + \frac{1}{2}\sqrt{(\lambda_1 - \lambda_2)^2 + 4\lambda_5^2}\right| < 8\pi, \\ &|\lambda_3 + 2\lambda_4 - 3\lambda_5| < 8\pi,\ |\lambda_3 - \lambda_5| < 8\pi, \\ &|\lambda_3 + 2\lambda_4 + 3\lambda_5| < 8\pi, \\ &|\lambda_3 + \lambda_5| < 8\pi,\ |\lambda_3 + \lambda_4| < 8\pi,\ |\lambda_3 - \lambda_4| < 8\pi. \end{aligned} \tag{D24}$$

It can be seen in Eq. (D23) that, large t_β will result in large $|\lambda_3|$ unless $s_\delta \left(\lambda_5 v_H^2 + m_A^2\right)/(c_\beta v_H^2) \propto \mathcal{O}(1)$, therefore s_δ must be small enough.

References

1. D. Jurčiukonis, L. Lavoura, JHEP **03**, 106 (2022). arXiv:2107.14207 [hep-ph]
2. R.H. Parker, C. Yu, W. Zhong, B. Estey, H. Müller, Science **360**, 191 (2018). arXiv:1812.04130 [physics.atom-ph]
3. X. Fan, T.G. Myers, B.A.D. Sukra, G. Gabrielse, Phys. Rev. Lett. **130**(7), 071801 (2023). arXiv:2209.13084 [physics.atom-ph]
4. D.P. Aguillard et al. (Muon g-2), Phys. Rev. Lett. **131**(16), 161802 (2023). arXiv:2308.06230 [hep-ex]
5. T. Mondal, H. Okada, Nucl. Phys. B **976**, 115716 (2022). arXiv:2103.13149 [hep-ph]
6. L.T. Hue, H.N. Long, V.H. Binh, H.L.T. Mai, T.P. Nguyen, Nucl. Phys. B **992**, 116244 (2023). arXiv:2301.05407 [hep-ph]
7. A. Crivellin, M. Hoferichter, P. Schmidt-Wellenburg, Phys. Rev. D **98**(11), 113002 (2018). arXiv:1807.11484 [hep-ph]
8. T.T. Hong, N.H.T. Nha, T.P. Nguyen, L.T.T. Phuong, L.T. Hue, PTEP **2022**(9), 093B05 (2022). arXiv:2206.08028 [hep-ph]
9. I. Cortes Maldonado, A. Moyotl, G. Tavares-Velasco, Int. J. Mod. Phys. A **26**, 4171–4185 (2011). arXiv:1109.0661 [hep-ph]
10. R. Dermisek, K. Hermanek, N. McGinnis, N. McGinnis, Phys. Rev. Lett. **126**(19), 191801 (2021). arXiv:2011.11812 [hep-ph]
11. R. Dermisek, K. Hermanek, N. McGinnis, Phys. Rev. D **104**(5), 055033 (2021). arXiv:2103.05645 [hep-ph]
12. R. Dermisek, K. Hermanek, N. McGinnis, S. Yoon, Phys. Rev. Lett. **129**(22), 221801 (2022). arXiv:2205.14243 [hep-ph]
13. A.S. De Jesus, S. Kovalenko, F.S. Queiroz, C. Siqueira, K. Sinha, Phys. Rev. D **102**(3), 035004 (2020). arXiv:2004.01200 [hep-ph]
14. D. Cogollo, Y.M. Oviedo-Torres, Y.S. Villamizar, Int. J. Mod. Phys. A **35**(23), 2050126 (2020). arXiv:2004.14792 [hep-ph]
15. R. Dermisek, K. Hermanek, N. McGinnis, S. Yoon, Phys. Rev. D **108**(5), 055019 (2023). arXiv:2306.13212 [hep-ph]
16. Á.S. de Jesus, F.S. Queiroz, J.W.F. Valle, Y. Villamizar, arXiv:2312.03851 [hep-ph]
17. E. Arganda, M.J. Herrero, X. Marcano, C. Weiland, Phys. Rev. D **91**(1), 015001 (2015). arXiv:1405.4300 [hep-ph]

18. M.J. Herrero, E. Arganda, X. Marcano, R. Morales, A. Szynkman, PoS **EPS-HEP2017**, 114 (2017). arXiv:1710.02510 [hep-ph]
19. E. Arganda, M.J. Herrero, X. Marcano, R. Morales, A. Szynkman, Phys. Rev. D **95**(9), 095029 (2017). arXiv:1612.09290 [hep-ph]
20. J.G. Korner, A. Pilaftsis, K. Schilcher, Phys. Lett. B **300**, 381–386 (1993). arXiv:hep-ph/9301290
21. V. De Romeri, M.J. Herrero, X. Marcano, F. Scarcella, Phys. Rev. D **95**(7), 075028 (2017). arXiv:1607.05257 [hep-ph]
22. G. Hernández-Tomé, J.I. Illana, M. Masip, G. López Castro, P. Roig, Phys. Rev. D **101**(7), 075020 (2020). arXiv:1912.13327 [hep-ph]
23. A. Abada, J. Kriewald, E. Pinsard, S. Rosauro-Alcaraz, A.M. Teixeira, Eur. Phys. J. C **83**(6), 494 (2023). arXiv:2207.10109 [hep-ph]
24. G. Aad et al. (ATLAS), JHEP **23**, 082 (2020). arXiv:2307.08567 [hep-ex]
25. T. Aoyama, N. Asmussen, M. Benayoun, J. Bijnens, T. Blum, M. Bruno, I. Caprini, C.M. Carloni Calame, M. Cè, G. Colangelo et al., Phys. Rep. **887**, 1–166 (2020). arXiv:2006.04822 [hep-ph]
26. M. Davier, A. Hoecker, B. Malaescu, Z. Zhang, Eur. Phys. J. C **71**, 1515 (2011). arXiv:1010.4180 [hep-ph]. [Erratum: Eur. Phys. J. C **72**, 1874 (2012)]
27. T. Aoyama, M. Hayakawa, T. Kinoshita, M. Nio, Phys. Rev. Lett. **109**, 111808 (2012). arXiv:1205.5370 [hep-ph]
28. T. Aoyama, T. Kinoshita, M. Nio, Atoms **7**(1), 28 (2019)
29. A. Czarnecki, W.J. Marciano, A. Vainshtein, Phys. Rev. D **67**, 073006 (2003). arXiv:hep-ph/0212229. [Erratum: Phys. Rev. D **73**, 119901 (2006)]
30. C. Gnendiger, D. Stöckinger, H. Stöckinger-Kim, Phys. Rev. D **88**, 053005 (2013). arXiv:1306.5546 [hep-ph]
31. I. Danilkin, M. Vanderhaeghen, Phys. Rev. D **95**(1), 014019 (2017). arXiv:1611.04646 [hep-ph]
32. M. Davier, A. Hoecker, B. Malaescu, Z. Zhang, Eur. Phys. J. C **77**(12), 827 (2017). arXiv:1706.09436 [hep-ph]
33. A. Keshavarzi, D. Nomura, T. Teubner, Phys. Rev. D **97**(11), 114025 (2018). arXiv:1802.02995 [hep-ph]
34. G. Colangelo, M. Hoferichter, P. Stoffer, JHEP **02**, 006 (2019). arXiv:1810.00007 [hep-ph]
35. M. Hoferichter, B.L. Hoid, B. Kubis, JHEP **08**, 137 (2019). arXiv:1907.01556 [hep-ph]
36. M. Davier, A. Hoecker, B. Malaescu, Z. Zhang, Eur. Phys. J. C **80**(3), 241 (2020). arXiv:1908.00921 [hep-ph]. [Erratum: Eur. Phys. J. C **80**(5), 410 (2020)]
37. A. Keshavarzi, D. Nomura, T. Teubner, Phys. Rev. D **101**(1), 014029 (2020). arXiv:1911.00367 [hep-ph]
38. A. Kurz, T. Liu, P. Marquard, M. Steinhauser, Phys. Lett. B **734**, 144–147 (2014). arXiv:1403.6400 [hep-ph]
39. K. Melnikov, A. Vainshtein, Phys. Rev. D **70**, 113006 (2004). arXiv:hep-ph/0312226
40. P. Masjuan, P. Sanchez-Puertas, Phys. Rev. D **95**(5), 054026 (2017). arXiv:1701.05829 [hep-ph]
41. G. Colangelo, M. Hoferichter, M. Procura, P. Stoffer, JHEP **04**, 161 (2017). arXiv:1702.07347 [hep-ph]
42. M. Hoferichter, B.L. Hoid, B. Kubis, S. Leupold, S.P. Schneider, JHEP **10**, 141 (2018). arXiv:1808.04823 [hep-ph]
43. A. Gérardin, H.B. Meyer, A. Nyffeler, Phys. Rev. D **100**(3), 034520 (2019). arXiv:1903.09471 [hep-lat]
44. J. Bijnens, N. Hermansson-Truedsson, A. Rodríguez-Sánchez, Phys. Lett. B **798**, 134994 (2019). arXiv:1908.03331 [hep-ph]
45. G. Colangelo, F. Hagelstein, M. Hoferichter, L. Laub, P. Stoffer, JHEP **03**, 101 (2020). arXiv:1910.13432 [hep-ph]
46. T. Blum, N. Christ, M. Hayakawa, T. Izubuchi, L. Jin, C. Jung, C. Lehner, Phys. Rev. Lett. **124**(13), 132002 (2020). arXiv:1911.08123 [hep-lat]
47. G. Colangelo, M. Hoferichter, A. Nyffeler, M. Passera, P. Stoffer, Phys. Lett. B **735**, 90–91 (2014). arXiv:1403.7512 [hep-ph]
48. V. Pauk, M. Vanderhaeghen, Eur. Phys. J. C **74**(8), 3008 (2014). arXiv:1401.0832 [hep-ph]
49. F. Jegerlehner, Springer Tracts Mod. Phys. **274**, 1–693 (2017)
50. M. Knecht, S. Narison, A. Rabemananjara, D. Rabetiarivony, Phys. Lett. B **787**, 111–123 (2018). arXiv:1808.03848 [hep-ph]
51. G. Eichmann, C.S. Fischer, R. Williams, Phys. Rev. D **101**(5), 054015 (2020). arXiv:1910.06795 [hep-ph]
52. P. Roig, P. Sanchez-Puertas, Phys. Rev. D **101**(7), 074019 (2020). arXiv:1910.02881 [hep-ph]
53. S. Ghosh, P. Ko, arXiv:2311.14099 [hep-ph]
54. D. Hanneke, S. Fogwell, G. Gabrielse, Phys. Rev. Lett. **100**, 120801 (2008). arXiv:0801.1134 [physics.atom-ph]
55. L. Morel, Z. Yao, P. Cladé, S. Guellati-Khélifa, Nature **588**(7836), 61–65 (2020)
56. T. Aoyama, M. Hayakawa, T. Kinoshita, M. Nio, Phys. Rev. Lett. **109**, 111807 (2012). arXiv:1205.5368 [hep-ph]
57. S. Laporta, Phys. Lett. B **772**, 232–238 (2017). arXiv:1704.06996 [hep-ph]
58. T. Aoyama, T. Kinoshita, M. Nio, Phys. Rev. D **97**(3), 036001 (2018). arXiv:1712.06060 [hep-ph]
59. H. Terazawa, Nonlinear Phenom. Complex Syst. **21**(3), 268–272 (2018)
60. S. Volkov, Phys. Rev. D **100**(9), 096004 (2019). arXiv:1909.08015 [hep-ph]
61. A. Gérardin, Eur. Phys. J. A **57**(4), 116 (2021). arXiv:2012.03931 [hep-lat]
62. B. Aubert et al. (BaBar), Phys. Rev. Lett. **104**, 021802 (2010). arXiv:0908.2381 [hep-ex]
63. A.M. Baldini et al. (MEG), Eur. Phys. J. C **76**(8), 434 (2016). arXiv:1605.05081 [hep-ex]
64. A. Abdesselam et al. (Belle), JHEP **10**, 19 (2021). arXiv:2103.12994 [hep-ex]
65. A.M. Baldini et al. (MEG II), Eur. Phys. J. C **78**(5), 380 (2018). arXiv:1801.04688 [physics.ins-det]
66. E. Kou et al. (Belle-II), PTEP **2019**(12), 123C01 (2019). arXiv:1808.10567 [hep-ex]. [Erratum: PTEP **2020**(2), 029201 (2020)]
67. A.M. Sirunyan et al. (CMS), Phys. Rev. D **104**(3), 032013 (2021). arXiv:2105.03007 [hep-ex]
68. (ATLAS), Search for the decays of the Higgs boson $H \to ee$ and $H \to e\mu$ in pp collisions at $\sqrt{s} = 13$ TeV with the ATLAS detector. ATLAS-CONF-2019-037
69. Q. Qin, Q. Li, C.D. Lü, F.S. Yu, S.H. Zhou, Eur. Phys. J. C **78**(10), 835 (2018). arXiv:1711.07243 [hep-ph]
70. R.K. Barman, P.S.B. Dev, A. Thapa, Phys. Rev. D **107**(7), 075018 (2023). arXiv:2210.16287 [hep-ph]
71. M. Aoki, S. Kanemura, M. Takeuchi, L. Zamakhsyari, Phys. Rev. D **107**(5), 055037 (2023). arXiv:2302.08489 [hep-ph]
72. G. Aad et al. (ATLAS), Phys. Rev. Lett. **127**, 271801 (2022). arXiv:2105.12491 [hep-ex]
73. G. Aad et al. (ATLAS), Phys. Rev. D **108**, 032015 (2023). arXiv:2204.10783 [hep-ex]
74. M. Dam, SciPost Phys. Proc. **1**, 041 (2019). arXiv:1811.09408 [hep-ex]
75. A. Abada et al. (FCC), Eur. Phys. J. C **79**(6), 474 (2019)
76. W. Grimus, L. Lavoura, Phys. Rev. D **66**, 014016 (2002). arXiv:hep-ph/0204070
77. H.K. Dreiner, H.E. Haber, S.P. Martin, Phys. Rep. **494**, 1–196 (2010). arXiv:0812.1594 [hep-ph]
78. G. 't Hooft, M.J.G. Veltman, Nucl. Phys. B **153**, 365–401 (1979)
79. J.A.M. Vermaseren, arXiv:math-ph/0010025
80. J. Kuipers, T. Ueda, J.A.M. Vermaseren, J. Vollinga, Comput. Phys. Commun. **184**, 1453–1467 (2013). arXiv:1203.6543 [cs.SC]

81. G.C. Branco, P.M. Ferreira, L. Lavoura, M.N. Rebelo, M. Sher, J.P. Silva, Phys. Rep. **516**, 1–102 (2012). arXiv:1106.0034 [hep-ph]
82. A.L. Cherchiglia, G. De Conto, C.C. Nishi, JHEP **08**, 170 (2023). arXiv:2304.00038 [hep-ph]
83. J.A. Casas, A. Ibarra, Nucl. Phys. B **618**, 171–204 (2001). arXiv:hep-ph/0103065
84. R.L. Workman et al. (Particle Data Group), PTEP **2022**, 083C01 (2022)
85. N.H. Thao, L.T. Hue, H.T. Hung, N.T. Xuan, Nucl. Phys. B **921**, 159–180 (2017). arXiv:1703.00896 [hep-ph]
86. L.T. Hue, K.H. Phan, T.P. Nguyen, H.N. Long, H.T. Hung, Eur. Phys. J. C **82**(8), 722 (2022). arXiv:2109.06089 [hep-ph]
87. A. Pilaftsis, Phys. Lett. B **285**, 68–74 (1992)
88. E. Arganda, A.M. Curiel, M.J. Herrero, D. Temes, Phys. Rev. D **71**, 035011 (2005). arXiv:hep-ph/0407302
89. D. de Florian et al. (LHC Higgs Cross Section Working Group), CERN Yellow Reports: Monographs, 2/2017, arXiv:1610.07922 [hep-ph]
90. L. Lavoura, Eur. Phys. J. C **29**, 191–195 (2003). arXiv:hep-ph/0302221
91. L.T. Hue, L.D. Ninh, T.T. Thuc, N.T.T. Dat, Eur. Phys. J. C **78**(2), 128 (2018). arXiv:1708.09723 [hep-ph]
92. L.T. Hue, A.E. Cárcamo Hernández, H.N. Long, T.T. Hong, Nucl. Phys. B **984**, 115962 (2022). arXiv:2110.01356 [hep-ph]
93. N.H. Thao, D.T. Binh, T.T. Hong, L.T. Hue, D.P. Khoi, PTEP **2023**, 8 (2023). arXiv:2302.07576 [hep-ph]
94. N. Aghanim et al. (Planck), Astron. Astrophys. **641**, A6 (2020). arXiv:1807.06209 [astro-ph.CO]. [Erratum: Astron. Astrophys. **652**, C4 (2021)]
95. N.R. Agostinho, G.C. Branco, P.M.F. Pereira, M.N. Rebelo, J.I. Silva-Marcos, Eur. Phys. J. C **78**(11), 895 (2018). arXiv:1711.06229 [hep-ph]
96. A.M. Coutinho, A. Crivellin, C.A. Manzari, Phys. Rev. Lett. **125**(7), 071802 (2020). arXiv:1912.08823 [hep-ph]
97. C. Biggio, E. Fernandez-Martinez, M. Filaci, J. Hernandez-Garcia, J. Lopez-Pavon, JHEP **05**, 022 (2020). arXiv:1911.11790 [hep-ph]
98. P. Escribano, J. Terol-Calvo, A. Vicente, Phys. Rev. D **103**(11), 115018 (2021). arXiv:2104.03705 [hep-ph]
99. G. 't Hooft, M.J.G. Veltman, Nucl. Phys. B **44**, 189–213 (1972)
100. T. Hahn, M. Perez-Victoria, Comput. Phys. Commun. **118**, 153–165 (1999). arXiv:hep-ph/9807565
101. M.E. Peskin, D.V. Schroeder (Addison-Wesley, 1995). ISBN:978-0-201-50397-5
102. T.P. Nguyen, T.T. Thuc, D.T. Si, T.T. Hong, L.T. Hue, PTEP **2022**(2), 023B01 (2022). arXiv:2011.12181 [hep-ph]
103. T.P. Nguyen, T.T. Le, T.T. Hong, L.T. Hue, Phys. Rev. D **97**(7), 073003 (2018). arXiv:1802.00429 [hep-ph]
104. L.T. Hue, H.N. Long, T.T. Thuc, T. Phong Nguyen, Nucl. Phys. B **907**, 37–76 (2016). arXiv:1512.03266 [hep-ph]